

# Strange-Meson Spectroscopy – from COMPASS to AMBER

Stefan Wallner for the COMPASS and AMBER Collaborations  
(swallner@mpp.mpg.de)

Max Planck Institute for Physics

Hadron Spectroscopy with Strangeness Workshop  
April 3, 2024

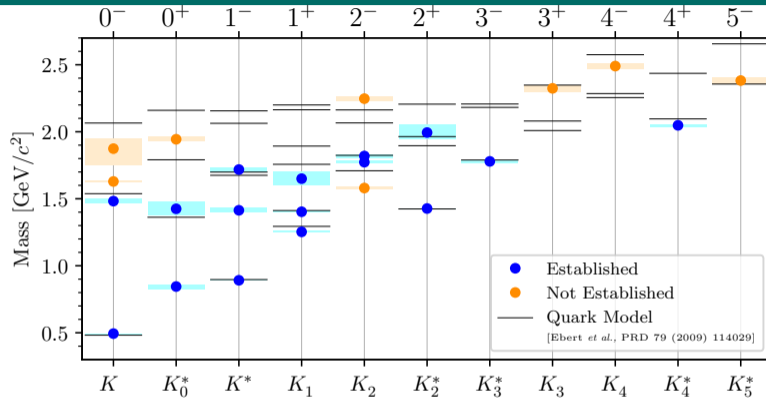


AMBER

Apparatus for Meson and Baryon  
Experimental Research



MAX PLANCK INSTITUTE  
FOR PHYSICS



PDG lists 25 strange mesons

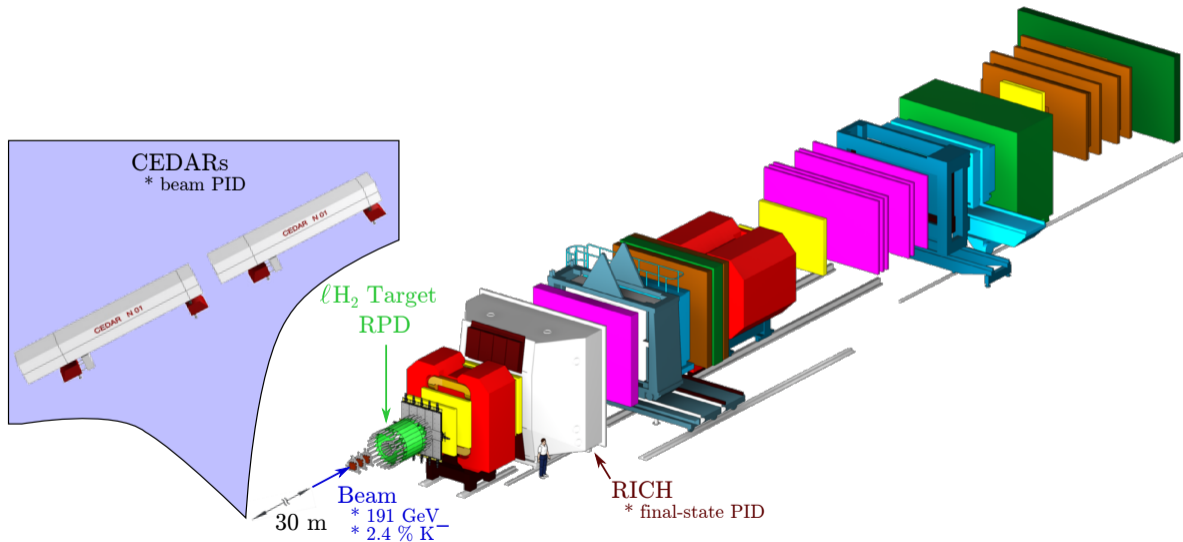
(2022)

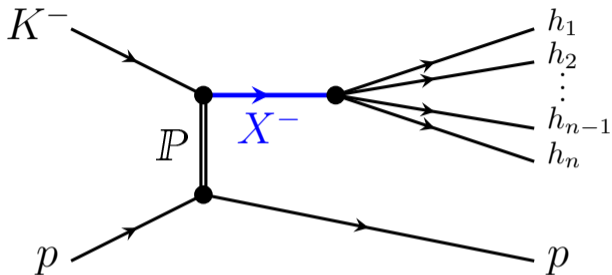
- ▶ 16 established states, 9 need further confirmation
- ▶ Missing states with respect to quark-model predictions
- ▶ Many measurements performed more than 30 years ago

# Strange-Meson Spectroscopy with COMPASS

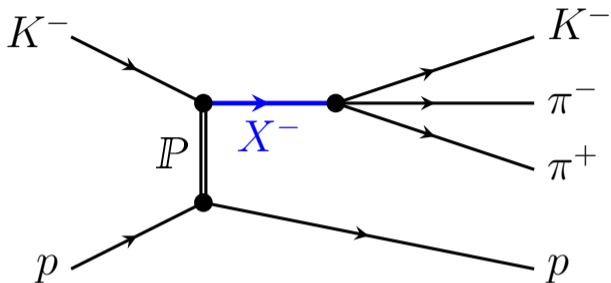
COMPASS Setup for Hadron Beams

[COMPASS, Nucl. Instrum. Methods 779 (2015) 69]





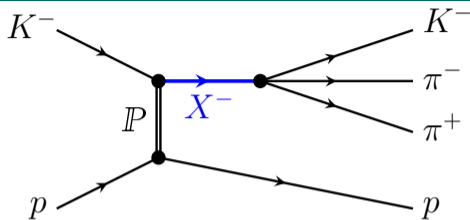
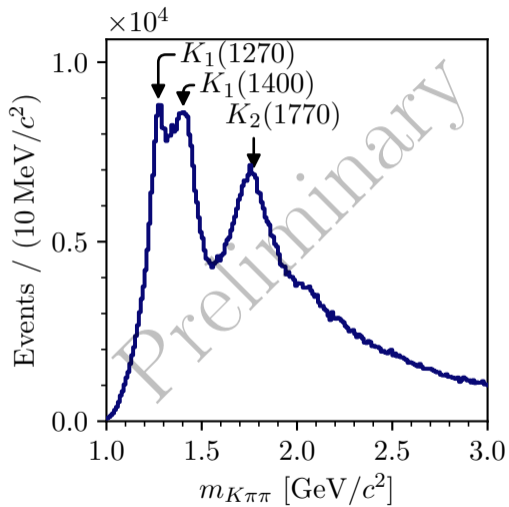
- ▶ Diffractive scattering of high-energy kaon beam
- ▶ Strange mesons appear as **intermediate resonances**  $X^-$
- ▶ Decay to multi-body hadronic final states
- ▶  $K^- \pi^- \pi^+$  final state
  - ▶ Study in principle all strange mesons
  - ▶ Study a wide mass range
  - ▶ Study different decay modes



- ▶ Diffractive scattering of high-energy kaon beam
- ▶ Strange mesons appear as **intermediate resonances**  $X^-$
- ▶ Decay to multi-body hadronic final states
- ▶  **$K^- \pi^- \pi^+$  final state**
  - ▶ Study in principle **all strange mesons**
  - ▶ Study a **wide mass range**
  - ▶ Study **different decay modes**

# Strange-Meson Spectroscopy with COMPASS

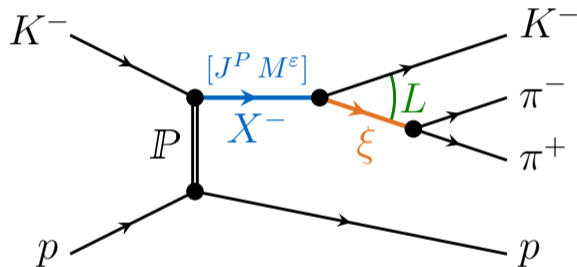
The  $K^- \pi^- \pi^+$  Data Sample



- ▶ World's largest data set of about 720 k events
- ▶ Rich spectrum of **overlapping and interfering**  $X^-$ 
  - ▶ Dominant well known states
  - ▶ States with lower intensity are "hidden"

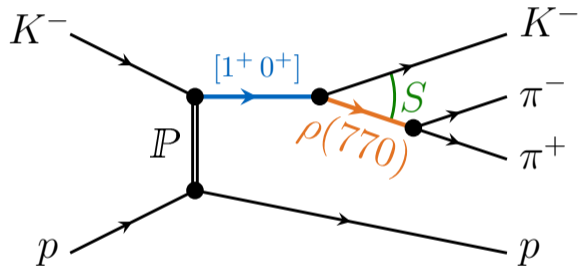
Partial wave:  $J^P M^\epsilon \xi b^- L$

- ▶  $J^P$  spin and parity
- ▶  $M^\epsilon$  spin projection
- ▶  $\xi$  isobar resonance
- ▶  $b^-$  bachelor particle
- ▶  $L$  orbital angular momentum



Partial wave:  $J^P M^{\xi} b^- L$

- ▶  $J^P$  spin and parity
- ▶  $M^{\xi}$  spin projection
- ▶  $\xi$  isobar resonance
- ▶  $b^-$  bachelor particle
- ▶  $L$  orbital angular momentum





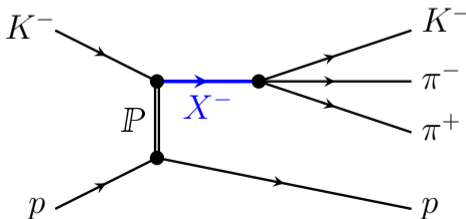
**Data:** 720 k diffractively produced  $K^- \pi^- \pi^+$  candidates

**Data:** 720 k diffractively produced  $K^-\pi^-\pi^+$  candidates

## (I) Partial-Wave Decomposition

Performed independently in narrow  $(m_{K\pi\pi}, t')$  cells  
No assumption about  $K\pi\pi$  resonances

**Partial waves:** Intensities and relative phases as a function of  $(m_{K\pi\pi}, t')$

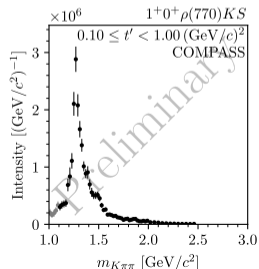
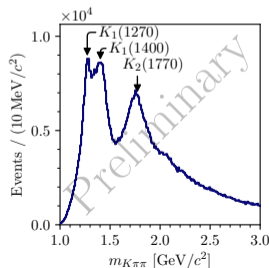


**Data:** 720 k diffractively produced  $K^-\pi^-\pi^+$  candidates

## (I) Partial-Wave Decomposition

Performed independently in narrow ( $m_{K\pi\pi}, t'$ ) cells  
 No assumption about  $K\pi\pi$  resonances

**Partial waves:** Intensities and relative phases as a function of ( $m_{K\pi\pi}, t'$ )



**Data:** 720 k diffractively produced  $K^-\pi^-\pi^+$  candidates

## (I) Partial-Wave Decomposition

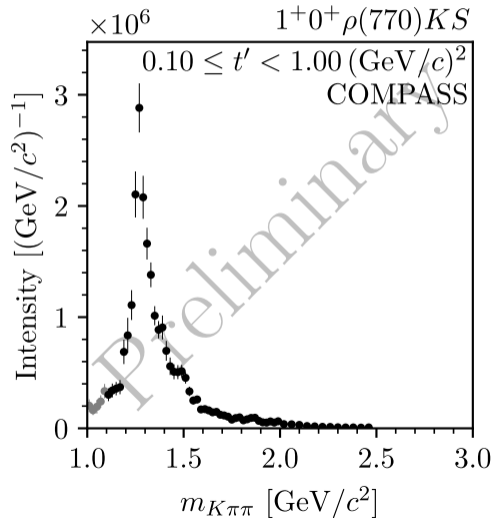
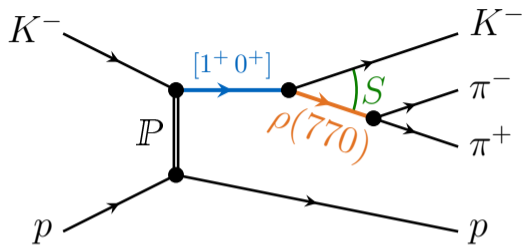
Performed independently in narrow  $(m_{K\pi\pi}, t')$  cells  
No assumption about  $K\pi\pi$  resonances

**Partial waves:** Intensities and relative phases as a function of  $(m_{K\pi\pi}, t')$

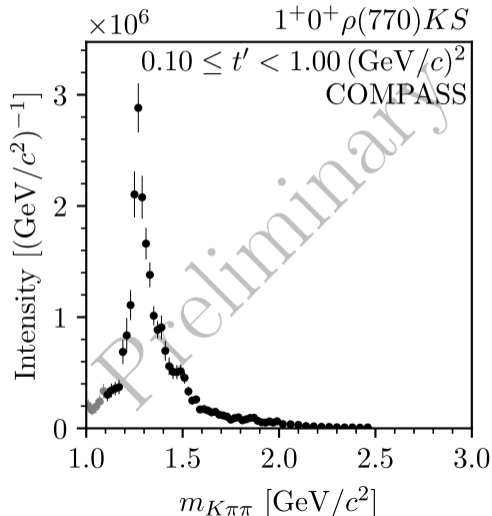
## (II) Resonance-Model Fit

Model  $m_{K\pi\pi}$  dependence of partial waves  
 $K\pi\pi$  resonances and background

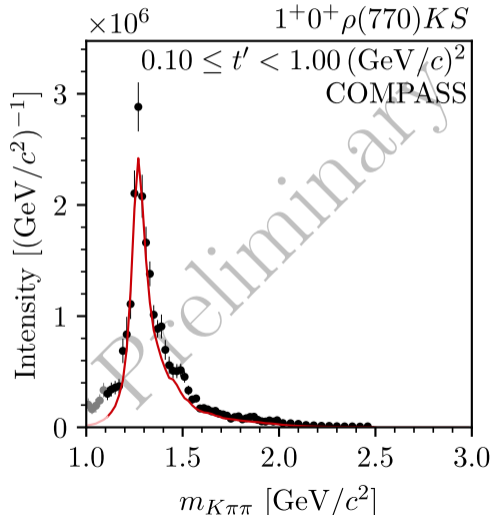
**Resonance parameters:** Masses and widths of the strange-meson resonances



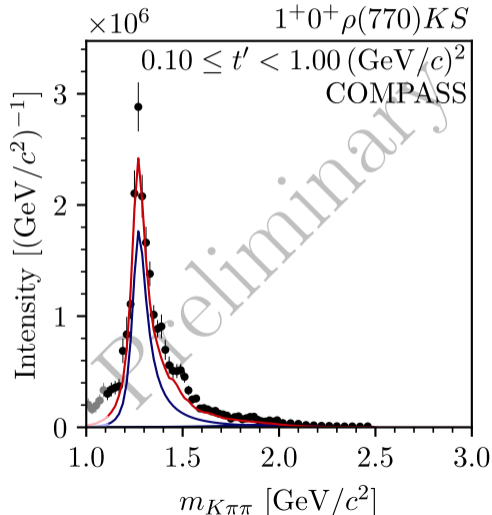
- ▶ Partial-wave amplitudes in  $(m_{K\pi\pi}, t')$  bins
  - ▶ Inferred wave set from data using regularization-based model-selection techniques
  - ▶ Bootstrap resampling to improve uncertainty estimates
  - ▶ Detailed Monte Carlo input-output studies
- ▶ Model  $m_{K\pi\pi}$  dependence of partial-wave amplitudes
- ▶ Breit-Wigner amplitudes for  $K^-\pi^-\pi^+$  resonance components
- ▶ Coherent non-resonant component parameterizing other  $K^-\pi^-\pi^+$  production mechanisms
- ▶ Developed scheme to handle incoherent backgrounds
  - ▶ Incoherent background from  $\pi^-$  diffraction to  $\pi^-\pi^+\pi^-$  explicitly modeled by COMPASS  $\pi^-\pi^-\pi^+$  analysis
  - ▶ Incoherent effective background component parameterizing other background processes



- ▶ Partial-wave amplitudes in  $(m_{K\pi\pi}, t')$  bins
  - ▶ Inferred wave set from data using regularization-based model-selection techniques
  - ▶ Bootstrap resampling to improve uncertainty estimates
  - ▶ Detailed Monte Carlo input-output studies
- ▶ Model  $m_{K\pi\pi}$  dependence of **partial-wave amplitudes**
- ▶ Breit-Wigner amplitudes for  $K^-\pi^-\pi^+$  resonance components
- ▶ Coherent non-resonant component parameterizing other  $K^-\pi^-\pi^+$  production mechanisms
- ▶ Developed scheme to handle incoherent backgrounds
  - ▶ Incoherent background from  $\pi^-\pi^-\pi^+$  diffraction to  $\pi^-\pi^-\pi^+$  explicitly modeled by COMPASS  $\pi^-\pi^-\pi^+$  analysis
  - ▶ Incoherent effective background component parameterizing other background processes

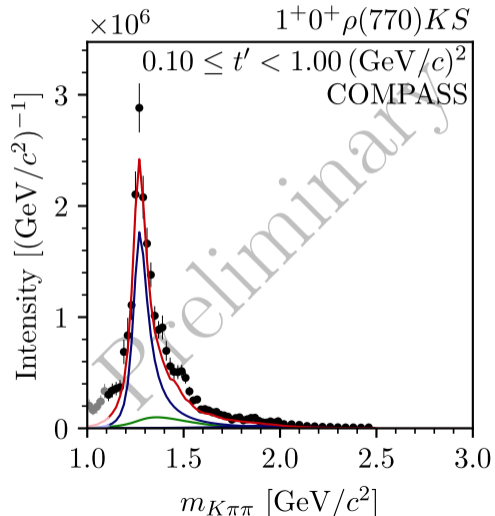


- ▶ Partial-wave amplitudes in  $(m_{K\pi\pi}, t')$  bins
  - ▶ Inferred wave set from data using regularization-based model-selection techniques
  - ▶ Bootstrap resampling to improve uncertainty estimates
  - ▶ Detailed Monte Carlo input-output studies
- ▶ Model  $m_{K\pi\pi}$  dependence of **partial-wave amplitudes**
- ▶ Breit-Wigner amplitudes for  $K^-\pi^-\pi^+$  **resonance components**
- ▶ **Coherent non-resonant component** parameterizing other  $K^-\pi^-\pi^+$  production mechanisms
- ▶ Developed scheme to handle incoherent backgrounds
  - ▶ Incoherent background from  $\pi^-\pi^-\pi^+$  diffraction to  $\pi^-\pi^-\pi^+$  explicitly modeled by COMPASS  $\pi^-\pi^-\pi^+$  analysis
  - ▶ Incoherent effective background component parameterizing other background processes

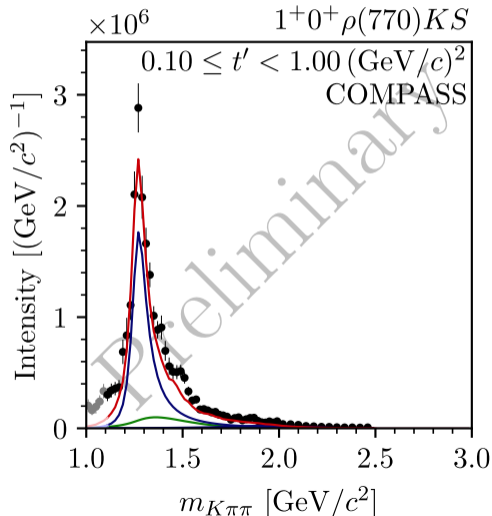




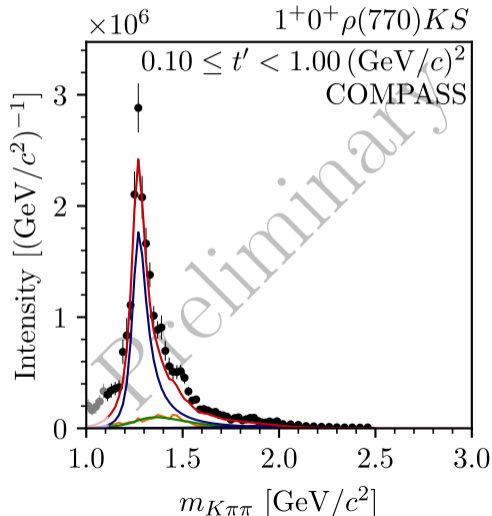
- ▶ Partial-wave amplitudes in  $(m_{K\pi\pi}, t')$  bins
  - ▶ Inferred wave set from data using regularization-based model-selection techniques
  - ▶ Bootstrap resampling to improve uncertainty estimates
  - ▶ Detailed Monte Carlo input-output studies
- ▶ Model  $m_{K\pi\pi}$  dependence of **partial-wave amplitudes**
- ▶ Breit-Wigner amplitudes for  $K^-\pi^-\pi^+$  **resonance components**
- ▶ **Coherent non-resonant component** parameterizing other  $K^-\pi^-\pi^+$  production mechanisms
- ▶ Developed scheme to handle incoherent backgrounds
  - ▶ Incoherent background from  $\pi^-\pi^-\pi^+$  diffraction to  $\pi^-\pi^-\pi^+$  explicitly modeled by COMPASS  $\pi^-\pi^-\pi^+$  analysis
  - ▶ Incoherent effective background component parameterizing other background processes



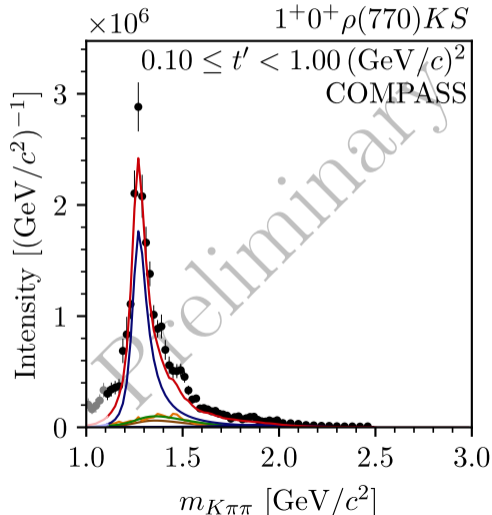
- ▶ Partial-wave amplitudes in  $(m_{K\pi\pi}, t')$  bins
  - ▶ Inferred wave set from data using regularization-based model-selection techniques
  - ▶ Bootstrap resampling to improve uncertainty estimates
  - ▶ Detailed Monte Carlo input-output studies
- ▶ Model  $m_{K\pi\pi}$  dependence of **partial-wave amplitudes**
- ▶ Breit-Wigner amplitudes for  $K^-\pi^-\pi^+$  **resonance components**
- ▶ **Coherent non-resonant component** parameterizing other  $K^-\pi^-\pi^+$  production mechanisms
- ▶ Developed scheme to handle incoherent backgrounds
  - ▶ **Incoherent background** from  $\pi^-$  diffraction to  $\pi^-\pi^-\pi^+$  explicitly modeled by COMPASS  $\pi^-\pi^-\pi^+$  analysis
  - ▶ **Incoherent effective background component** parameterizing other background processes



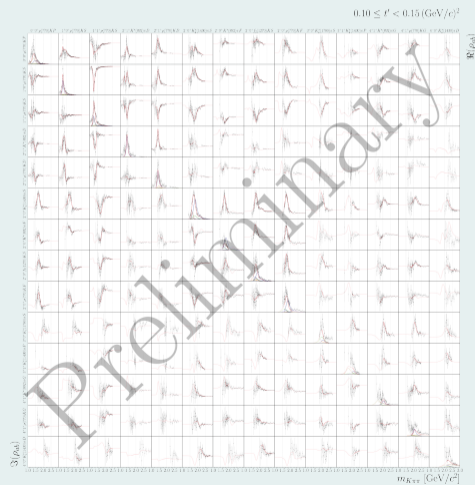
- ▶ Partial-wave amplitudes in  $(m_{K\pi\pi}, t')$  bins
  - ▶ Inferred wave set from data using regularization-based model-selection techniques
  - ▶ Bootstrap resampling to improve uncertainty estimates
  - ▶ Detailed Monte Carlo input-output studies
- ▶ Model  $m_{K\pi\pi}$  dependence of **partial-wave amplitudes**
- ▶ Breit-Wigner amplitudes for  $K^-\pi^-\pi^+$  **resonance components**
- ▶ **Coherent non-resonant component** parameterizing other  $K^-\pi^-\pi^+$  production mechanisms
- ▶ Developed scheme to handle incoherent backgrounds
  - ▶ **Incoherent background** from  $\pi^-$  diffraction to  $\pi^-\pi^-\pi^+$  explicitly modeled by COMPASS  $\pi^-\pi^-\pi^+$  analysis
  - ▶ **Incoherent effective background component** parameterizing other background processes

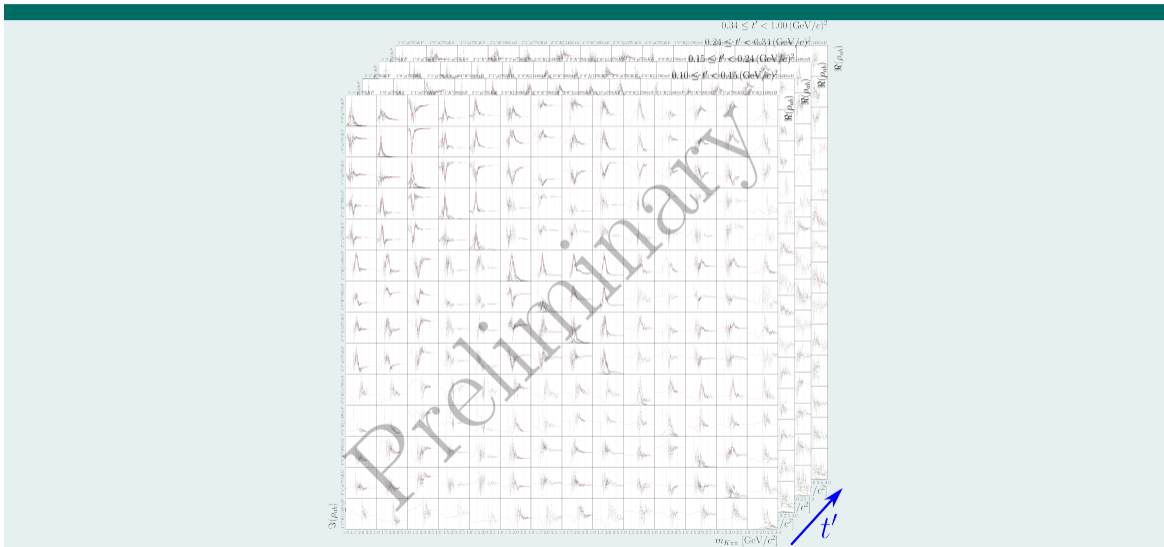


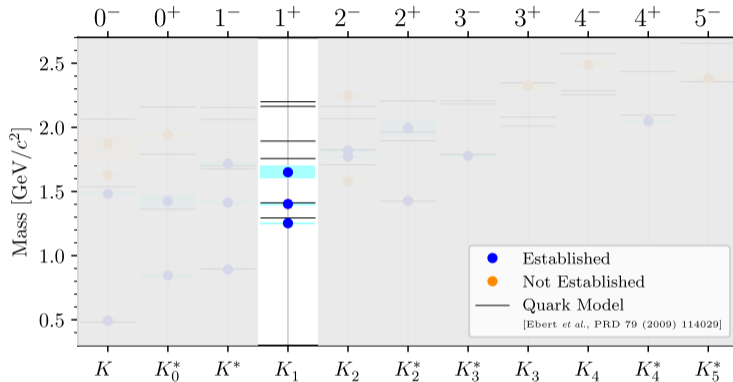
- ▶ Partial-wave amplitudes in  $(m_{K\pi\pi}, t')$  bins
  - ▶ Inferred wave set from data using regularization-based model-selection techniques
  - ▶ Bootstrap resampling to improve uncertainty estimates
  - ▶ Detailed Monte Carlo input-output studies
- ▶ Model  $m_{K\pi\pi}$  dependence of **partial-wave amplitudes**
- ▶ Breit-Wigner amplitudes for  $K^-\pi^-\pi^+$  **resonance components**
- ▶ **Coherent non-resonant component** parameterizing other  $K^-\pi^-\pi^+$  production mechanisms
- ▶ Developed scheme to handle incoherent backgrounds
  - ▶ **Incoherent background** from  $\pi^-$  diffraction to  $\pi^-\pi^-\pi^+$  explicitly modeled by COMPASS  $\pi^-\pi^-\pi^+$  analysis
  - ▶ **Incoherent effective background component** parameterizing other background processes



- ▶ Simultaneously included 14 partial waves in resonance-model fit
- ▶ Modeled by 13 strange-meson resonance components
- ▶ Using measured intensities and interference terms (relative phases)







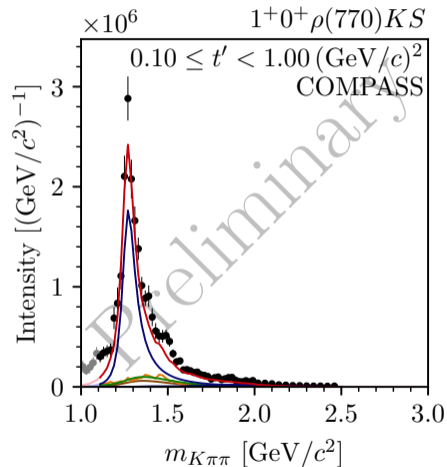
PDG

(2022)

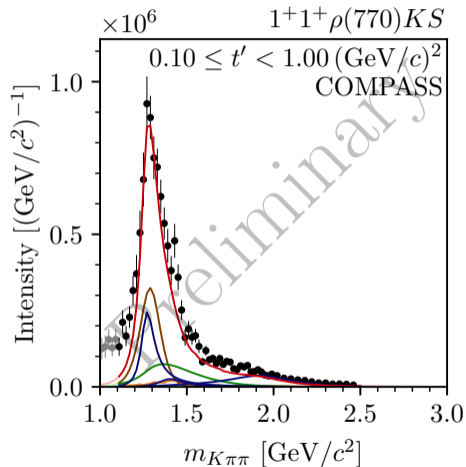
- ▶ Two near-by states  $K_1(1270)$  and  $K_1(1400)$
- ▶ Excited  $K_1(1650)$

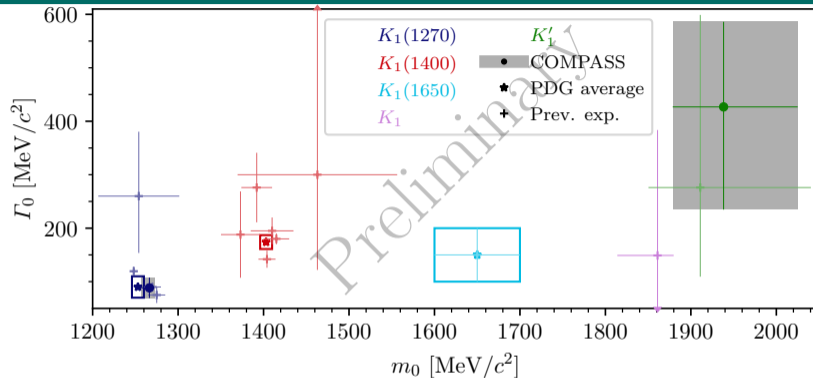


- ▶ Study  $K_1$  states in  $\rho(770)K$  decay with  $M^\epsilon = 0^+$
- ▶ Dominated by  $K_1(1270)$
- ▶ Similar spectrum also in  $M^\epsilon = 1^+$  wave
- ▶ Indications for excited  $K_1'$  mainly in  $M^\epsilon = 1^+$  wave



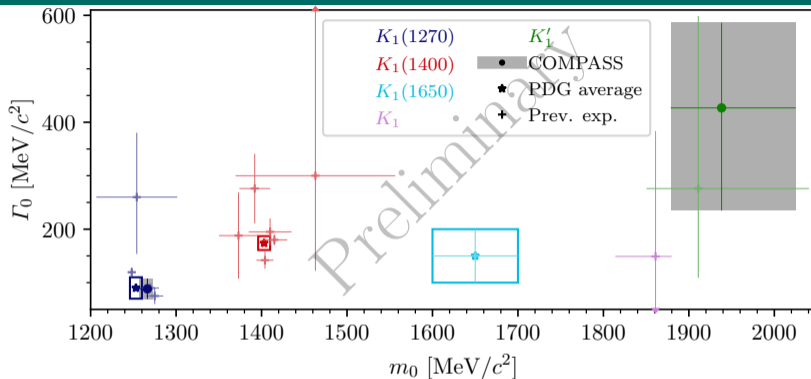
- ▶ Study  $K_1$  states in  $\rho(770)K$  decay with  $M^\epsilon = 0^+$
- ▶ Dominated by  $K_1(1270)$
- ▶ Similar spectrum also in  $M^\epsilon = 1^+$  wave
- ▶ Indications for excited  $K_1'$  mainly in  $M^\epsilon = 1^+$  wave





## $K_1(1270)$

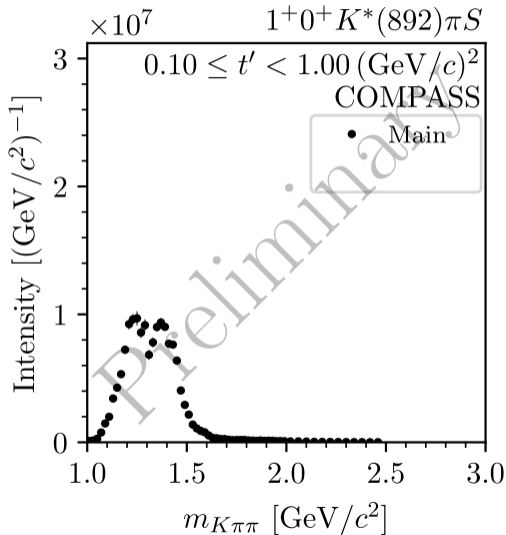
- ▶ Resonance parameters in agreement with previous measurements
- ▶ Our estimates from only  $\rho(770)K$  waves yields slightly larger mass and smaller width compared to PDG average



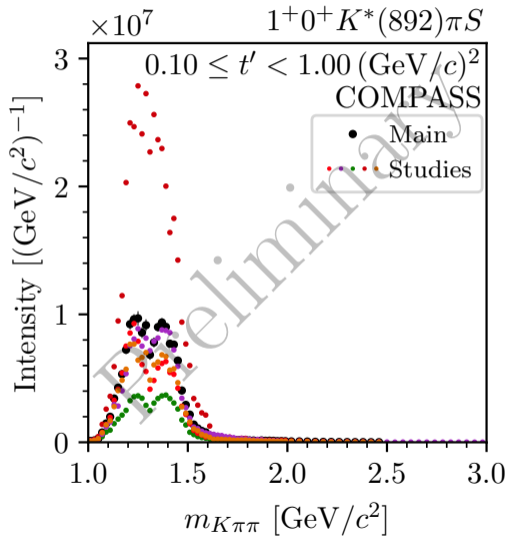
## $K_1'$

- ▶ Larger mass and width compared to PDG average of  $K_1(1650)$
- ▶ PDG average from single measurement at CERN Omega spectrometer extracted from fit to only intensity spectrum [NPB 276 (1986) 667]
- ▶ Our estimates consistent with recent measurement in  $B^+ \rightarrow J/\psi \phi K^+$  at LHCb

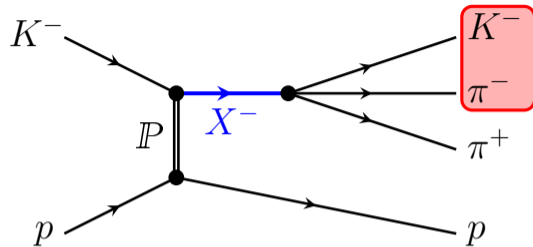
- ▶ Want to study  $K_1$  states also in  $K^*(892)\pi$  decays
- ▶ Very sensitive to systematic effects
- ▶ Event selection requires to identify one of the two negative particles
  - Limited acceptance due to limited kinematic range of final-state PID
  - Reduced differentiability of certain partial waves
  - Causes analysis artifacts in affected waves
- ▶ Only a sub-set of partial waves affected



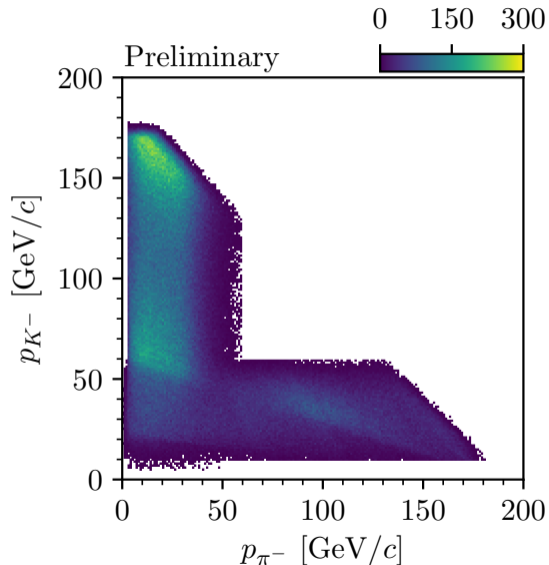
- ▶ Want to study  $K_1$  states also in  $K^*(892)\pi$  decays
- ▶ Very sensitive to systematic effects
- ▶ Event selection requires to identify one of the two negative particles
  - Limited acceptance due to limited kinematic range of final-state PID
  - Reduced differentiability of certain partial waves
  - Causes analysis artifacts in affected waves
- ▶ Only a sub-set of partial waves affected



- ▶ Want to study  $K_1$  states also in  $K^*(892)\pi$  decays
- ▶ Very sensitive to systematic effects
- ▶ Event selection requires to identify one of the two negative particles
  - Limited acceptance due to limited kinematic range of final-state PID
  - Reduced differentiability of certain partial waves
  - Causes analysis artifacts in affected waves
- ▶ Only a sub-set of partial waves affected

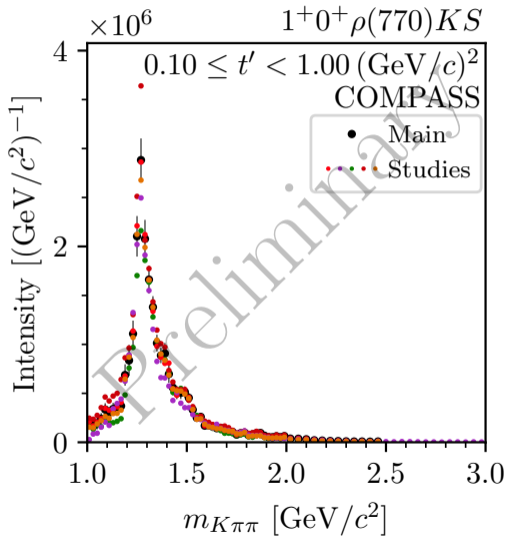


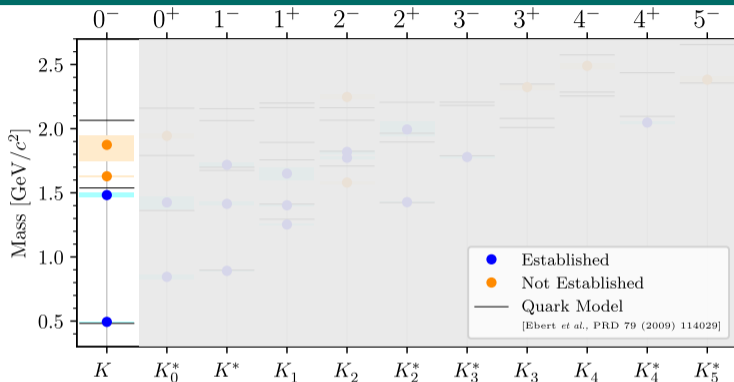
- ▶ Want to study  $K_1$  states also in  $K^*(892)\pi$  decays
- ▶ Very sensitive to systematic effects
- ▶ Event selection requires to identify one of the two negative particles
  - ➡ Limited acceptance due to limited kinematic range of final-state PID
  - ➡ Reduced differentiability of certain partial waves
  - ➡ Causes analysis artifacts in affected waves
- ▶ Only a sub-set of partial waves affected



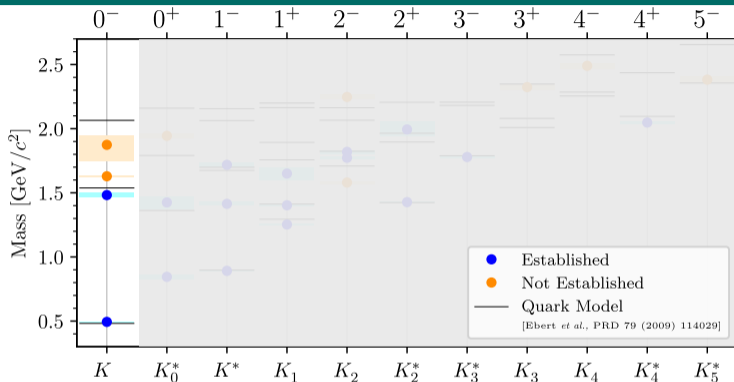


- ▶ Want to study  $K_1$  states also in  $K^*(892)\pi$  decays
- ▶ Very sensitive to systematic effects
- ▶ Event selection requires to identify one of the two negative particles
  - ➡ Limited acceptance due to limited kinematic range of final-state PID
  - ➡ Reduced differentiability of certain partial waves
  - ➡ Causes analysis artifacts in affected waves
- ▶ Only a sub-set of partial waves affected





- ▶  $K(1460)$  and  $K(1830)$
- ▶  $K(1630)$ 
  - ▶ Unexpectedly small width of only  $16 \text{ MeV}/c^2$
  - ▶  $J^P$  of  $K(1630)$  unclear



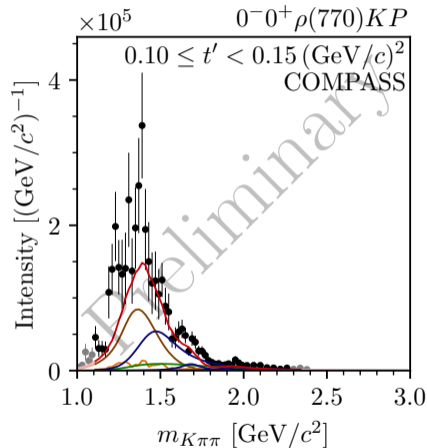
## PDG

(2022)

- ▶  $K(1460)$  and  $K(1830)$
- ▶  $K(1630)$ 
  - ▶ Unexpectedly small width of only  $16 \text{ MeV}/c^2$
  - ▶  $J^P$  of  $K(1630)$  unclear

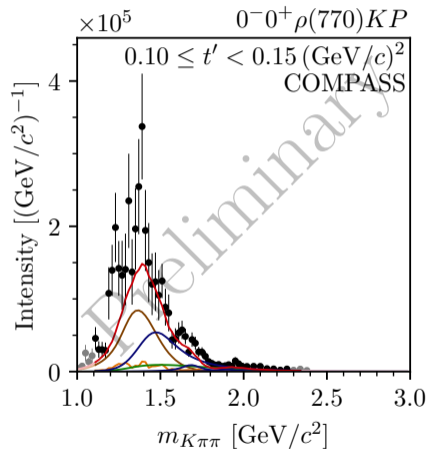
## COMPASS $K^-\pi^-\pi^+$ data

- ▶ Peak at about  $1.4 \text{ GeV}/c^2$ 
  - ▶ Established  $K(1460)$
  - ▶ But,  $m_{K\pi\pi} \lesssim 1.5 \text{ GeV}/c^2$  region weakly affected by known analysis artifacts
- ▶ Second peak at about  $1.7 \text{ GeV}/c^2$ 
  - ▶  $K(1630)$  signal with  $8.3\sigma$  statistical significance
  - ▶ Accompanied by rising phase
- ▶ Weak signal at about  $2.0 \text{ GeV}/c^2$ 
  - ▶  $K(1830)$  signal with  $5.4\sigma$  statistical significance



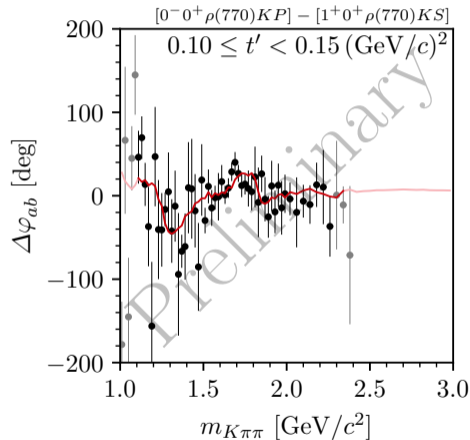
## COMPASS $K^-\pi^-\pi^+$ data

- ▶ Peak at about  $1.4 \text{ GeV}/c^2$ 
  - ▶ Established  $K(1460)$
  - ▶ But,  $m_{K\pi\pi} \lesssim 1.5 \text{ GeV}/c^2$  region weakly affected by known analysis artifacts
- ▶ Second peak at about  $1.7 \text{ GeV}/c^2$ 
  - ▶  $K(1630)$  signal with  $8.3\sigma$  statistical significance
  - ▶ Accompanied by rising phase
- ▶ Weak signal at about  $2.0 \text{ GeV}/c^2$ 
  - ▶  $K(1830)$  signal with  $5.4\sigma$  statistical significance



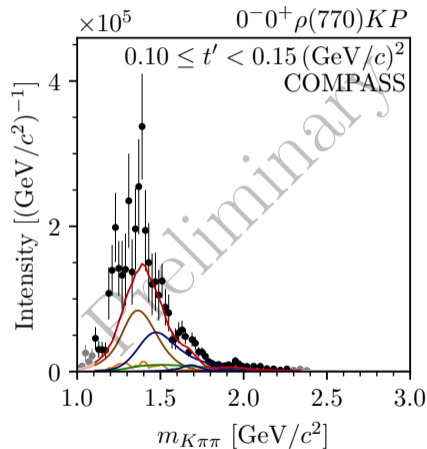
## COMPASS $K^- \pi^- \pi^+$ data

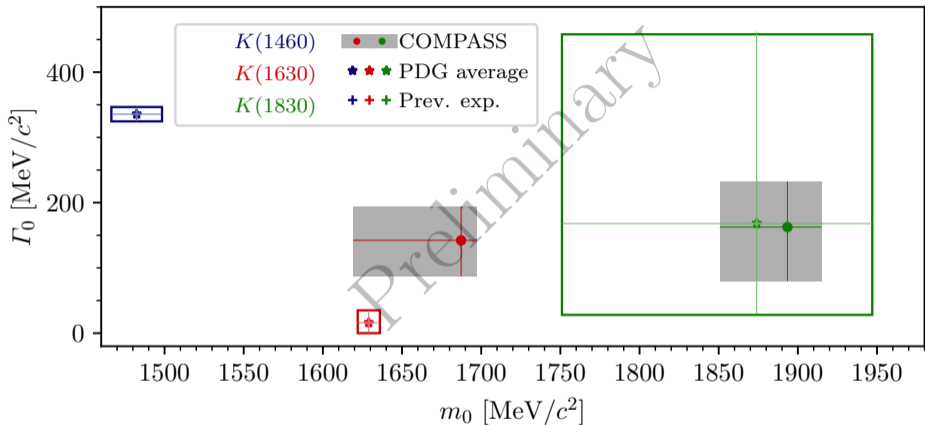
- ▶ Peak at about  $1.4 \text{ GeV}/c^2$ 
  - ▶ Established  $K(1460)$
  - ▶ But,  $m_{K\pi\pi} \lesssim 1.5 \text{ GeV}/c^2$  region weakly affected by known analysis artifacts
- ▶ Second peak at about  $1.7 \text{ GeV}/c^2$ 
  - ▶  $K(1630)$  signal with  $8.3\sigma$  statistical significance
  - ▶ Accompanied by rising phase
- ▶ Weak signal at about  $2.0 \text{ GeV}/c^2$ 
  - ▶  $K(1830)$  signal with  $5.4\sigma$  statistical significance



## COMPASS $K^-\pi^-\pi^+$ data

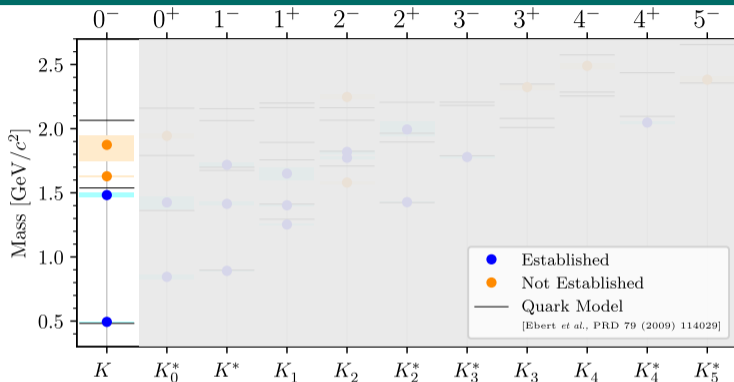
- ▶ Peak at about  $1.4 \text{ GeV}/c^2$ 
  - ▶ Established  $K(1460)$
  - ▶ But,  $m_{K\pi\pi} \lesssim 1.5 \text{ GeV}/c^2$  region weakly affected by known analysis artifacts
- ▶ Second peak at about  $1.7 \text{ GeV}/c^2$ 
  - ▶  $K(1630)$  signal with  $8.3\sigma$  statistical significance
  - ▶ Accompanied by rising phase
- ▶ Weak signal at about  $2.0 \text{ GeV}/c^2$ 
  - ▶  $K(1830)$  signal with  $5.4\sigma$  statistical significance



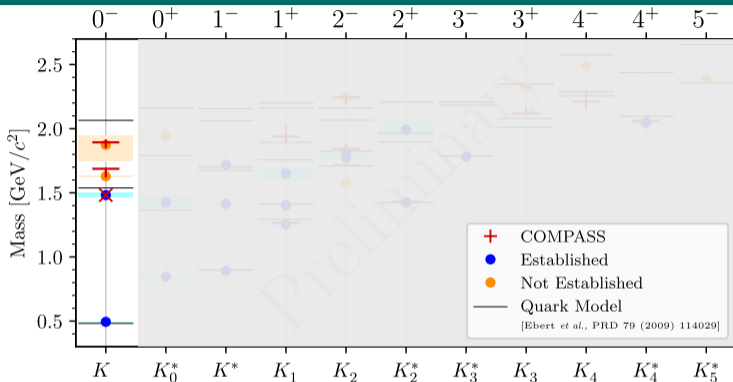


- ▶  $K(1830)$  parameters in good agreement with LChb measurement [PRL 118 (2017) 022003]
- ▶ Expected  $K(1630)$  width of about 140 MeV/c<sup>2</sup>

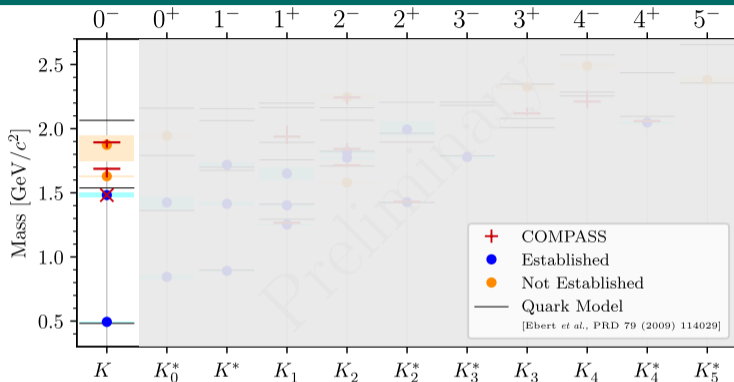




- ▶ Indications for 3 excited  $K$  from a single analysis
- ▶ Quark-model predicts only two excited states: potentially  $K(1460)$  and  $K(1830)$ 
  - $K(1630)$  supernumerary signal
  - Candidate for **exotic non- $q\bar{q}$  state**; other explanations possible ( $K^*(892)$   $\omega$  threshold nearby)



- ▶ Indications for 3 excited  $K$  from a single analysis
- ▶ Quark-model predicts only two excited states: potentially  $K(1460)$  and  $K(1830)$ 
  - $K(1630)$  supernumerary signal
  - Candidate for exotic non- $q\bar{q}$  state; other explanations possible ( $K^*(892)$   $\omega$  threshold nearby)



- ▶ Indications for 3 excited  $K$  from a single analysis
- ▶ Quark-model predicts only two excited states: potentially  $K(1460)$  and  $K(1830)$ 
  - ➡  $K(1630)$  supernumerary signal
  - ➡ Candidate for **exotic non- $q\bar{q}$  state**; other explanations possible ( $K^*(892)$   $\omega$  threshold nearby)

## Main limiting factors

- ▶ Final-state **particle identification**
  - ↳ Analysis artifacts in some partial waves
  - ↳ Background from reactions like  $\pi^- + p \rightarrow \pi^- \pi^- \pi^+ + p$
- ▶ **Size of the data sample**
  - ▶ **Low kaon fraction in the beam** ( $\approx 2\%$ )
  - ▶ Sample for strange-mesons about **150-times smaller** than sample for non-strange mesons
    - ▶ 720 k  $K^- + p \rightarrow K^- \pi^- \pi^+ + p$  events
    - ▶ 115 M  $\pi^- + p \rightarrow \pi^- \pi^- \pi^+ + p$  events

- ▶ High-precision measurement of various final states:  $\pi^-\pi^-\pi^+$ ,  $\eta^{(\prime)}\pi^-$ ,  $\omega\pi^0\pi^-$ ,  $K_S^0K^-$ , ...
- ▶ Most comprehensive analysis of  $\pi^-\pi^-\pi^+$ :  
88 partial waves; fine  $t'$  binning; 11 isovector resonances; novel methods
- ▶ Large variety of results: [\[PLB 740 \(2015\) 303\]](#), [\[PRL 115 \(2015\) 82001\]](#), [\[PRD 95 \(2017\) 032004\]](#), [\[PRD 98 \(2018\) 092003\]](#), [\[PRD 105 \(2022\) 012005\]](#)

## Spin-exotic $\pi_1(1600)$

- ▶ Certain  $J^{PC}$  quantum numbers not possible for pure quark-model state, e.g.  $1^{-+}$  ( $\pi_1$ )
- ▶ COMPASS studied partial waves with  $J^{PC} = 1^{-+}$ 
  - ▶ Consistent picture of spin-exotic  $\pi_1(1600)$  emerging
- ▶ Fitting unitary and analytic models to COMPASS data on  $\eta^{(\prime)}\pi^-$  final states yields no evidence for  $\pi_1(1400)$

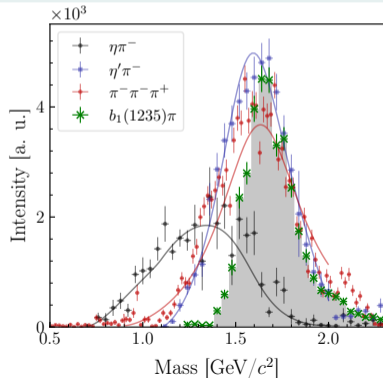
[\[PRL 112 \(2019\) 042002\]](#), [\[EPJ C 81 \(2021\) 1056\]](#)

- ▶ High-precision measurement of various final states:  $\pi^- \pi^- \pi^+$ ,  $\eta^{(\prime)} \pi^-$ ,  $\omega \pi^0 \pi^-$ ,  $K_S^0 K^-$ , ...
- ▶ Most comprehensive analysis of  $\pi^- \pi^- \pi^+$ :  
88 partial waves; fine  $t'$  binning; 11 isovector resonances; novel methods
- ▶ Large variety of results: [\[PLB 740 \(2015\) 303\]](#), [\[PRL 115 \(2015\) 82001\]](#), [\[PRD 95 \(2017\) 032004\]](#), [\[PRD 98 \(2018\) 092003\]](#), [\[PRD 105 \(2022\) 012005\]](#)

## Spin-exotic $\pi_1(1600)$

- ▶ Certain  $J^{PC}$  quantum numbers not possible for pure quark-model state, e.g.  $1^{-+}$  ( $\pi_1$ )
- ▶ COMPASS studied partial waves with  $J^{PC} = 1^{-+}$ 
  - ▶ Consistent picture of spin-exotic  $\pi_1(1600)$  emerging
- ▶ Fitting unitary and analytic models to COMPASS data on  $\eta^{(\prime)} \pi^-$  final states yields no evidence for  $\pi_1(1400)$

[\[PRL 112 \(2019\) 042002\]](#), [\[EPJ C 81 \(2021\) 1056\]](#)



# AMBER

## Apparatus for Meson and Baryon Experimental Research

Phase I: After long shutdown 2 of LHC  
[[CERN-SPSC-2019-022](#)]

- ▶ Proton charge-radius measurement
- ▶ Drell-Yan and charmonium production
- ▶  $p$ -induced  $\bar{p}$  production cross section

Phase II: After long shutdown 3 of LHC  
[[arXiv:1808.00848](#)]

- ▶ Physics with kaon beams
  - ▶ **Strange-meson spectroscopy**  
goal:  $10\times$  larger data sample
  - ▶ Kaon-induced charmonium production
  - ▶ ...
- ▶ ...



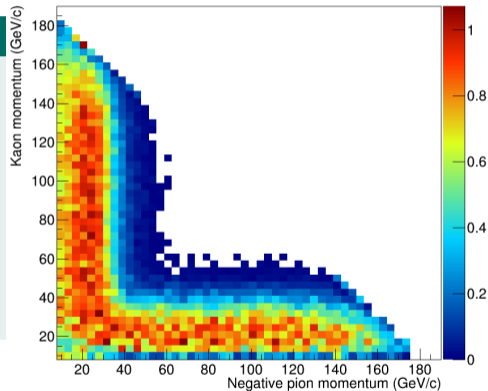
- ▶ Upgrade of **final-state particle identification**
    - ▶ **Cover wide momentum range**
    - ▶ **Large** and uniform acceptance
  - ▶ Dedicated trigger for kaon-induced events
  - ▶ Efficient **beam-particle identification** for high-purity sample
  - ▶ High-resolution track reconstruction
  - ▶ Efficient photon detection for access to final states with neutral particles
- 
- ▶ Eliminate artifacts caused by limited final-state particle identification
  - ▶ Increase size of the data sample by increasing acceptance



$$p_{\text{beam}} = 190 \text{ GeV}/c$$

## Various options under study

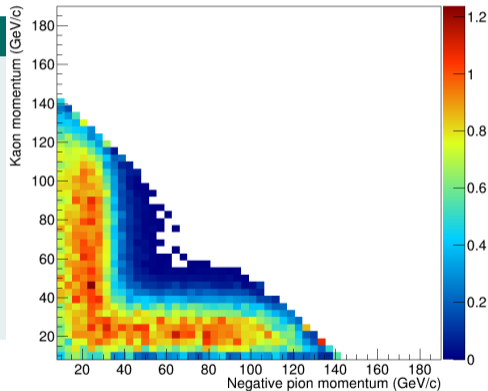
- ▶ New detector for high-momentum particle identification
- ▶ Adjust the momentum range of the existing COMPASS RICH
- ▶ Reduce the beam momentum to better fit the current momentum coverage
  - ▶ However, lower fraction of kaons in the beam at lower momenta



$$p_{\text{beam}} = 150 \text{ GeV}/c$$

## Various options under study

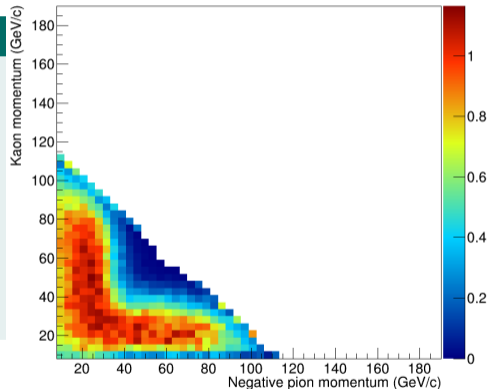
- ▶ New detector for high-momentum particle identification
- ▶ Adjust the momentum range of the existing COMPASS RICH
- ▶ Reduce the beam momentum to better fit the current momentum coverage
  - ▶ However, lower fraction of kaons in the beam at lower momenta



$$p_{\text{beam}} = 120 \text{ GeV}/c$$

## Various options under study

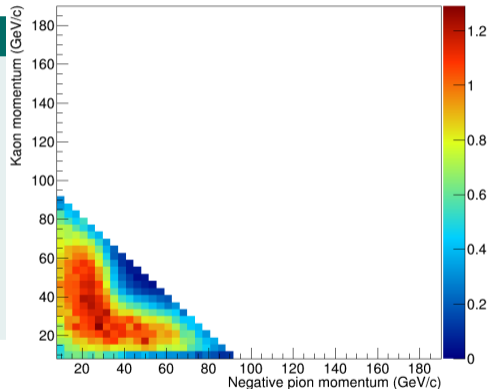
- ▶ New detector for high-momentum particle identification
- ▶ Adjust the momentum range of the existing COMPASS RICH
- ▶ Reduce the beam momentum to better fit the current momentum coverage
  - ▶ However, lower fraction of kaons in the beam at lower momenta

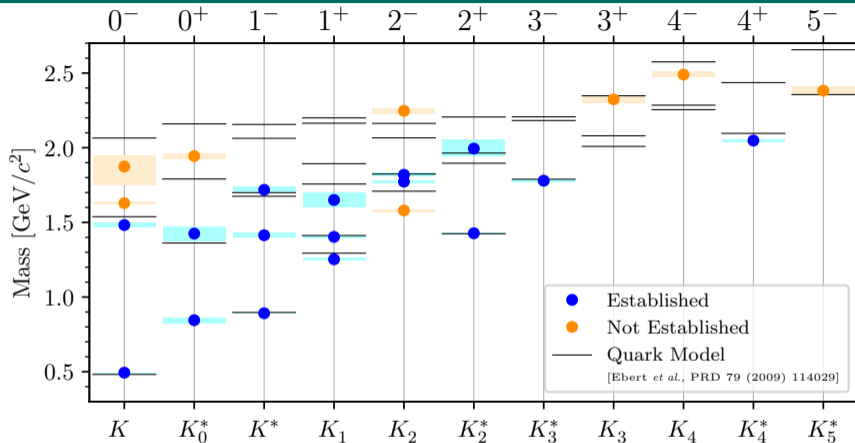


$$p_{\text{beam}} = 100 \text{ GeV}/c$$

## Various options under study

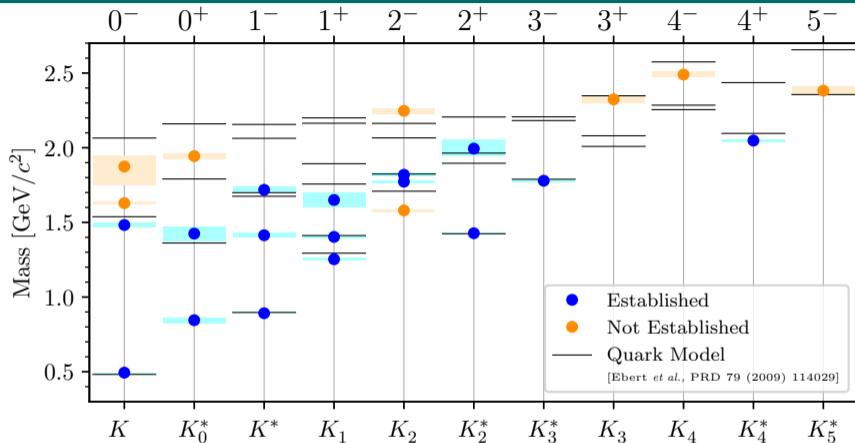
- ▶ New detector for high-momentum particle identification
- ▶ Adjust the momentum range of the existing COMPASS RICH
- ▶ Reduce the beam momentum to better fit the current momentum coverage
  - ▶ However, lower fraction of kaons in the beam at lower momenta





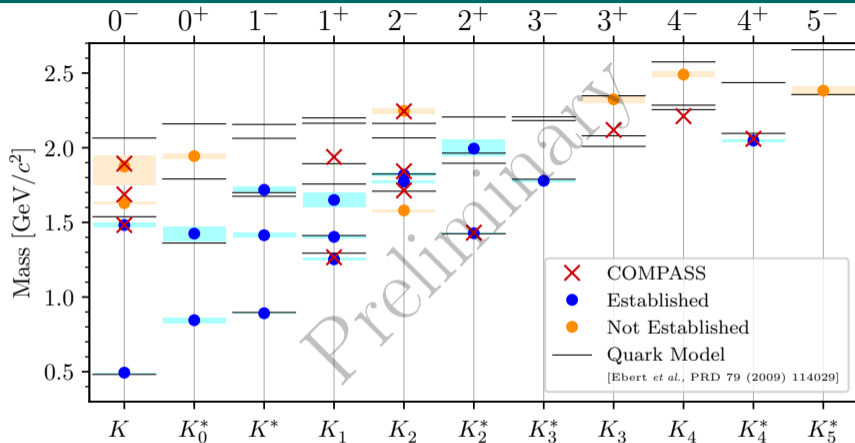
## The Strange-Meson Spectrum

- ▶ Many strange mesons require further confirmation
- ▶ Search for strange partners of exotic non-strange light mesons



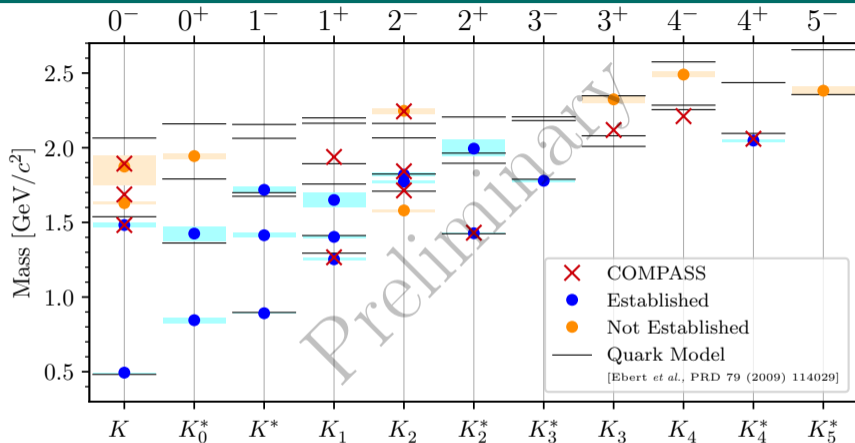
## COMPASS

- ▶ World's largest data sample on  $K^- \pi^- \pi^+$   $\Rightarrow$  Most detailed and comprehensive analysis
- ▶ Candidate for exotic strange-meson signal with  $J^P = 0^-$



## COMPASS

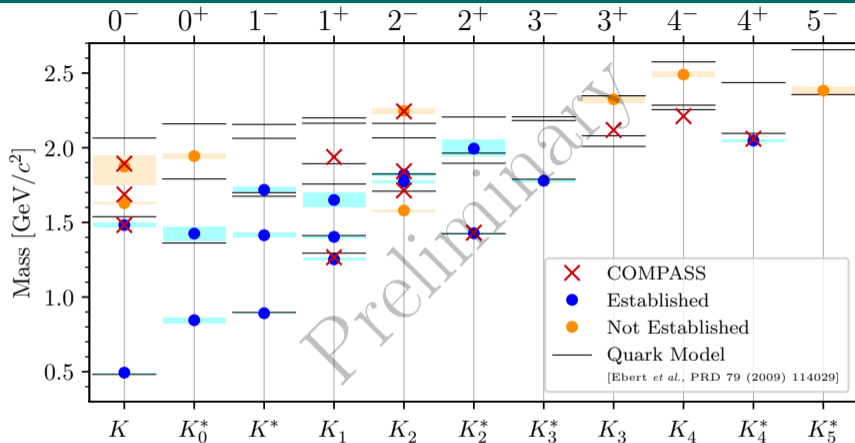
- ▶ World's largest data sample on  $K^- \pi^- \pi^+$   $\Rightarrow$  Most detailed and comprehensive analysis
- ▶ Candidate for exotic strange-meson signal with  $J^P = 0^-$



## AMBER: Proposal for High-Precision Strange-Meson Spectroscopy

- ▶ Goal: Collect  $10 - 20 \times 10^6$   $K^- \pi^- \pi^+$  events using high-energy kaon beam
- ▶ AMBER is open for interested collaborators to join





## COMPASS

- ▶ World's largest data sample on  $K^- \pi^- \pi^+$   $\Rightarrow$  Most detailed and comprehensive analysis
- ▶ Candidate for exotic strange-meson signal with  $J^P = 0^-$

# Backup

## 10 Partial-Wave Decomposition

- Treating the  $\pi^-\pi^-\pi^+$  and Other Backgrounds

## 11 Resonance-Model Fit

- Modeling the  $K^-\pi^-\pi^+$  Signal
- Modeling the  $\pi^-\pi^-\pi^+$  Background
- Modeling the Effective Background
- $\chi^2$  Fit Procedure

## 12 Wave-Set Selection

- Regularization: LASSO
- Regularization: Generalized Pareto
- Regularization: Cauchy
- For the  $K^-\pi^-\pi^+$  Final State

## 13 14-Wave Resonance-Model Fit

- Searching for Exotic Strange Mesons with  $J^P = 0^-$
- Partial Waves with  $J^P = 2^+$
- Partial Waves with  $J^P = 2^-$
- Partial Waves with  $J^P = 4^+$

## 14 Kinematic Distribution of $K^-\pi^-\pi^+$ Events

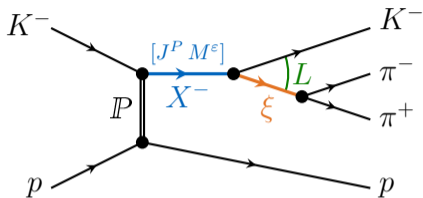
- Subsystem
- $m_{K^-\pi^-}$
- $t'$  Spectrum
- Exclusivity

## 15 Systematic Studies of the Partial-Wave Decomposition

- 14 Waves
- Leakage Waves

## 16 Leakage Effect

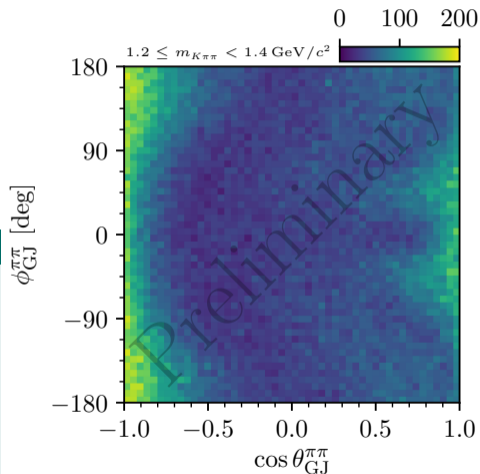
## 17 Incoherent $\pi^-\pi^-\pi^+$ Background



## Partial wave

$$J^P M^E \xi b L$$

- ▶  $J^P M^E$ : Spin, parity, and spin projection of  $X^-$
- ▶  $\xi$ : Isobar
- ▶  $b$ : Bachelor particle. Here: Spectator  $K^-$
- ▶  $L$ : Angular momentum between bachelor and isobar



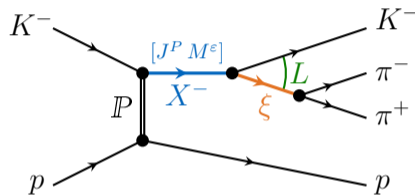
## Model intensity

$$\mathcal{I}(\tau, m_{K\pi\pi}, t') = \sum_z \left| \sum_{a \in \mathbb{W}_z(m_{K\pi\pi}, t')} \mathcal{T}_a^z(m_{K\pi\pi}, t') \Psi_a^z(\tau, m_{K\pi\pi}) \right|^2$$

### ► Model intensity distribution

- in 5D  $K^- \pi^- \pi^+$  phase-space
- for a given  $(m_{K\pi\pi}, t')$  cell
- as **incoherent sum** over **coherent sectors**  $z$ 
  - “Rank” of the partial-wave model = number of coherent sectors

- $\Psi_a^z$  known, assuming the isobar model
- Wave set  $\mathbb{W}_z(m_{K\pi\pi}, t')$  inferred from data using regularization-based model-selection techniques
- $\mathcal{T}_a^z$  extracted in maximum-likelihood fit, independently for each  $(m_{K\pi\pi}, t')$  cell



## Spin-Density Matrix

$$\rho_{ab} = \sum_z \mathcal{T}_a^z [\mathcal{T}_b^z]^*$$

## Model intensity

$$\mathcal{I}(\tau, m_{K\pi\pi}, t') = \sum_z \left| \sum_{a \in \mathbb{W}_z(m_{K\pi\pi}, t')} \mathcal{T}_a^z(m_{K\pi\pi}, t') \Psi_a^z(\tau, m_{K\pi\pi}) \right|^2$$

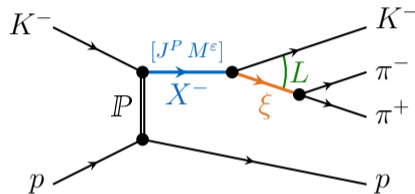
### ► Model intensity distribution

- in 5D  $K^- \pi^- \pi^+$  phase-space
- for a given  $(m_{K\pi\pi}, t')$  cell
- as incoherent sum over coherent sectors  $z$ 
  - “Rank” of the partial-wave model = number of coherent sectors

►  $\Psi_a^z$  known, assuming the isobar model

► Wave set  $\mathbb{W}_z(m_{K\pi\pi}, t')$  inferred from data using regularization-based model-selection techniques

►  $\mathcal{T}_a^z$  extracted in maximum-likelihood fit, independently for each  $(m_{K\pi\pi}, t')$  cell



## Spin-Density Matrix

$$\rho_{ab} = \sum_z \mathcal{T}_a^z [\mathcal{T}_b^z]^*$$

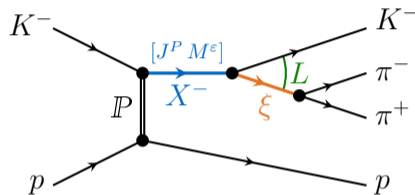
## Model intensity

$$\mathcal{I}(\tau, m_{K\pi\pi}, t') = \sum_z \left| \sum_{a \in \mathbb{W}_z(m_{K\pi\pi}, t')} \mathcal{T}_a^z(m_{K\pi\pi}, t') \Psi_a^z(\tau, m_{K\pi\pi}) \right|^2$$

### ► Model intensity distribution

- in 5D  $K^- \pi^- \pi^+$  phase-space
- for a given  $(m_{K\pi\pi}, t')$  cell
- as incoherent sum over coherent sectors  $z$ 
  - “Rank” of the partial-wave model = number of coherent sectors

- $\Psi_a^z$  known, assuming the isobar model
- Wave set  $\mathbb{W}_z(m_{K\pi\pi}, t')$  inferred from data using regularization-based model-selection techniques
- $\mathcal{T}_a^z$  extracted in maximum-likelihood fit, independently for each  $(m_{K\pi\pi}, t')$  cell



## Spin-Density Matrix

$$\rho_{ab} = \sum_z \mathcal{T}_a^z [\mathcal{T}_b^z]^*$$

### Approach

- ▶ Effectively take into account in partial-wave decomposition by **incoherently adding additional coherent sectors  $z$**   
(Model background by  $K^-\pi^-\pi^+$  partial waves)
  - ➔ Increasing the rank of the spin-density matrix  $\rho_{ab}$
  - ➔ Signal not separated from background in partial-wave decomposition
  - ➔ Partial-wave amplitudes include background
- ▶ Model signal and background contributions in resonance-model fit using more constrained signal model
  - ➔ Separate signal from background

$$\mathcal{I}(\tau, m_{K\pi\pi}, t') = \sum_z \left| \sum_{a \in \mathbb{W}_z(m_{K\pi\pi}, t')} \mathcal{T}_a^z(m_{K\pi\pi}, t') \Psi_a^z(\tau, m_{K\pi\pi}) \right|^2$$

$$\rho_{ab} = \sum_z \mathcal{T}_a^z [\mathcal{T}_b^z]^*$$



### True physics intensity distribution

$$\mathcal{I}(\tau) = \left| \sum_a^{\text{waves}} \mathcal{T}_a \Psi_a(\tau) \right|^2$$

### Experimentally measured intensity distribution

$$\mathcal{I}_{\text{measured}}(\tau) = \eta(\tau) \mathcal{I}(\tau)$$

- ▶ Take into account different processes  $\mathfrak{p}$ 
  - ▶ Different model intensities  $\mathcal{I}^{\mathfrak{p}}$
  - ▶ Different experimental acceptance  $\eta^{\mathfrak{p}}$
  - ▶ Formulated in terms of different phase-space variables  $\tau^{\mathfrak{p}}$ 
    - ▶ Jacobian terms  $J(\tau^{K\pi\pi} \rightarrow \tau^{\mathfrak{p}})$  from variable transformation

True physics intensity distribution for process  $p$

$$\mathcal{I}^p(\tau) = \left| \sum_a^{\text{waves}} \mathcal{T}_a^p \Psi_a^p(\tau) \right|^2$$

Experimentally measured intensity distribution

$$\mathcal{I}_{\text{measured}}(\tau) = \sum_p \eta^p(\tau) \mathcal{I}^p(\tau)$$

- ▶ Take into account different processes  $p$ 
  - ▶ Different model intensities  $\mathcal{I}^p$
  - ▶ Different experimental acceptance  $\eta^p$
  - ▶ Formulated in terms of different phase-space variables  $\tau^p$ 
    - ▶ Jacobian terms  $J(\tau^{K\pi\pi} \rightarrow \tau^p)$  from variable transformation

### True physics intensity distribution for process $\mathbf{p}$

$$\mathcal{I}^{\mathbf{p}}(\tau^{\mathbf{p}}) = \left| \sum_a^{\text{waves}} \mathcal{T}_a^{\mathbf{p}} \Psi_a^{\mathbf{p}}(\tau^{\mathbf{p}}) \right|^2$$

### Experimentally measured intensity distribution

$$\mathcal{I}_{\text{measured}}(\tau^{K\pi\pi}) = \sum_{\mathbf{p}} \eta^{\mathbf{p}}(\tau^{\mathbf{p}}) \mathcal{I}^{\mathbf{p}}(\tau^{\mathbf{p}}) J(\tau^{K\pi\pi} \rightarrow \tau^{\mathbf{p}})$$

- ▶ Take into account different processes  $\mathbf{p}$ 
  - ▶ Different model intensities  $\mathcal{I}^{\mathbf{p}}(\tau^{\mathbf{p}})$
  - ▶ Different experimental acceptance  $\eta^{\mathbf{p}}(\tau^{\mathbf{p}})$
  - ▶ Formulated in terms of different phase-space variables  $\tau^{\mathbf{p}}$ 
    - ▶ Jacobian terms  $J(\tau^{K\pi\pi} \rightarrow \tau^{\mathbf{p}})$  from variable transformation

True physics intensity distribution for process  $p$

$$\mathcal{I}^p(\tau^p) = \left| \sum_a^{\text{waves}} \mathcal{T}_a^p \Psi_a^p(\tau^p) \right|^2$$

- ▶  $\mathcal{I}^{\pi\pi\pi}$  known by COMPASS analysis
- ▶  $\eta^{\pi\pi\pi}$  from detector simulation

Experimentally measured intensity distribution

$$\mathcal{I}_{\text{measured}}(\tau^{K\pi\pi}) = \sum_p \eta^p(\tau^p) \mathcal{I}^p(\tau^p) J(\tau^{K\pi\pi} \rightarrow \tau^p)$$

- ▶  $\eta^{\pi\pi\pi}$  computationally expensive
- ▶ Different  $m_{3\pi}$  bins enter one  $m_{K\pi\pi}$  bin
- ▶ Other background channels:  $K^-K^-K^+$ , ...
  - ▶  $\mathcal{I}^p$  unknown
  - ▶ Unknown background channels

True physics intensity distribution for process  $p$

$$\mathcal{I}^p(\tau^p) = \left| \sum_a^{\text{waves}} \mathcal{T}_a^p \Psi_a^p(\tau^p) \right|^2$$

- ▶  $\mathcal{I}^{\pi\pi\pi}$  known by COMPASS analysis
- ▶  $\eta^{\pi\pi\pi}$  from detector simulation

Experimentally measured intensity distribution

$$\mathcal{I}_{\text{measured}}(\tau^{K\pi\pi}) = \sum_p \eta^p(\tau^p) \mathcal{I}^p(\tau^p) J(\tau^{K\pi\pi} \rightarrow \tau^p)$$

- ▶  $\eta^{\pi\pi\pi}$  computationally expensive
- ▶ Different  $m_{3\pi}$  bins enter one  $m_{K\pi\pi}$  bin
- ▶ Other background channels:  $K^-K^-\pi^+$ , ...
  - ▶  $\mathcal{I}^p$  unknown
  - ▶ Unknown background channels

True physics intensity distribution for process  $p$

$$\mathcal{I}^p(\tau^p) = \left| \sum_a^{\text{waves}} \mathcal{T}_a^p \Psi_a^p(\tau^p) \right|^2$$

- ▶  $\mathcal{I}^{\pi\pi\pi}$  known by COMPASS analysis
- ▶  $\eta^{\pi\pi\pi}$  from detector simulation

Experimentally measured intensity distribution

$$\mathcal{I}_{\text{measured}}(\tau^{K\pi\pi}) = \sum_p \eta^p(\tau^p) \mathcal{I}^p(\tau^p) J(\tau^{K\pi\pi} \rightarrow \tau^p)$$

- ▶  $\eta^{\pi\pi\pi}$  computationally expensive
- ▶ Different  $m_{3\pi}$  bins enter one  $m_{K\pi\pi}$  bin
- ▶ Other background channels:  $K^-K^-K^+$ , ...
  - ▶  $\mathcal{I}^p$  unknown
  - ▶ Unknown background channels

Approximate model for process  $p$  by  $K^-\pi^-\pi^+$  partial waves

$$\eta^p(\tau^p) \left| \sum_a^{\text{waves}} \mathcal{T}_a^p \Psi_a^p(\tau^p) \right|^2 \approx \eta^{K\pi\pi}(\tau^{K\pi\pi}) \left| \sum_a^{\text{waves}} \tilde{\mathcal{T}}_a^p \Psi_a^{K\pi\pi}(\tau^{K\pi\pi}) \right|^2$$

Total true physics intensity distribution

$$\mathcal{I}(\tau^{K\pi\pi}) = \sum_p \left| \sum_a^{\text{waves}} \mathcal{T}_a^p \Psi_a^{K\pi\pi}(\tau^{K\pi\pi}) \right|^2$$

Experimentally measured intensity distribution

$$\mathcal{I}_{\text{measured}}(\tau^{K\pi\pi}) = \eta^{K\pi\pi}(\tau^{K\pi\pi}) \mathcal{I}(\tau^{K\pi\pi})$$

- ▶ How well can  $K^-\pi^-\pi^+$  partial waves approximate the distribution of process  $p$ 
  - ▶ Is the set of  $K^-\pi^-\pi^+$  partial waves sufficient?
    - ➔ Automatic wave-set selection using model-selection techniques

Approximate model for process  $p$  by  $K^-\pi^-\pi^+$  partial waves

$$\eta^p(\tau^p) \left| \sum_a^{\text{waves}} \mathcal{T}_a^p \Psi_a^p(\tau^p) \right|^2 \approx \eta^{K\pi\pi}(\tau^{K\pi\pi}) \left| \sum_a^{\text{waves}} \tilde{\mathcal{T}}_a^p \Psi_a^{K\pi\pi}(\tau^{K\pi\pi}) \right|^2$$

Total true physics intensity distribution

$$\mathcal{I}(\tau^{K\pi\pi}) = \sum_p \left| \sum_a^{\text{waves}} \mathcal{T}_a^p \Psi_a^{K\pi\pi}(\tau^{K\pi\pi}) \right|^2$$

Experimentally measured intensity distribution

$$\mathcal{I}_{\text{measured}}(\tau^{K\pi\pi}) = \eta^{K\pi\pi}(\tau^{K\pi\pi}) \mathcal{I}(\tau^{K\pi\pi})$$

- ▶ How well can  $K^-\pi^-\pi^+$  partial waves approximate the distribution of process  $p$ 
  - ▶ Is the set of  $K^-\pi^-\pi^+$  partial waves sufficient?
    - Automatic wave-set selection using model-selection techniques



Approximate model for process  $p$  by  $K^-\pi^-\pi^+$  partial waves

$$\eta^p(\tau^p) \left| \sum_a^{\text{waves}} \mathcal{T}_a^p \Psi_a^p(\tau^p) \right|^2 \approx \eta^{K\pi\pi}(\tau^{K\pi\pi}) \left| \sum_a^{\text{waves}} \tilde{\mathcal{T}}_a^p \Psi_a^{K\pi\pi}(\tau^{K\pi\pi}) \right|^2$$

Total true physics intensity distribution

$$\mathcal{I}(\tau^{K\pi\pi}) = \sum_{a,b}^{\text{waves}} \Psi_a^{K\pi\pi}(\tau^{K\pi\pi}) \rho_{a,b} [\Psi_b^{K\pi\pi}(\tau^{K\pi\pi})]^*$$

Spin-density matrix with rank  $N_r > 1$

$$\rho_{a,b} = \sum_p \mathcal{T}_a^p [T_b^p]^*$$

- ▶ How well can  $K^-\pi^-\pi^+$  partial waves approximate the distribution of process  $p$ 
  - ▶ Is the set of  $K^-\pi^-\pi^+$  partial waves sufficient?
    - ➔ Automatic wave-set selection using model-selection techniques

Approximate model for process  $p$  by  $K^-\pi^-\pi^+$  partial waves

$$\eta^p(\tau^p) \left| \sum_a^{\text{waves}} \mathcal{T}_a^p \Psi_a^p(\tau^p) \right|^2 \approx \eta^{K\pi\pi}(\tau^{K\pi\pi}) \left| \sum_a^{\text{waves}} \tilde{\mathcal{T}}_a^p \Psi_a^{K\pi\pi}(\tau^{K\pi\pi}) \right|^2$$

Total true physics intensity distribution

$$\mathcal{I}(\tau^{K\pi\pi}) = \sum_{a,b}^{\text{waves}} \Psi_a^{K\pi\pi}(\tau^{K\pi\pi}) \rho_{a,b} [\Psi_b^{K\pi\pi}(\tau^{K\pi\pi})]^*$$

Spin-density matrix with rank  $N_r > 1$

$$\rho_{a,b} = \sum_p \mathcal{T}_a^p [\mathcal{T}_b^p]^*$$

- ▶ How well can  $K^-\pi^-\pi^+$  partial waves approximate the distribution of process  $p$ 
  - ▶ Is the set of  $K^-\pi^-\pi^+$  partial waves sufficient?
    - ➔ Automatic wave-set selection using model-selection techniques

Approximate model for process  $p$  by  $K^-\pi^-\pi^+$  partial waves

$$\eta^p(\tau^p) \left| \sum_a^{\text{waves}} \mathcal{T}_a^p \Psi_a^p(\tau^p) \right|^2 \approx \eta^{K\pi\pi}(\tau^{K\pi\pi}) \left| \sum_a^{\text{waves}} \tilde{\mathcal{T}}_a^p \Psi_a^{K\pi\pi}(\tau^{K\pi\pi}) \right|^2$$

Total true physics intensity distribution

$$\mathcal{I}(\tau^{K\pi\pi}) = \sum_{a,b}^{\text{waves}} \Psi_a^{K\pi\pi}(\tau^{K\pi\pi}) \rho_{a,b} [\Psi_b^{K\pi\pi}(\tau^{K\pi\pi})]^*$$

Spin-density matrix with rank  $N_r > 1$

$$\rho_{a,b} = \sum_r^{N_r} \mathcal{T}_a^r [T_b^r]^*$$

▶ Experimentally measurable quantities are spin-density matrix elements

- ➡ Transition amplitudes  $\mathcal{T}_a^p$  are only effective parameters
- ➡ Cannot determine  $\mathcal{T}_a^p$  of individual processes
- ➡ Cannot separate different processes

Approximate model for process  $p$  by  $K^-\pi^-\pi^+$  partial waves

$$\eta^p(\tau^p) \left| \sum_a^{\text{waves}} \mathcal{T}_a^p \Psi_a^p(\tau^p) \right|^2 \approx \eta^{K\pi\pi}(\tau^{K\pi\pi}) \left| \sum_a^{\text{waves}} \tilde{\mathcal{T}}_a^p \Psi_a^{K\pi\pi}(\tau^{K\pi\pi}) \right|^2$$

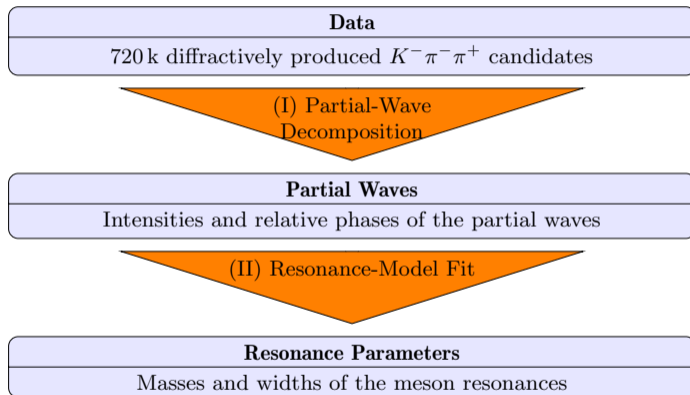
Total true physics intensity distribution

$$\mathcal{I}(\tau^{K\pi\pi}) = \sum_{a,b}^{\text{waves}} \Psi_a^{K\pi\pi}(\tau^{K\pi\pi}) \rho_{a,b} [\Psi_b^{K\pi\pi}(\tau^{K\pi\pi})]^*$$

Spin-density matrix with rank  $N_r > 1$

$$\rho_{a,b} = \sum_r^{N_r} \mathcal{T}_a^r [T_b^r]^*$$

- ▶ Large number of fit parameters:  $N_{\text{para}} = N_r(2N_{\text{waves}} - N_r)$
- ▶ Sufficient rank of spin-density matrix must be determined
  - ▶ Rank two needed to describe pure  $\pi^-\pi^-\pi^+$  Monte Carlo sample using  $K^-\pi^-\pi^+$  partial waves
  - ▶ Used rank three to model  $K^-\pi^-\pi^+$  sample



- ▶ Spin-density matrix  $\rho_{ab}(m_{K\pi\pi}, t')$  measured in partial-wave decomposition
- ▶ Model spin-density matrix in resonance-model fit

$$\hat{\rho}_{ab}(m_{K\pi\pi}, t') = \hat{\rho}_{ab}^{K\pi\pi}(m_{K\pi\pi}, t') + \hat{\rho}_{ab}^{3\pi}(m_{K\pi\pi}, t') + \hat{\rho}_{ab}^{\text{Bkg}}(m_{K\pi\pi}, t')$$

### Model transition amplitudes as coherent sum over various components

$$\hat{T}_a^z(m_{K\pi\pi}, t') = \sum_{k \in \mathbb{S}_a} K(m_{K\pi\pi}, t')^k C_a^{K\pi\pi}(t') \mathcal{D}_k(m_{K\pi\pi}; \zeta_k)$$

- ▶ Dynamic functions  $\mathcal{D}_k(m_{K\pi\pi}; \zeta_k)$ 
  - ▶ For resonances: rel. Breit-Wigner
  - ▶ For non-resonant terms:  $\mathcal{D}_k^{\text{NR}}(m_{K\pi\pi}; a_k, c_k) = (m_{K\pi\pi} - m_{\text{thr}})^{a_k} e^{-b(c_k) \tilde{q}_k^2(m_{K\pi\pi})}$
- ▶ “Coupling amplitudes”:  ${}^k C_a^z(t')$ 
  - ▶ Independent coupling amplitude for each  $t'$  bin
- ▶ Kinematic factor  $K(m_{K\pi\pi}, t')$
- ▶ Coherently summed over all assumed model components

### Model transition amplitudes as coherent sum over various components

$$\hat{T}_a^z(m_{K\pi\pi}, t') = \sum_{k \in \mathbb{S}_a} K(m_{K\pi\pi}, t')^k C_a^{K\pi\pi}(t') \mathcal{D}_k(m_{K\pi\pi}; \zeta_k)$$

- ▶ Dynamic functions  $\mathcal{D}_k(m_{K\pi\pi}; \zeta_k)$ 
  - ▶ For resonances: rel. Breit-Wigner
  - ▶ For non-resonant terms:  $\mathcal{D}_k^{\text{NR}}(m_{K\pi\pi}; a_k, c_k) = (m_{K\pi\pi} - m_{\text{thr}})^{a_k} e^{-b(c_k) \tilde{q}_k^2(m_{K\pi\pi})}$
- ▶ “Coupling amplitudes”:  ${}^k C_a^z(t')$ 
  - ▶ Independent coupling amplitude for each  $t'$  bin
- ▶ Kinematic factor  $K(m_{K\pi\pi}, t')$
- ▶ Coherently summed over all assumed model components



### Model transition amplitudes as coherent sum over various components

$$\hat{T}_a^z(m_{K\pi\pi}, t') = \sum_{k \in \mathbb{S}_a} K(m_{K\pi\pi}, t')^k C_a^{K\pi\pi}(t') \mathcal{D}_k(m_{K\pi\pi}; \zeta_k)$$

- ▶ Dynamic functions  $\mathcal{D}_k(m_{K\pi\pi}; \zeta_k)$ 
  - ▶ For resonances: rel. Breit-Wigner
  - ▶ For non-resonant terms:  $\mathcal{D}_k^{\text{NR}}(m_{K\pi\pi}; a_k, c_k) = (m_{K\pi\pi} - m_{\text{thr}})^{a_k} e^{-b(c_k) \tilde{q}_k^2(m_{K\pi\pi})}$
- ▶ “Coupling amplitudes”:  ${}^k C_a^z(t')$ 
  - ▶ Independent coupling amplitude for each  $t'$  bin
- ▶ Kinematic factor  $K(m_{K\pi\pi}, t')$
- ▶ Coherently summed over all assumed model components

### Model transition amplitudes as coherent sum over various components

$$\hat{T}_a^z(m_{K\pi\pi}, t') = \sum_{k \in \mathbb{S}_a} K(m_{K\pi\pi}, t')^k C_a^{K\pi\pi}(t') \mathcal{D}_k(m_{K\pi\pi}; \zeta_k)$$

- ▶ Dynamic functions  $\mathcal{D}_k(m_{K\pi\pi}; \zeta_k)$ 
  - ▶ For resonances: rel. Breit-Wigner
  - ▶ For non-resonant terms:  $\mathcal{D}_k^{\text{NR}}(m_{K\pi\pi}; a_k, c_k) = (m_{K\pi\pi} - m_{\text{thr}})^{a_k} e^{-b(c_k) \tilde{q}_k^2(m_{K\pi\pi})}$
- ▶ “Coupling amplitudes”:  ${}^k C_a^z(t')$ 
  - ▶ Independent coupling amplitude for each  $t'$  bin
- ▶ Kinematic factor  $K(m_{K\pi\pi}, t')$
- ▶ **Coherently summed** over all assumed model components

### 3 $\pi$ spin-density matrix

$$\hat{\rho}_{ab}^{\pi\pi\pi}(m_{K\pi\pi}, t') = \left| C^{\pi\pi\pi} \right|^2 \rho_{ab}^{\pi\pi\pi}(m_{K\pi\pi}, t')$$

- ▶  $\rho_{ab}^{\pi\pi\pi}(m_{K\pi\pi}, t')$  obtained from PWD of  $\pi^- \pi^- \pi^+$  pseudodata sample
  - ▶  $m_{K\pi\pi}$  dependence fixed
  - ▶  $t'$  dependence fixed
  - ▶ Rel. strength between partial waves fixed (freed in a study)
- ▶ One global real-valued yield parameter  $\left| C^{\pi\pi\pi} \right|^2$

### Background spin-density matrix

- ▶ Additional incoherent contribution from other processes:  $K^- K^- K^+$ , ...
- ▶ Transition amplitudes modeled by non-resonant parameterizations for each partial wave

$$\hat{\mathcal{T}}_a^{\text{eBKG}}(m_{K\pi\pi}, t') = K(m_{K\pi\pi}, t') \mathcal{C}_a^{\text{eBKG}}(t') \mathcal{D}_{k_a}^{\text{eBKG}}(m_{K\pi\pi}; a_{k_a}, c_{k_a})$$

- ▶  $\chi^2$  fit of the real and imaginary parts of the spin-density matrix
  - ▶ Taking into account correlations between spin-density matrix elements
  - ▶ Shape parameters ( $m_0, \Gamma_0, \dots$ ) and coupling amplitudes are free parameters
- ▶ For the main fit, we performed 2000 fit attempts with random start-parameter values for the shape parameters, e.g. mass and width parameters, and the coupling and branching amplitudes.
- ▶ Start-parameter ranges for the shape parameters are chosen according to previous measurements (see note)
- ▶ The best result is the one which yielded the smallest  $\chi^2$  value

- ▶  $\chi^2$  fit of the real and imaginary parts of the spin-density matrix
  - ▶ Taking into account correlations between spin-density matrix elements
  - ▶ Shape parameters ( $m_0, \Gamma_0, \dots$ ) and coupling amplitudes are free parameters
- ▶ For the main fit, we performed 2000 fit attempts with random start-parameter values for the shape parameters, e.g. mass and width parameters, and the coupling and branching amplitudes.
- ▶ Start-parameter ranges for the shape parameters are chosen according to previous measurements (see note)
- ▶ The best result is the one which yielded the smallest  $\chi^2$  value

$$\mathcal{I}(\tau, m_{K\pi\pi}, t') = \left| \sum_{a \in \mathbb{W}(m_{K\pi\pi}, t')} \mathcal{T}_a(m_{K\pi\pi}, t') \Psi_a(\tau, m_{K\pi\pi}) \right|^2$$

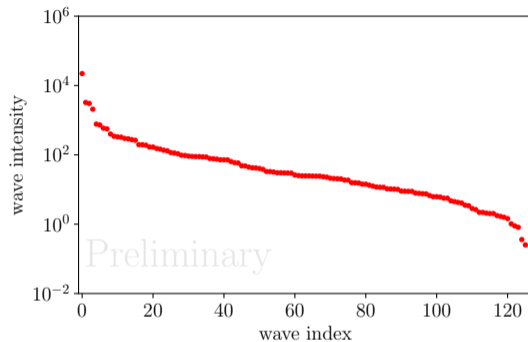
Challenge: Find the “best” set of waves that describes the data

- ▶ If the wave set is too large
  - ↳ Starting to describe statistical fluctuations
- ▶ If waves that contribute to the data are missing
  - ↳ Intensity can be wrongly attributed to other waves
  - ↳ Model leakage

## Infer wave set from data

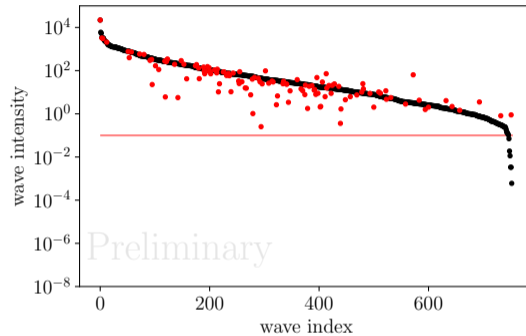
- ▶ **Systematically construct** large set of allowed partial waves
  - ↳ “Wave pool”
- ▶ Fit wave pool to data
  - ▶ Impose penalty on  $|\mathcal{T}_a|^2 \Rightarrow$  **regularization**
  - ▶ Suppress insignificant waves
- ▶ **Select waves** that significantly contribute to data
  - ↳ “Best” subset of waves that describe the data





- ▶  $\pi^- \pi^- \pi^+$  Monte Carlo mock data set with 126 partial waves
- ▶ Fitting wave pool of 753 waves
  - ▶ Massive overfitting
  - ▶ Almost all waves pick up intensity

Courtesy F. Kaspar, TUM



- ▶  $\pi^- \pi^- \pi^+$  Monte Carlo mock data set with 126 partial waves
- ▶ Fitting wave pool of 753 waves
  - Massive overfitting
  - Almost all waves pick up intensity

Courtesy F. Kaspar, TUM

$$\ln \mathcal{L}_{\text{fit}} = \ln \mathcal{L}_{\text{extended}} + \sum_a^{\text{waves}} \ln \mathcal{L}_{\text{reg}}(|\mathcal{T}_a|; \{c_{\text{para}}\})$$

### LASSO/L1 regularization<sup>1</sup>

$$\ln \mathcal{L}_{\text{reg}}(|\mathcal{T}_a|; \lambda) = -\lambda |\mathcal{T}_a|$$

- ▶ Maximum at  $|\mathcal{T}_a| = 0$
- ▶ Well established<sup>2</sup>
- ▶ “Smoothing” at  $|\mathcal{T}_a| = 0$

$$|\mathcal{T}_a| \rightarrow \sqrt{|\mathcal{T}_a|^2 + \varepsilon}$$

<sup>1</sup> Robert Tibshirani. “Regression Shrinkage and Selection via the Lasso”. In: Journal of the Royal Statistical Society. Series B 58.1 (1996)

<sup>2</sup> Baptiste Guegan et al. “Model selection for amplitude analysis”. In: JINST 10.09 (2015), P09002

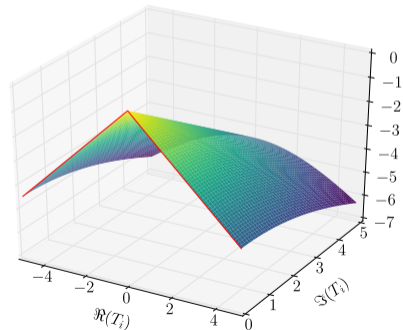
$$\ln \mathcal{L}_{\text{fit}} = \ln \mathcal{L}_{\text{extended}} + \sum_a^{\text{waves}} \ln \mathcal{L}_{\text{reg}}(|\mathcal{T}_a|; \{c_{\text{para}}\})$$

## LASSO/L1 regularization<sup>1</sup>

$$\ln \mathcal{L}_{\text{reg}}(|\mathcal{T}_a|; \lambda) = -\lambda |\mathcal{T}_a|$$

- ▶ Maximum at  $|\mathcal{T}_a| = 0$
- ▶ Well established<sup>2</sup>
- ▶ “Smoothing” at  $|\mathcal{T}_a| = 0$

$$|\mathcal{T}_a| \rightarrow \sqrt{|\mathcal{T}_a|^2 + \varepsilon}$$



<sup>1</sup> Robert Tibshirani. “Regression Shrinkage and Selection via the Lasso”. In: Journal of the Royal Statistical Society. Series B 58.1 (1996)

<sup>2</sup> Baptiste Guegan et al. “Model selection for amplitude analysis”. In: JINST 10.09 (2015), P09002

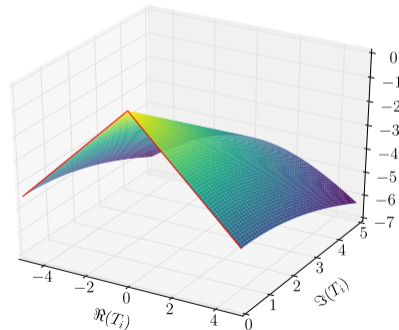
$$\ln \mathcal{L}_{\text{fit}} = \ln \mathcal{L}_{\text{extended}} + \sum_a^{\text{waves}} \ln \mathcal{L}_{\text{reg}}(|\mathcal{T}_a|; \{c_{\text{para}}\})$$

### LASSO/L1 regularization<sup>1</sup>

$$\ln \mathcal{L}_{\text{reg}}(|\mathcal{T}_a|; \lambda) = -\lambda |\mathcal{T}_a|$$

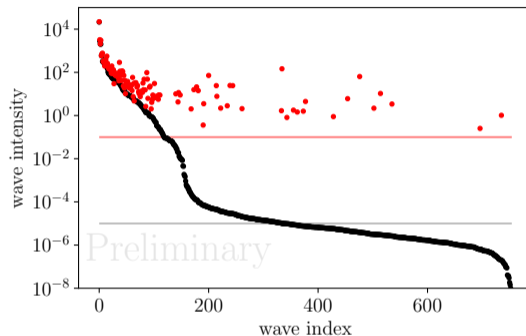
- ▶ Maximum at  $|\mathcal{T}_a| = 0$
- ▶ Well established<sup>2</sup>
- ▶ “Smoothing” at  $|\mathcal{T}_a| = 0$

$$|\mathcal{T}_a| \rightarrow \sqrt{|\mathcal{T}_a|^2 + \varepsilon}$$



<sup>1</sup> Robert Tibshirani. “Regression Shrinkage and Selection via the Lasso”. In: Journal of the Royal Statistical Society. Series B 58.1 (1996)

<sup>2</sup> Baptiste Guegan et al. “Model selection for amplitude analysis”. In: JINST 10.09 (2015), P09002



$$\lambda = 0.3$$

$$\varepsilon = 10^{-5}$$

- ▶ Bias also on large transition amplitudes
- ▶ Some additional waves
- ▶ Some waves missing

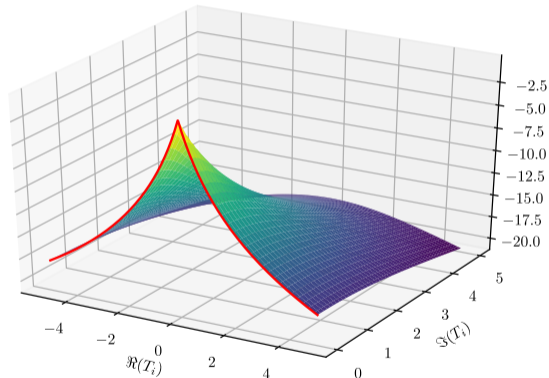
Courtesy F. Kaspar, TUM

### Generalized Pareto<sup>1</sup>

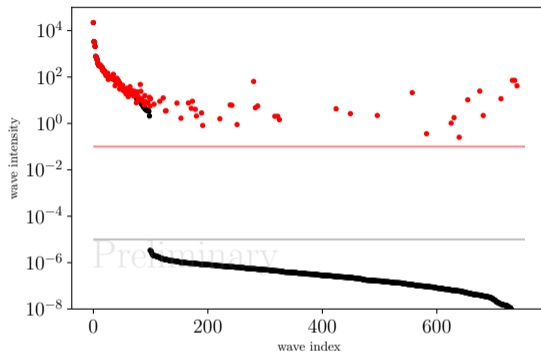
$$\ln \mathcal{L}_{\text{reg}}(|\mathcal{T}_a|; \Gamma, \zeta) = -\frac{1}{\zeta} \ln \left[ 1 + \zeta \frac{|\mathcal{T}_a|}{\Gamma} \right]$$

- ▶ Wave **intensities** spread over **orders of magnitudes**
- ▶ Use **logarithmic prior**
  - ➔ Heavy-tailed
  - ➔ Less bias on large waves
- ▶ LASSO-like for  $|\mathcal{T}_a| \rightarrow 0$
- ▶ “Smoothing” at  $|\mathcal{T}_a| = 0$

$$|\mathcal{T}_a| \rightarrow \sqrt{|\mathcal{T}_a|^2 + \varepsilon}$$



<sup>1</sup> Artin Armagan, David B. Dunson, and Jaeyong Lee. “Generalized double Pareto shrinkage”. In: *Statistica Sinica* (2013). doi: 10.5705/ss.2011.048.



$$\zeta = 0.5$$

$$\Gamma = 0.1$$

$$\varepsilon = 10^{-5}$$

- ▶ Less bias on large transition amplitudes
- ▶ Clear **kink** in intensity distribution to smoothing scale  $\Rightarrow$  Selection
- ▶ Less additional waves
- ▶ Some small waves missing

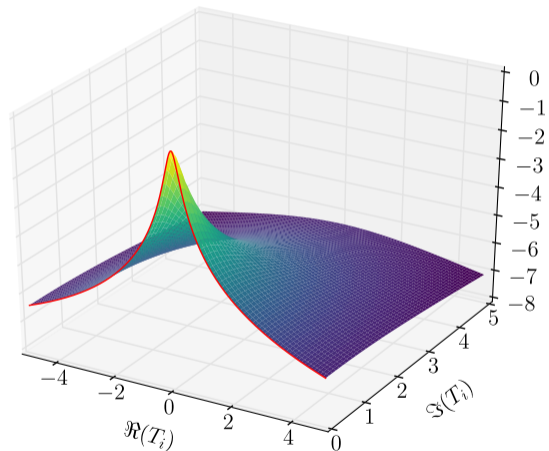
Courtesy F. Kaspar, TUM



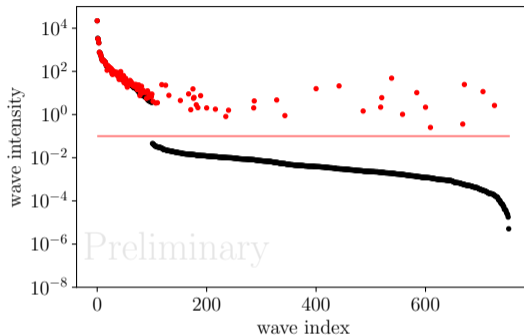
## “Cauchy”

$$\ln \mathcal{L}_{\text{reg}}(|\mathcal{T}_a|; \Gamma) = -\ln \left[ 1 + \frac{|\mathcal{T}_a|^2}{\Gamma_a^2} \right]$$

- ▶ Logarithmic prior
- ▶ L2-like for  $|\mathcal{T}_a| \rightarrow 0$



$$\Gamma = 0.2$$



- ▶ Less bias on large transition amplitudes
- ▶ Clear kink in intensity distribution
- ▶ Few additional waves
- ▶ Few small waves missing

Courtesy F. Kaspar, TUM

## Wave pool

- ▶ Spin  $J \leq 7$
  - ▶ Angular momentum  $L \leq 7$
  - ▶ Positive naturality of exchange particle
  - ▶ 12 isobars
    - ▶  $[K\pi]_S^{K\pi}$ ,  $[K\pi]_S^{K\eta}$ ,  $K^*(892)$ ,  $K^*(1680)$ ,  $K_2^*(1430)$ ,  $K_3^*(1780)$
    - ▶  $[\pi\pi]_S$ ,  $f_0(980)$ ,  $f_0(1500)$ ,  $\rho(770)$ ,  $f_2(1270)$ ,  $\rho_3(1690)$
- ⇒ “Wave pool” of 596 waves

“only” 720 k events

## Wave pool

- ▶ Spin  $J \leq 7$
  - ▶ Angular momentum  $L \leq 7$
  - ▶ Positive naturality of exchange particle
  - ▶ 12 isobars
    - ▶  $[K\pi]_S^{K\pi}$ ,  $[K\pi]_S^{K\eta}$ ,  $K^*(892)$ ,  $K^*(1680)$ ,  $K_2^*(1430)$ ,  $K_3^*(1780)$
    - ▶  $[\pi\pi]_S$ ,  $f_0(980)$ ,  $f_0(1500)$ ,  $\rho(770)$ ,  $f_2(1270)$ ,  $\rho_3(1690)$
- ⇒ “Wave pool” of 596 waves

“only” 720 k events

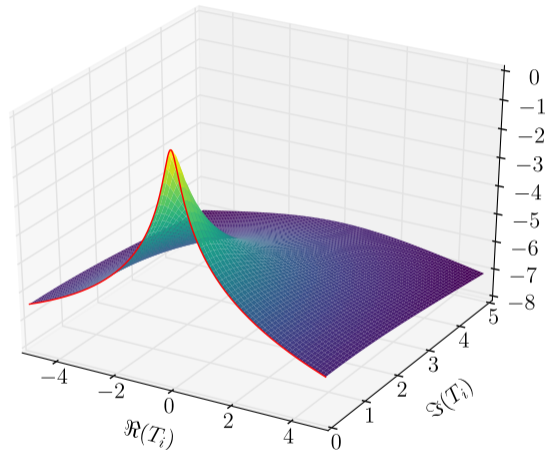
## Regularization

$$\ln \mathcal{L}_{\text{reg}}(|\mathcal{T}_a|; \Gamma) = -\ln \left[ 1 + \frac{|\mathcal{T}_a|^2}{\Gamma_a^2} \right]$$

- ▶ Use Cauchy regularization
- ▶ Scale of  $|\mathcal{T}_a|$  depends on experimental acceptance
  - ▶ Apply penalty on expected number  $\bar{N}_a$  of observed events

$$\Gamma_a = \frac{\Gamma}{\sqrt{\bar{n}_a}} \Rightarrow \frac{|\mathcal{T}_a|^2}{\Gamma_a^2} = \frac{\bar{N}_a}{\Gamma^2}$$

- ▶  $\Gamma$  is a universal parameter



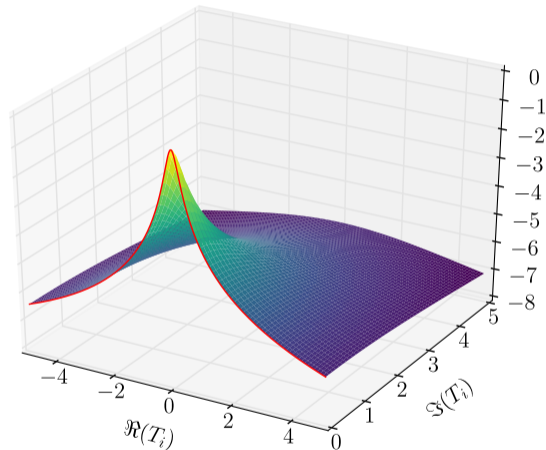
## Regularization

$$\ln \mathcal{L}_{\text{reg}}(|\mathcal{T}_a|; \Gamma) = -\ln \left[ 1 + \frac{|\mathcal{T}_a|^2}{\Gamma_a^2} \right]$$

- ▶ Use Cauchy regularization
- ▶ **Scale of  $|\mathcal{T}_a|$  depends on experimental acceptance**
  - ▶ Apply penalty on expected number  $\bar{N}_a$  of observed events

$$\Gamma_a = \frac{\Gamma}{\sqrt{\bar{\eta}_a}} \Rightarrow \frac{|\mathcal{T}_a|^2}{\Gamma_a^2} = \frac{\bar{N}_a}{\Gamma^2}$$

- ▶  $\Gamma$  is a universal parameter



## Regularization

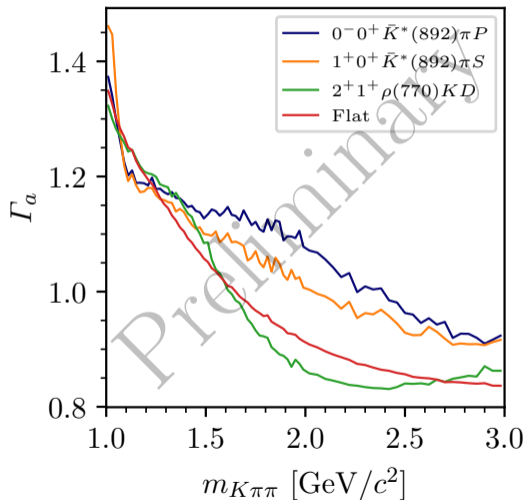
$$\ln \mathcal{L}_{\text{reg}}(|\mathcal{T}_a|; \Gamma) = -\ln \left[ 1 + \frac{|\mathcal{T}_a|^2}{\Gamma_a^2} \right]$$

- ▶ Use Cauchy regularization
- ▶ Scale of  $|\mathcal{T}_a|$  depends on experimental acceptance
  - ▶ Apply penalty on expected number  $\bar{N}_a$  of observed events

$$\Gamma_a = \frac{\Gamma}{\sqrt{\bar{\eta}_a}} \Rightarrow \frac{|\mathcal{T}_a|^2}{\Gamma_a^2} = \frac{\bar{N}_a}{\Gamma^2}$$

- ▶  $\Gamma$  is a universal parameter

## COMPASS



## Regularization

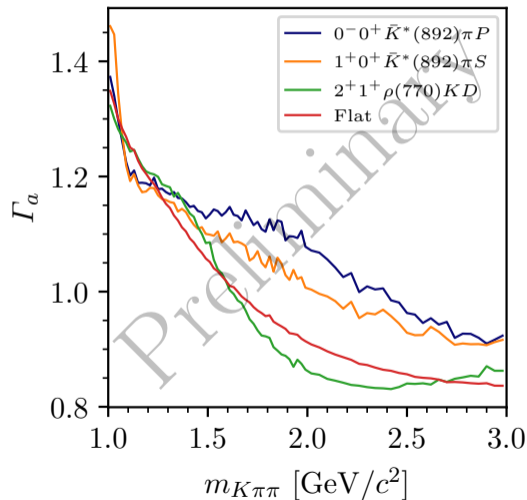
$$\ln \mathcal{L}_{\text{reg}}(|\mathcal{T}_a|; \Gamma) = -\ln \left[ 1 + \frac{|\mathcal{T}_a|^2}{\Gamma_a^2} \right]$$

- ▶ Use Cauchy regularization
- ▶ Scale of  $|\mathcal{T}_a|$  depends on experimental acceptance
  - ▶ Apply penalty on expected number  $\bar{N}_a$  of observed events

$$\Gamma_a = \frac{\Gamma}{\sqrt{\bar{\eta}_a}} \Rightarrow \frac{|\mathcal{T}_a|^2}{\Gamma_a^2} = \frac{\bar{N}_a}{\Gamma^2}$$

- ▶  $\Gamma$  is a universal parameter

## COMPASS





## Imposing continuity of the wave set

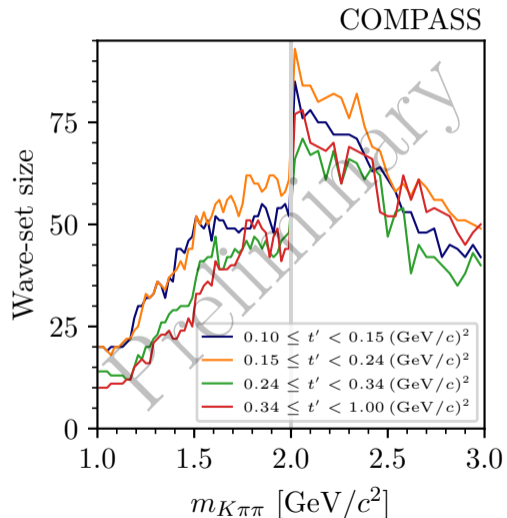
- ▶ Wave-set inferred independently for each  $(m_{K\pi\pi}, t')$  cell
- ▶ Impose continuity of the wave set in  $m_{K\pi\pi}$  by adding additional regularization term

$$\ln \mathcal{L}_{\text{cont}}(\{\mathcal{T}_a(m_{K\pi\pi}, t')\}; \lambda) = \sum_{j=i-3}^{j=i+3} \lambda \left| \mathcal{T}_a(m_{K\pi\pi}, t')(m_{K\pi\pi}^{j+1}) - \mathcal{T}_a(m_{K\pi\pi}, t')(m_{K\pi\pi}^j) \right|^2,$$

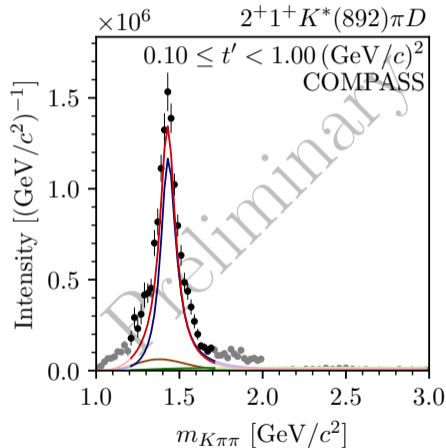
which suppresses fluctuations among neighboring  $m_{K\pi\pi}$  bins

## Wave-set size

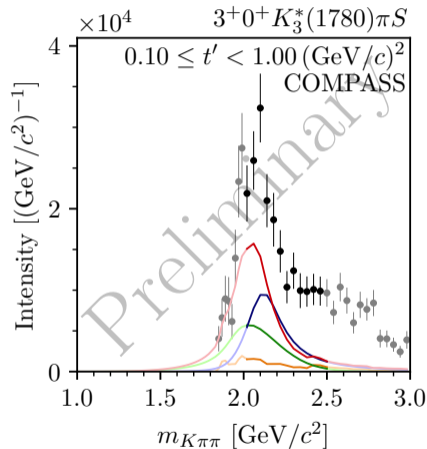
- ▶ 5 to 90 waves per  $(m_{K\pi\pi}, t')$  cell
- ▶ Larger wave set for larger binning in  $m_{K\pi\pi}$
- ▶ Larger wave set in  $t'$  bins with more events



- ▶ Selection of large signals
- ▶ as well as of signals at per-mil level

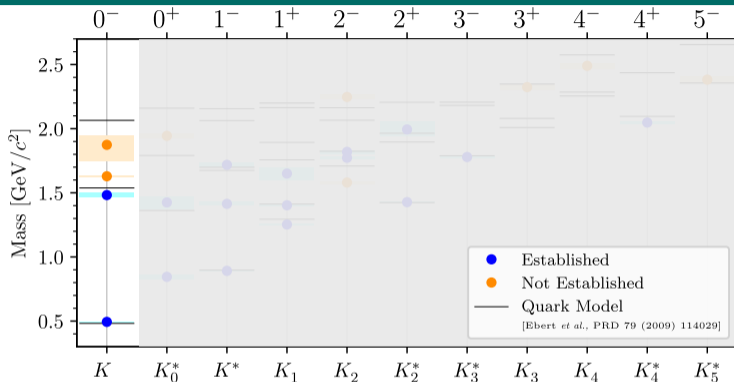


- ▶ Selection of large signals
- ▶ as well as of signals at per-mil level



# 14-Wave Resonance-Model Fit

Searching for Exotic Strange Mesons with  $J^P = 0^-$



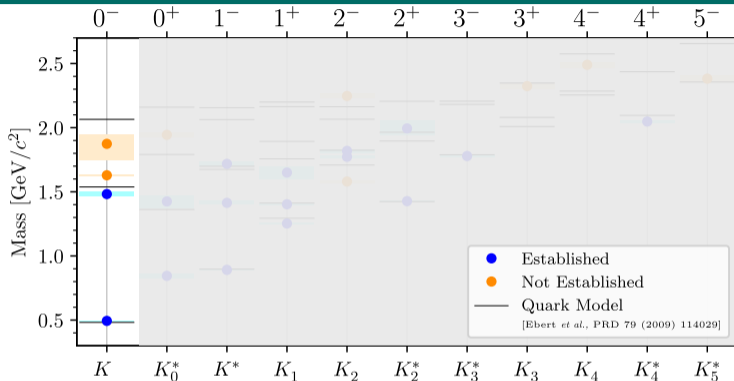
PDG

(2022)

- ▶  $K(1460)$  and  $K(1830)$
- ▶  $K(1630)$ 
  - ▶ Unexpectedly small width of only  $16 \text{ MeV}/c^2$
  - ▶  $J^P$  of  $K(1630)$  unclear

# 14-Wave Resonance-Model Fit

Searching for Exotic Strange Mesons with  $J^P = 0^-$



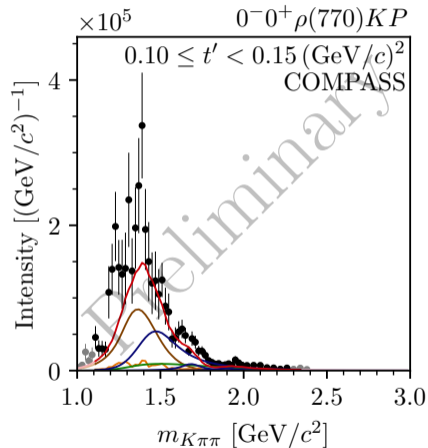
PDG

(2022)

- ▶  $K(1460)$  and  $K(1830)$
- ▶  $K(1630)$ 
  - ▶ Unexpectedly small width of only  $16 \text{ MeV}/c^2$
  - ▶  $J^P$  of  $K(1630)$  unclear

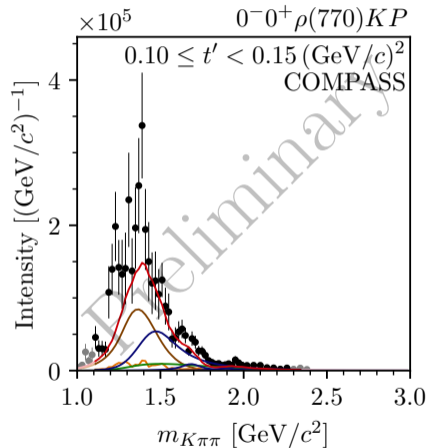
## COMPASS $K^-\pi^-\pi^+$ data

- ▶ Peak at about  $1.4 \text{ GeV}/c^2$ 
  - ▶ Potentially from established  $K(1460)$
  - ▶ But,  $m_{K\pi\pi} \lesssim 1.5 \text{ GeV}/c^2$  region affected by analysis artifacts
- ▶ Second peak at about  $1.7 \text{ GeV}/c^2$ 
  - ▶  $K(1630)$  signal with  $8.3\sigma$  statistical significance
  - ▶ Accompanied by rising phase
- ▶ Weak signal at about  $2.0 \text{ GeV}/c^2$ 
  - ▶  $K(1830)$  signal with  $5.4\sigma$  statistical significance



## COMPASS $K^-\pi^-\pi^+$ data

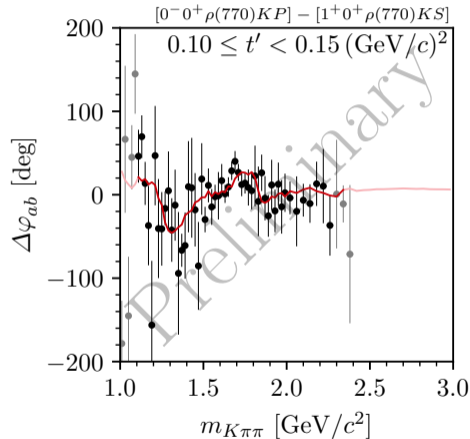
- ▶ Peak at about  $1.4 \text{ GeV}/c^2$ 
  - ▶ Potentially from established  $K(1460)$
  - ▶ But,  $m_{K\pi\pi} \lesssim 1.5 \text{ GeV}/c^2$  region affected by analysis artifacts
- ▶ Second peak at about  $1.7 \text{ GeV}/c^2$ 
  - ▶  $K(1630)$  signal with  $8.3\sigma$  statistical significance
  - ▶ Accompanied by rising phase
- ▶ Weak signal at about  $2.0 \text{ GeV}/c^2$ 
  - ▶  $K(1830)$  signal with  $5.4\sigma$  statistical significance





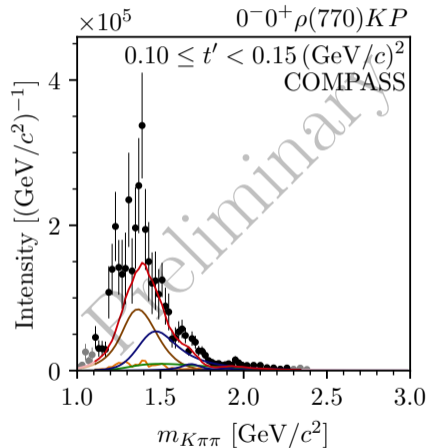
## COMPASS $K^- \pi^- \pi^+$ data

- ▶ Peak at about  $1.4 \text{ GeV}/c^2$ 
  - ▶ Potentially from established  $K(1460)$
  - ▶ But,  $m_{K\pi\pi} \lesssim 1.5 \text{ GeV}/c^2$  region affected by analysis artifacts
- ▶ Second peak at about  $1.7 \text{ GeV}/c^2$ 
  - ▶  $K(1630)$  signal with  $8.3\sigma$  statistical significance
  - ▶ Accompanied by rising phase
- ▶ Weak signal at about  $2.0 \text{ GeV}/c^2$ 
  - ▶  $K(1830)$  signal with  $5.4\sigma$  statistical significance



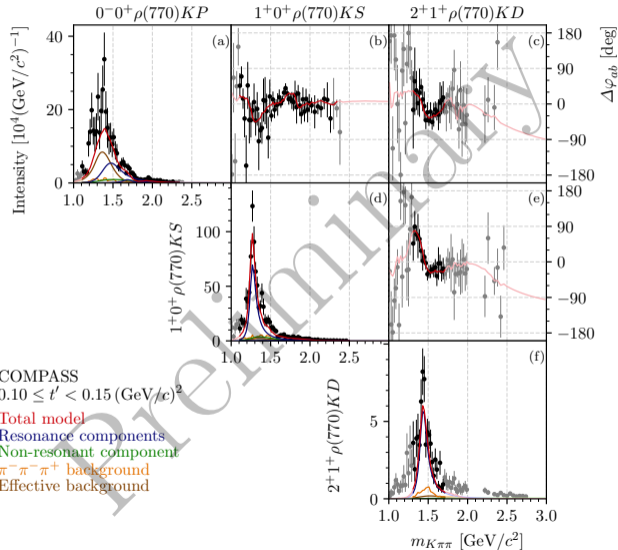
## COMPASS $K^-\pi^-\pi^+$ data

- ▶ Peak at about  $1.4 \text{ GeV}/c^2$ 
  - ▶ Potentially from established  $K(1460)$
  - ▶ But,  $m_{K\pi\pi} \lesssim 1.5 \text{ GeV}/c^2$  region affected by analysis artifacts
- ▶ Second peak at about  $1.7 \text{ GeV}/c^2$ 
  - ▶  $K(1630)$  signal with  $8.3\sigma$  statistical significance
  - ▶ Accompanied by rising phase
- ▶ Weak signal at about  $2.0 \text{ GeV}/c^2$ 
  - ▶  $K(1830)$  signal with  $5.4\sigma$  statistical significance



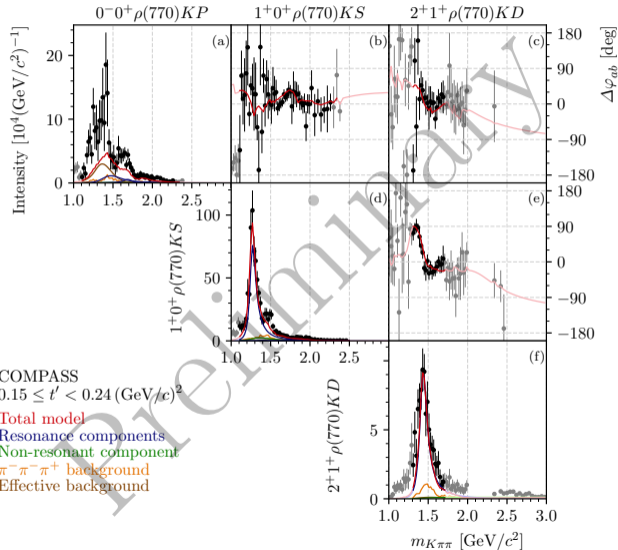
# 14-Wave Resonance-Model Fit

Searching for Exotic Strange Mesons with  $J^P = 0^-$



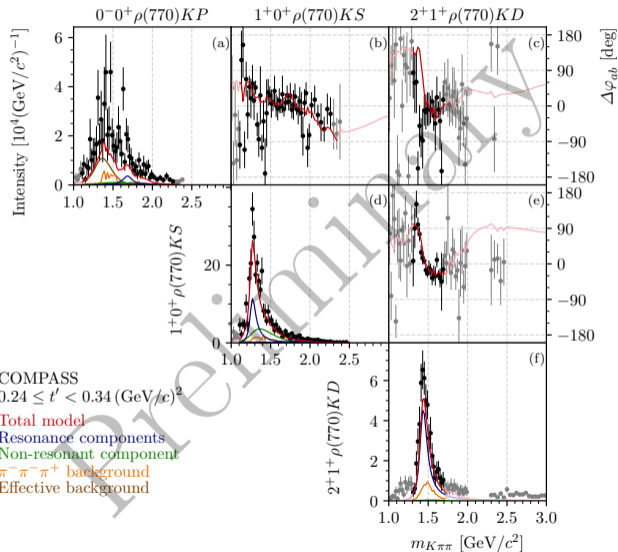
# 14-Wave Resonance-Model Fit

Searching for Exotic Strange Mesons with  $J^P = 0^-$



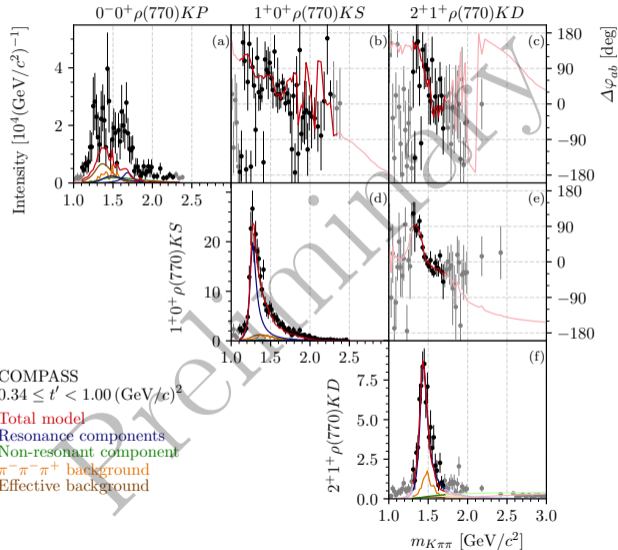
# 14-Wave Resonance-Model Fit

Searching for Exotic Strange Mesons with  $J^P = 0^-$



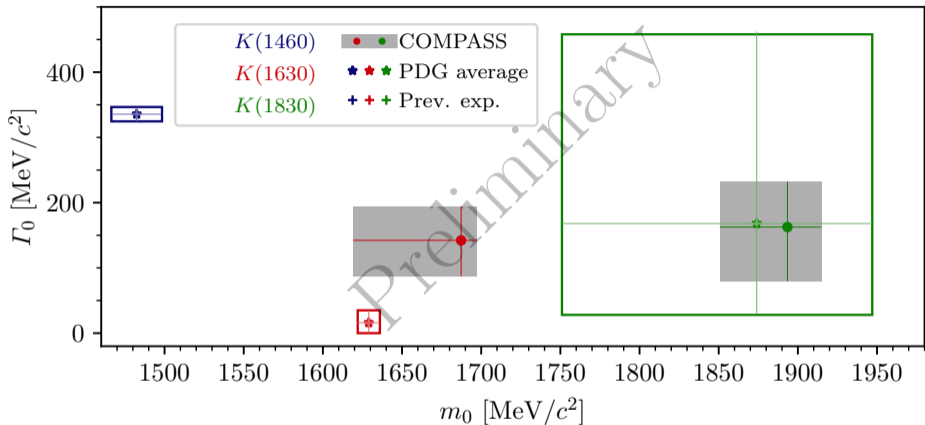
# 14-Wave Resonance-Model Fit

Searching for Exotic Strange Mesons with  $J^P = 0^-$



# 14-Wave Resonance-Model Fit

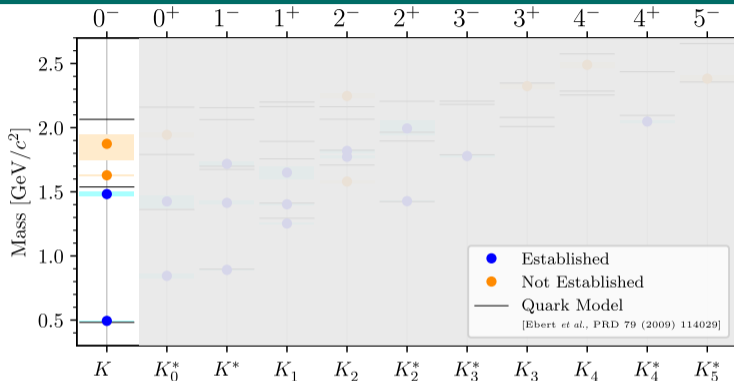
Searching for Exotic Strange Mesons with  $J^P = 0^-$



- ▶  $K(1830)$  parameters in good agreement with LCHb measurement [PRL 118 (2017) 022003]
- ▶ Realistic  $K(1630)$  width of about  $140 \text{ MeV}/c^2$

# 14-Wave Resonance-Model Fit

Searching for Exotic Strange Mesons with  $J^P = 0^-$

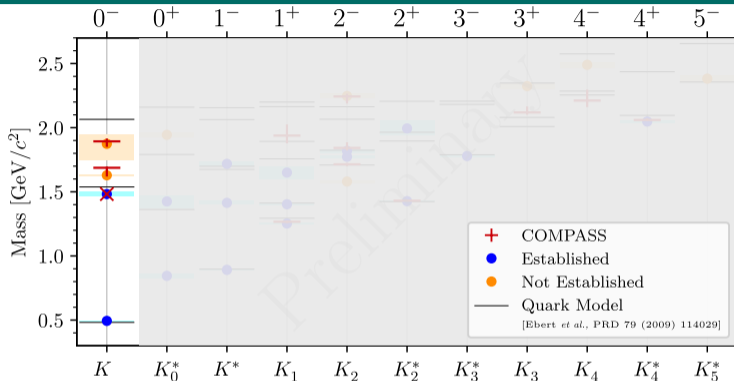


- ▶ Indications for 3 excited  $K$  from a single analysis
- ▶ Quark-model predicts only two excited states: potentially  $K(1460)$  and  $K(1830)$ 
  - $K(1630)$  supernumerary signal
  - Candidate for **exotic non- $q\bar{q}$  state**; other explanations possible ( $K^*(892)$   $\omega$  threshold nearby)



# 14-Wave Resonance-Model Fit

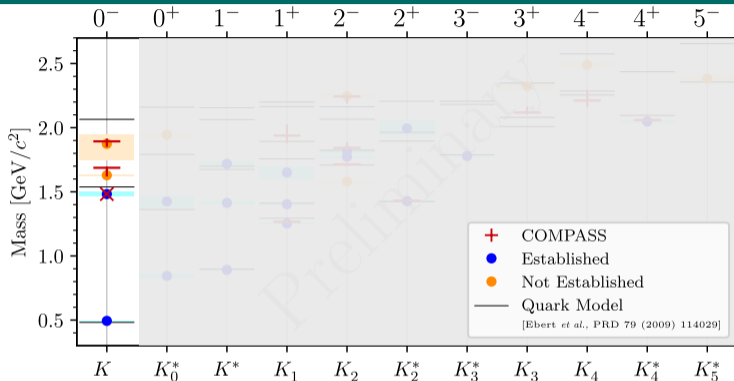
Searching for Exotic Strange Mesons with  $J^P = 0^-$



- ▶ Indications for 3 excited  $K$  from a single analysis
- ▶ Quark-model predicts only two excited states: potentially  $K(1460)$  and  $K(1830)$ 
  - $K(1630)$  supernumerary signal
  - Candidate for exotic non- $q\bar{q}$  state; other explanations possible ( $K^*(892)$   $\omega$  threshold nearby)

# 14-Wave Resonance-Model Fit

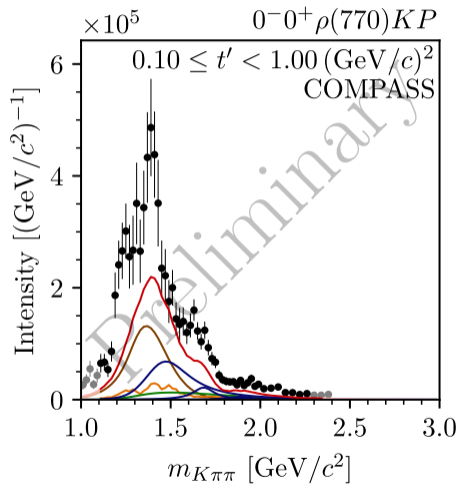
Searching for Exotic Strange Mesons with  $J^P = 0^-$



- ▶ Indications for 3 excited  $K$  from a single analysis
- ▶ Quark-model predicts only two excited states: potentially  $K(1460)$  and  $K(1830)$ 
  - ➔  $K(1630)$  supernumerary signal
  - ➔ Candidate for **exotic non- $q\bar{q}$  state**; other explanations possible ( $K^*(892)$   $\omega$  threshold nearby)

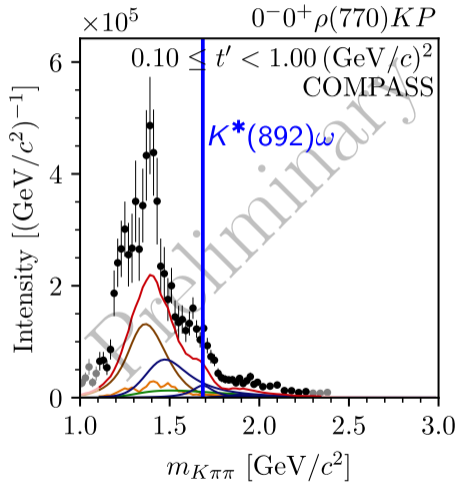
# 14-Wave Resonance-Model Fit

Searching for Exotic Strange Mesons with  $J^P = 0^-$



# 14-Wave Resonance-Model Fit

Searching for Exotic Strange Mesons with  $J^P = 0^-$

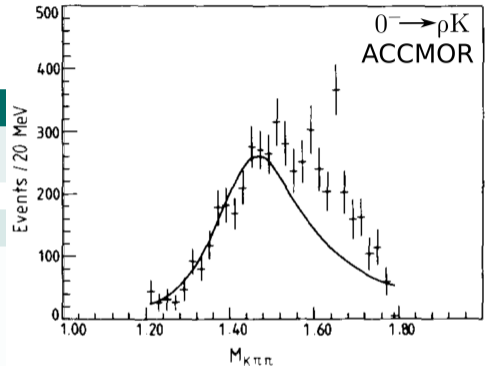


## $K^- \pi^- \pi^+$ from ACCMOR

- ▶ Potential  $K(1630)$  signal already in ACCMOR analysis

## $K^- \pi^- \pi^+$ from LHCb

- ▶ Measurement of  $D^0 \rightarrow K^\mp \pi^\pm \pi^\pm \pi^\mp$  at LHCb
  - ▶ Study strange mesons in  $K\pi\pi$  subsystem
  - ▶ MIPWA of  $J^P = 0^-$  amplitude
  - ▶ Potential signal above  $1.6 \text{ GeV}/c^2$
  - ▶ Limited by kinematic range

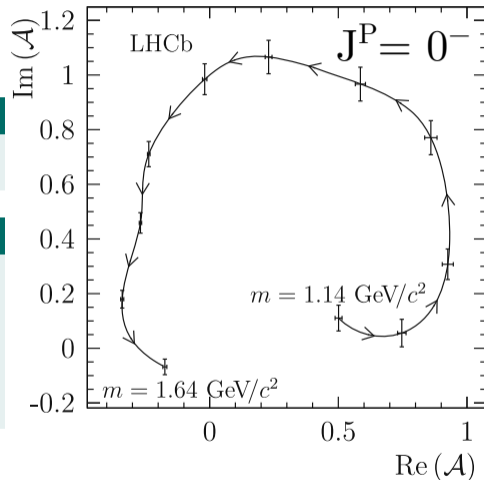


## $K^- \pi^- \pi^+$ from ACCMOR

- ▶ Potential  $K(1630)$  signal already in ACCMOR analysis

## $K^- \pi^- \pi^+$ from LHCb

- ▶ Measurement of  $D^0 \rightarrow K^\mp \pi^\pm \pi^\pm \pi^\mp$  at LHCb
  - ▶ Study strange mesons in  $K\pi\pi$  subsystem
  - ▶ MIPWA of  $J^P = 0^-$  amplitude
  - ▶ Potential signal above  $1.6 \text{ GeV}/c^2$
  - ▶ Limited by kinematic range

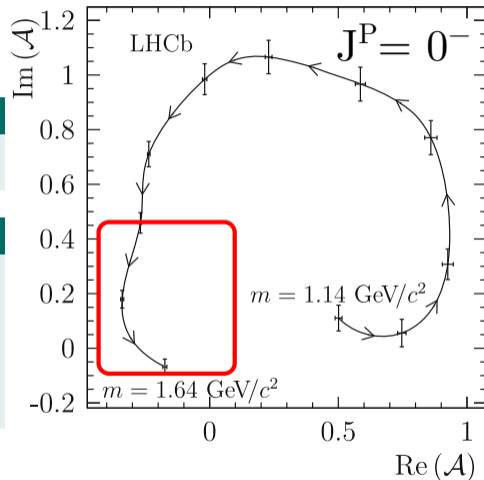


## $K^- \pi^- \pi^+$ from ACCMOR

- ▶ Potential  $K(1630)$  signal already in ACCMOR analysis

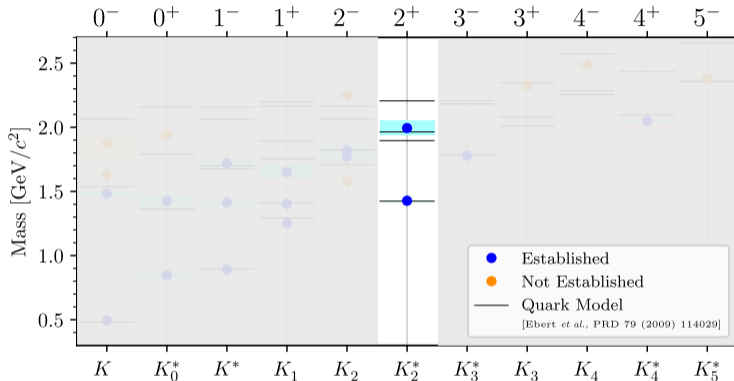
## $K^- \pi^- \pi^+$ from LHCb

- ▶ Measurement of  $D^0 \rightarrow K^\mp \pi^\pm \pi^\pm \pi^\mp$  at LHCb
  - ▶ Study strange mesons in  $K\pi\pi$  subsystem
  - ▶ MIPWA of  $J^P = 0^-$  amplitude
  - ▶ Potential signal above  $1.6 \text{ GeV}/c^2$
  - ▶ Limited by kinematic range



# 14-Wave Resonance-Model Fit

Partial Waves with  $J^P = 2^+$



PDG

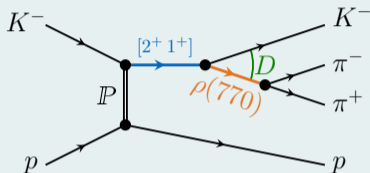
(2022)

►  $K_2^*(1430)$  well known resonance

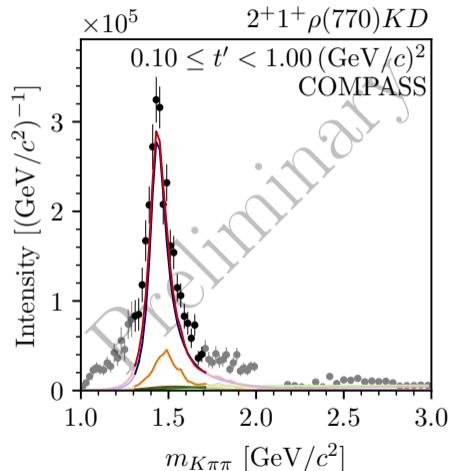


# 14-Wave Resonance-Model Fit

Partial Waves with  $J^P = 2^+$



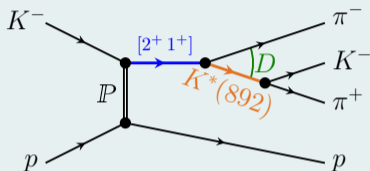
- ▶ Signal in  $K_2^*(1430)$  mass region
- ▶ In **different decays**
  - ▶  $\rho(770) K D$
  - ▶  $K^*(892) \pi D$
- ▶ In agreement with previous measurements
- ▶ **Cleaner** signal in **COMPASS** data



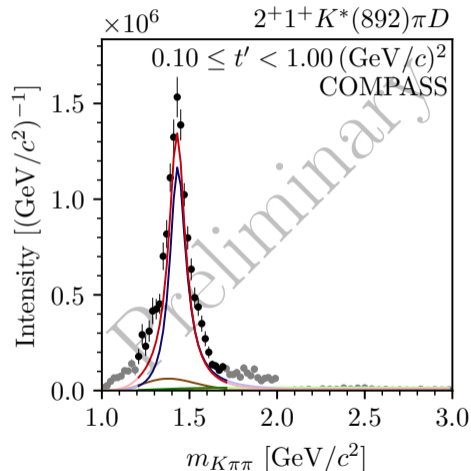
total resonance model, resonances, non-resonant,  $\pi\pi\pi$  background, effective background

# 14-Wave Resonance-Model Fit

Partial Waves with  $J^P = 2^+$



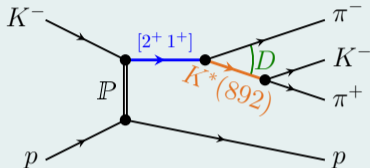
- ▶ Signal in  $K_2^*(1430)$  mass region
- ▶ In **different decays**
  - ▶  $\rho(770) K D$
  - ▶  $K^*(892) \pi D$
- ▶ In agreement with previous measurements
- ▶ **Cleaner** signal in **COMPASS** data



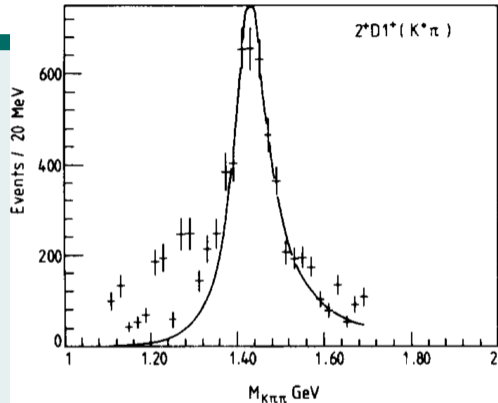
total resonance model, resonances, non-resonant,  $\pi\pi\pi$  background, effective background

# 14-Wave Resonance-Model Fit

Partial Waves with  $J^P = 2^+$

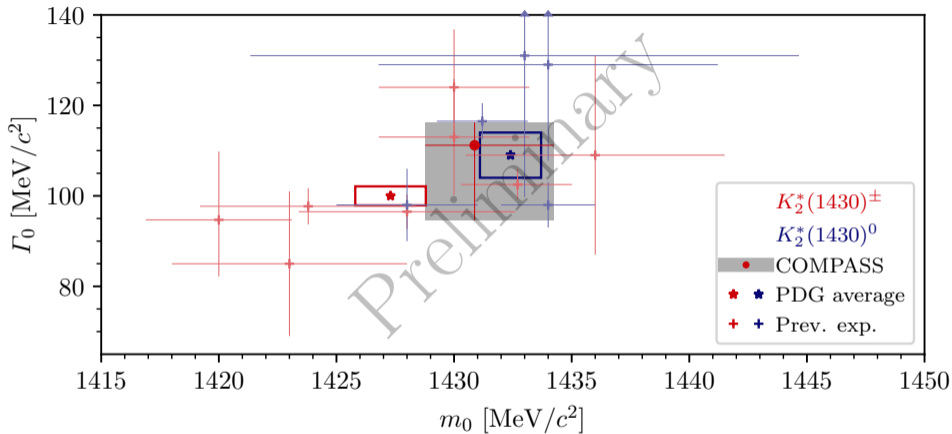


- ▶ Signal in  $K_2^*(1430)$  mass region
- ▶ In **different decays**
  - ▶  $\rho(770) K D$
  - ▶  $K^*(892) \pi D$
- ▶ In agreement with previous measurements
- ▶ **Cleaner** signal in **COMPASS** data



# 14-Wave Resonance-Model Fit

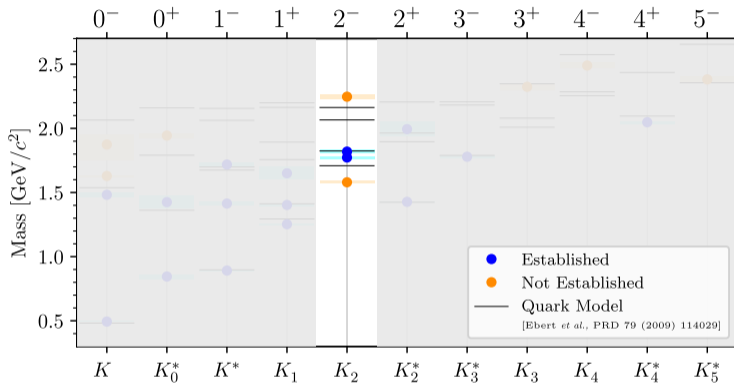
Partial Waves with  $J^P = 2^+$



- ▶  $K_2^*(1430)$  parameters consistent with previous observations
- ▶ Better agreement with PDG average values for neutral  $K_2^*(1430)$

# 14-Wave Resonance-Model Fit

Partial Waves with  $J^P = 2^-$



PDG

(2022)

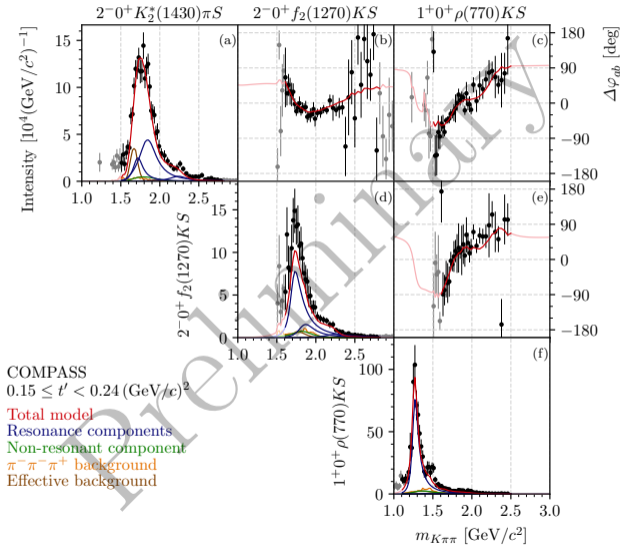
- ▶ Established  $K_2(1770)$  and  $K_2(1820)$
- ▶  $K_2(2250)$  need further confirmation

# 14-Wave Resonance-Model Fit

Partial Waves with  $J^P = 2^-$



- ▶ Simultaneously fit 4 waves with  $J^P = 2^-$
- ▶  $1.8 \text{ GeV}/c^2$  peak modeled by  $K_2(1770)$ ,  $K_2(1820)$
- ▶ High-mass shoulder modeled by  $K_2(2250)$
- ▶ Different intensity spectra and large phase motions among  $2^-$  waves

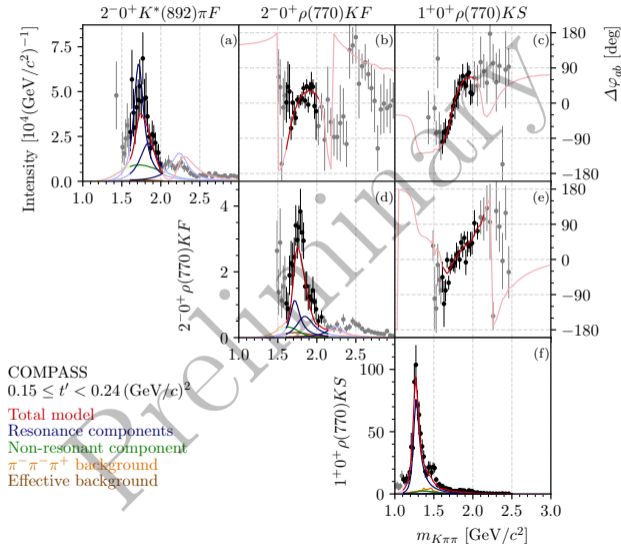


# 14-Wave Resonance-Model Fit

Partial Waves with  $J^P = 2^-$

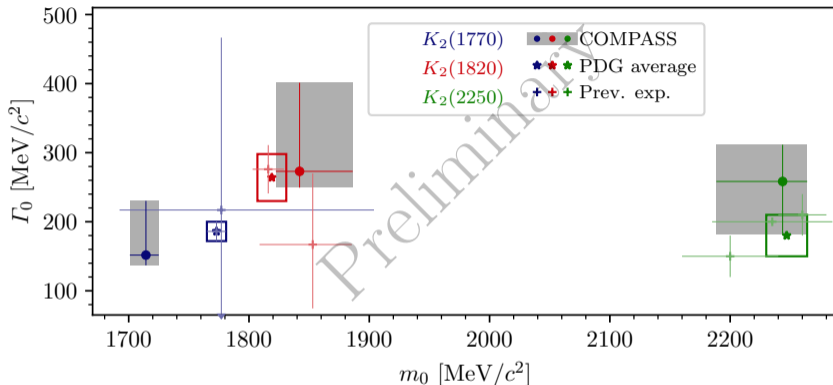


- ▶ Simultaneously fit 4 waves with  $J^P = 2^-$
- ▶  $1.8 \text{ GeV}/c^2$  peak modeled by  $K_2(1770)$ ,  $K_2(1820)$
- ▶ High-mass shoulder modeled by  $K_2(2250)$
- ▶ Different intensity spectra and large phase motions among  $2^-$  waves



# 14-Wave Resonance-Model Fit

Partial Waves with  $J^P = 2^-$



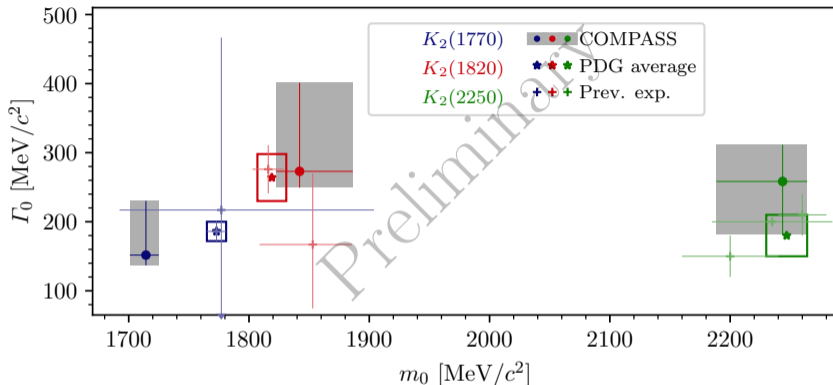
## $K_2(1770)$ and $K_2(1820)$

- ▶ Two states were considered by only three measurements ACCMOR, LASS, LHCb
- ▶ Only LHCb measurement could confirm two states ( $3\sigma$  statistical significance)
- ▶ We observe two states with  $11\sigma$  statistical significance



# 14-Wave Resonance-Model Fit

Partial Waves with  $J^P = 2^-$

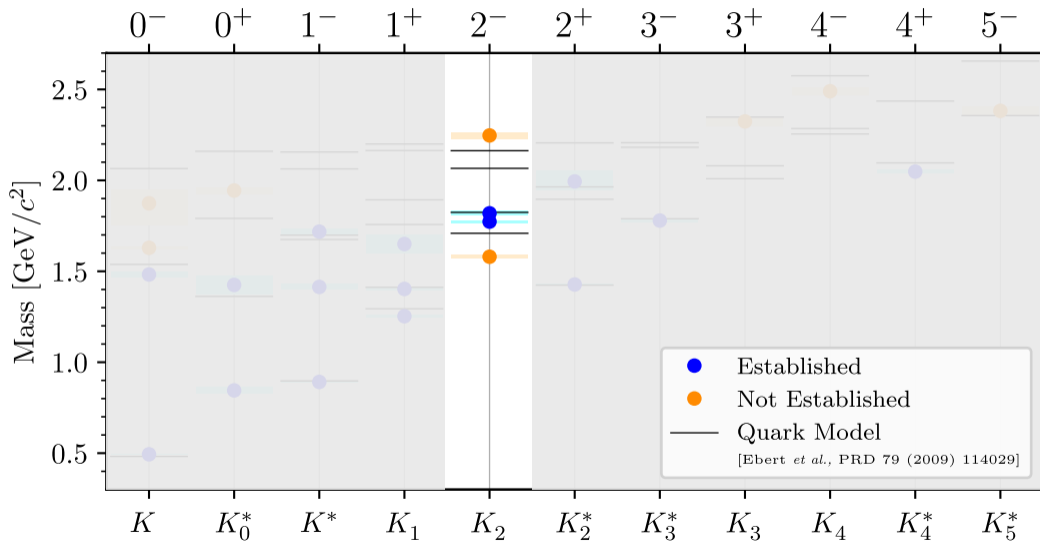


## $K_2(2250)$

- ▶ Studied so far mainly in  $\bar{\Lambda}(\bar{p})$  final states
- ▶ First simultaneous measurement of  $K_2(1770)$ ,  $K_2(1820)$ , and  $K_2(2250)$
- ▶ Resonance parameters consistent with previous observations

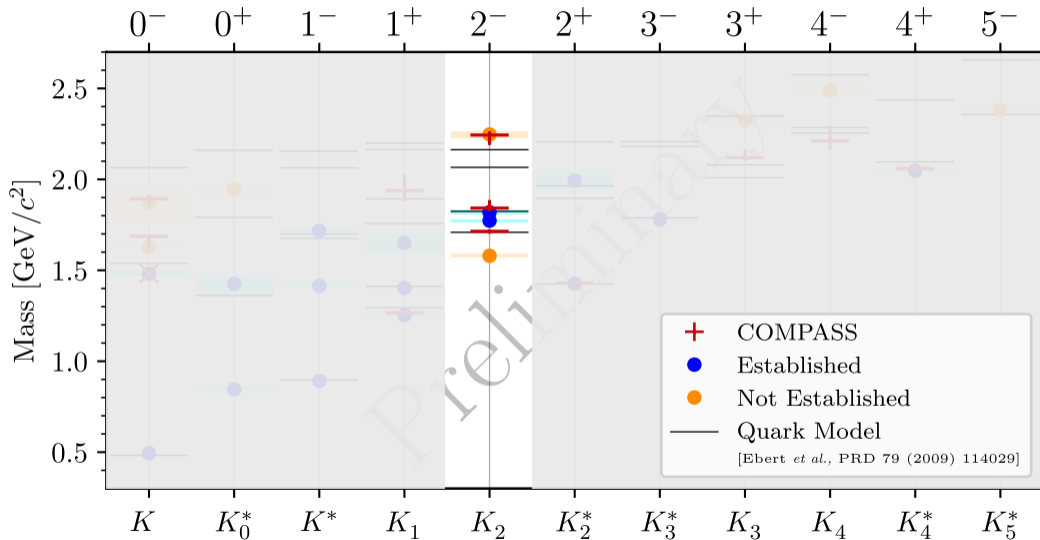
# 14-Wave Resonance-Model Fit

Partial Waves with  $J^P = 2^-$



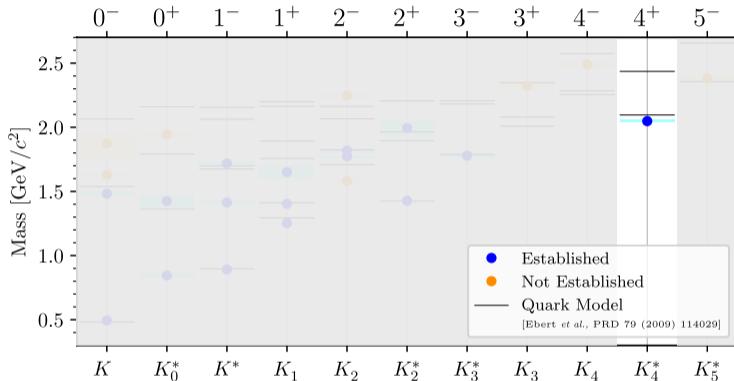
# 14-Wave Resonance-Model Fit

Partial Waves with  $J^P = 2^-$



# 14-Wave Resonance-Model Fit

Partial Waves with  $J^P = 4^+$



PDG

(2022)

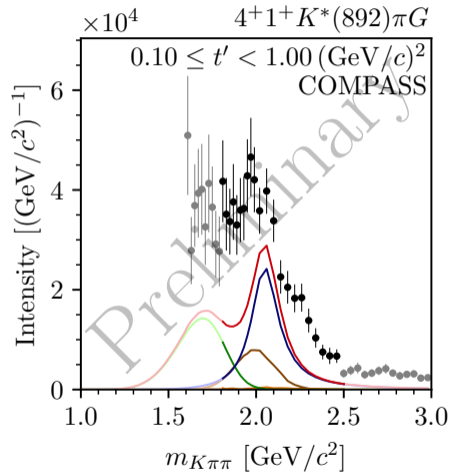
►  $K_4^*(2045)$  known resonance

# 14-Wave Resonance-Model Fit

Partial Waves with  $J^P = 4^+$



- ▶ Signal  $K_4^*(2045)$  signal in  $K^*(892) \pi$  and  $\rho(770) K$  decays



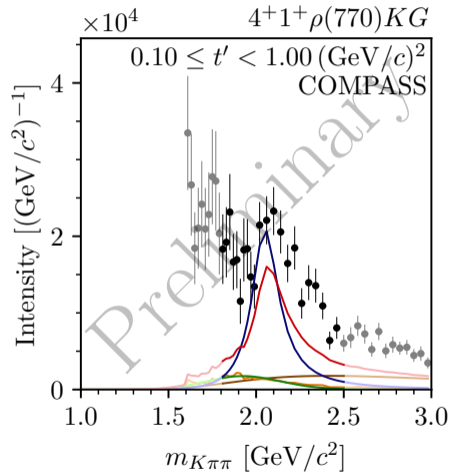
total resonance model, resonances, non-resonant,  $\pi\pi\pi$  background, effective background

# 14-Wave Resonance-Model Fit

Partial Waves with  $J^P = 4^+$



- ▶ Signal  $K_4^*(2045)$  signal in  $K^*(892) \pi$  and  $\rho(770) K$  decays



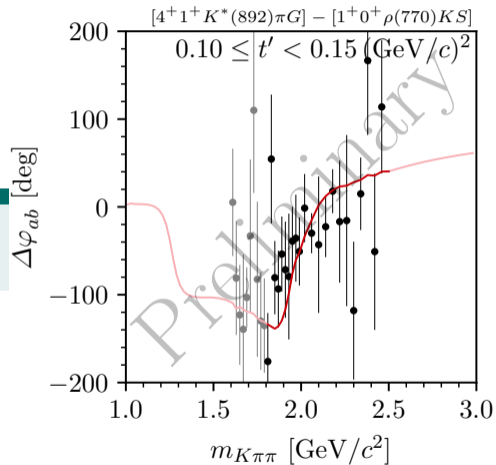
total resonance model, resonances, non-resonant,  $\pi\pi\pi$  background, effective background

# 14-Wave Resonance-Model Fit

Partial Waves with  $J^P = 4^+$



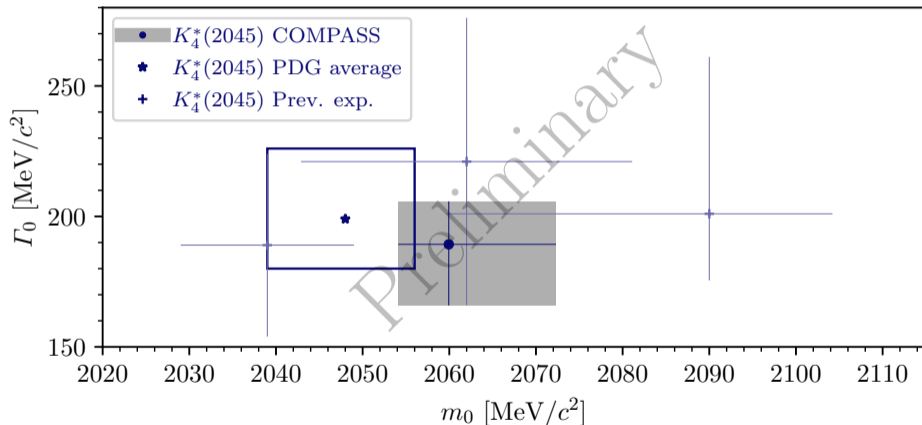
- Signal  $K_4^*(2045)$  signal in  $K^*(892) \pi$  and  $\rho(770) K$  decays



total resonance model, resonances, non-resonant,  $\pi\pi\pi$  background, effective background

# 14-Wave Resonance-Model Fit

Partial Waves with  $J^P = 4^+$





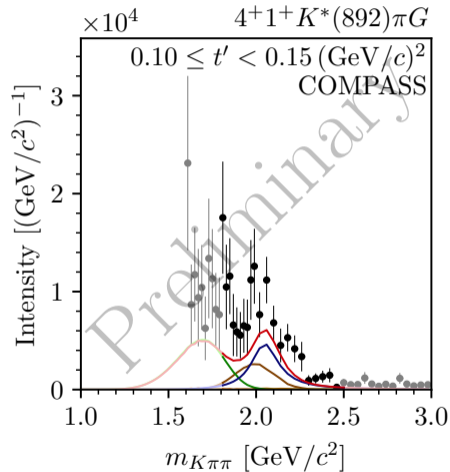
# 14-Wave Resonance-Model Fit

Partial Waves with  $J^P = 4^+$



- ▶ Imperfect description of magnitude of intensity,
- ▶ Also, real and imaginary parts of **interference terms described well, including their magnitude**
- ▶ Intensities and real and imaginary parts of interference terms not directly related as  $\text{Rank}[\rho_{ab}] > 1$   
 $|\rho_{ab}| \neq \sqrt{|\rho_{aa}| |\rho_{bb}|}$ 
  - ▶ Analysis artifacts in intensities of small waves, which are the least constrained by data

- ▶ Results validated by Monte Carlo input-output and systematic studies
- ▶ Imperfections considered in systematic uncertainties
- ▶ Results in agreement with previous experiments



total resonance model, resonances, non-resonant,  $\pi\pi\pi$  background, effective background

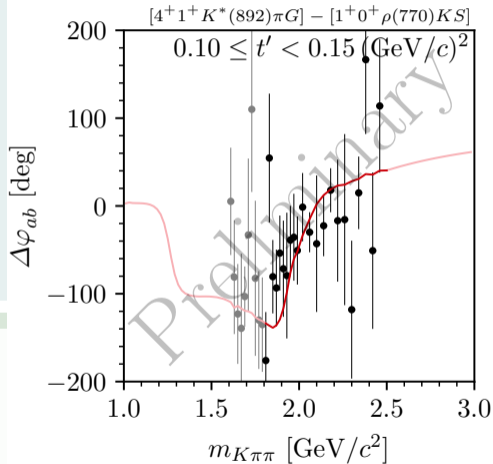
# 14-Wave Resonance-Model Fit

Partial Waves with  $J^P = 4^+$



- ▶ Imperfect description of magnitude of intensity, , while relative phase described well
- ▶ Also, real and imaginary parts of **interference terms described well, including their magnitude**
- ▶ Intensities and real and imaginary parts of interference terms not directly related as  $\text{Rank}[\rho_{ab}] > 1$   
 $|\rho_{ab}| \neq \sqrt{|\rho_{aa}| |\rho_{bb}|}$ 
  - ▶ Analysis artifacts in intensities of small waves, which are the least constrained by data

- ▶ Results validated by Monte Carlo input-output and systematic studies
- ▶ Imperfections considered in systematic uncertainties
- ▶ Results in agreement with previous experiments



total resonance model, resonances, non-resonant,  $\pi\pi\pi$  background, effective background

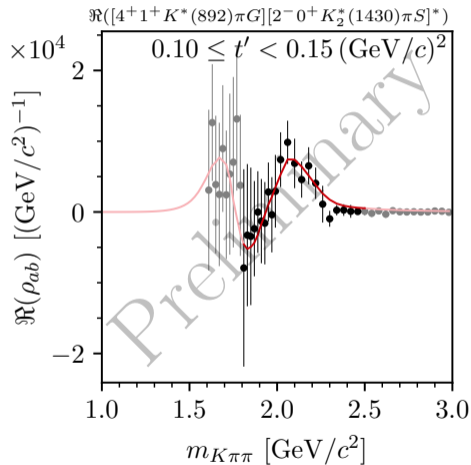
# 14-Wave Resonance-Model Fit

Partial Waves with  $J^P = 4^+$



- ▶ Imperfect description of magnitude of intensity, , while relative phase described well
- ▶ Also, real and imaginary parts of **interference terms described well, including their magnitude**
- ▶ Intensities and real and imaginary parts of interference terms not directly related as  $\text{Rank}[\rho_{ab}] > 1$   
 $|\rho_{ab}| \neq \sqrt{|\rho_{aa}| |\rho_{bb}|}$ 
  - ▶ Analysis artifacts in intensities of small waves, which are the least constrained by data

- ▶ Results validated by Monte Carlo input-output and systematic studies
- ▶ Imperfections considered in systematic uncertainties
- ▶ Results in agreement with previous experiments



total resonance model, resonances, non-resonant,  $\pi\pi\pi$  background, effective background

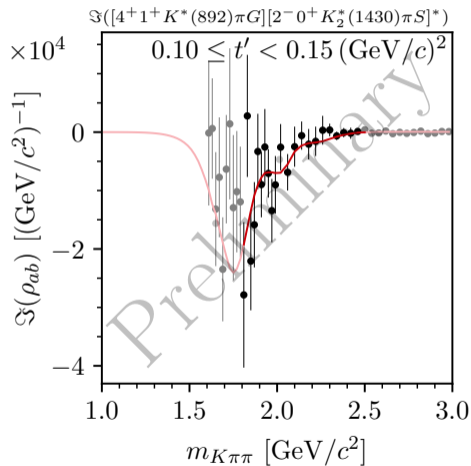
# 14-Wave Resonance-Model Fit

Partial Waves with  $J^P = 4^+$



- ▶ Imperfect description of magnitude of intensity, , while relative phase described well
- ▶ Also, real and imaginary parts of **interference terms described well, including their magnitude**
- ▶ Intensities and real and imaginary parts of interference terms not directly related as  $\text{Rank}[\rho_{ab}] > 1$   
 $|\rho_{ab}| \neq \sqrt{|\rho_{aa}| |\rho_{bb}|}$ 
  - ▶ Analysis artifacts in intensities of small waves, which are the least constrained by data

- ▶ Results validated by Monte Carlo input-output and systematic studies
- ▶ Imperfections considered in systematic uncertainties
- ▶ Results in agreement with previous experiments



total resonance model, resonances, non-resonant,  $\pi\pi\pi$  background, effective background

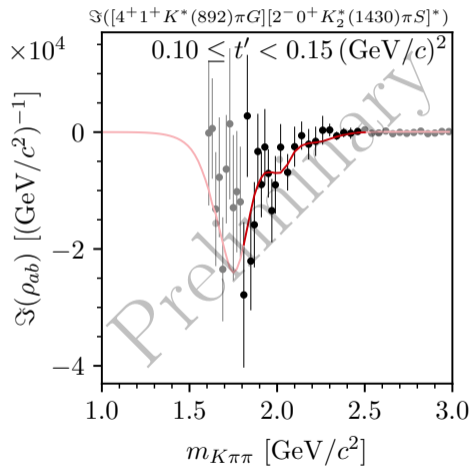
# 14-Wave Resonance-Model Fit

Partial Waves with  $J^P = 4^+$



- ▶ Imperfect description of magnitude of intensity, , while relative phase described well
- ▶ Also, real and imaginary parts of **interference terms described well, including their magnitude**
- ▶ Intensities and real and imaginary parts of interference terms not directly related as  $\text{Rank}[\rho_{ab}] > 1$   
 $|\rho_{ab}| \neq \sqrt{|\rho_{aa}| |\rho_{bb}|}$ 
  - ▶ Analysis artifacts in **intensities of small waves, which are the least constrained by data**

- ▶ Results validated by Monte Carlo input-output and systematic studies
- ▶ Imperfections considered in systematic uncertainties
- ▶ Results in agreement with previous experiments



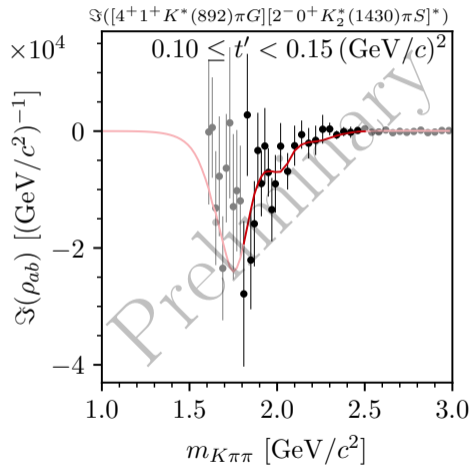
# 14-Wave Resonance-Model Fit

Partial Waves with  $J^P = 4^+$



- ▶ Imperfect description of magnitude of intensity, , while relative phase described well
- ▶ Also, real and imaginary parts of **interference terms described well, including their magnitude**
- ▶ Intensities and real and imaginary parts of interference terms not directly related as  $\text{Rank}[\rho_{ab}] > 1$   
 $|\rho_{ab}| \neq \sqrt{|\rho_{aa}| |\rho_{bb}|}$ 
  - ▶ Analysis artifacts in **intensities of small waves, which are the least constrained by data**

- ▶ Results validated by Monte Carlo input-output and systematic studies
- ▶ Imperfections considered in systematic uncertainties
- ▶ Results in agreement with previous experiments



total resonance model, resonances, non-resonant,  $\pi\pi\pi$  background, effective background

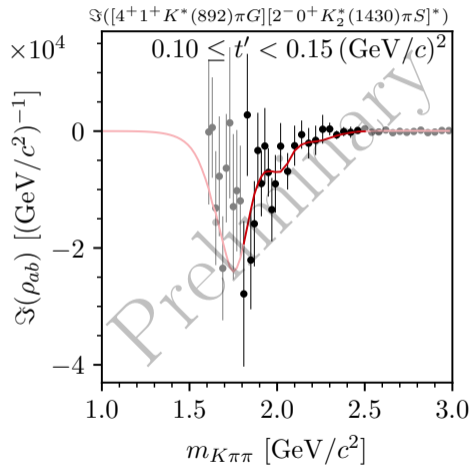
# 14-Wave Resonance-Model Fit

Partial Waves with  $J^P = 4^+$

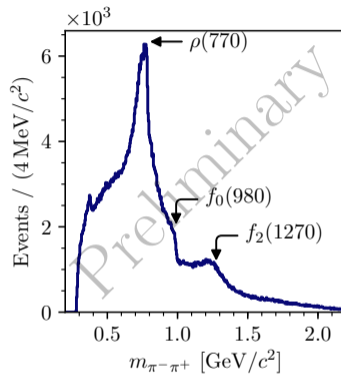
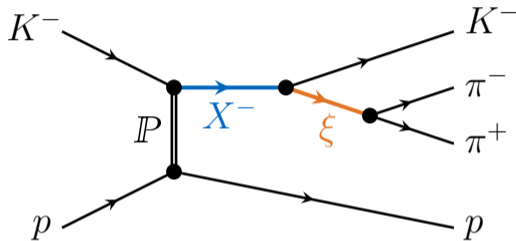


- ▶ Imperfect description of magnitude of intensity, , while relative phase described well
- ▶ Also, real and imaginary parts of **interference terms described well, including their magnitude**
- ▶ Intensities and real and imaginary parts of interference terms not directly related as  $\text{Rank}[\rho_{ab}] > 1$   
 $|\rho_{ab}| \neq \sqrt{|\rho_{aa}| |\rho_{bb}|}$ 
  - ▶ Analysis artifacts in **intensities of small waves, which are the least constrained by data**

- ▶ Results validated by Monte Carlo input-output and systematic studies
- ▶ Imperfections considered in systematic uncertainties
- ▶ Results in agreement with previous experiments

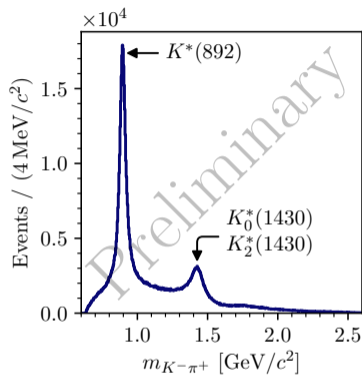
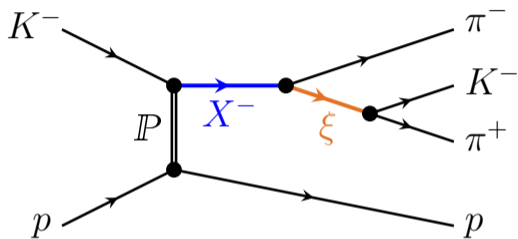


total resonance model, resonances, non-resonant,  $\pi\pi\pi$  background, effective background

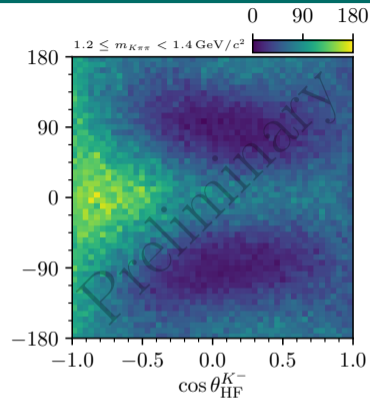
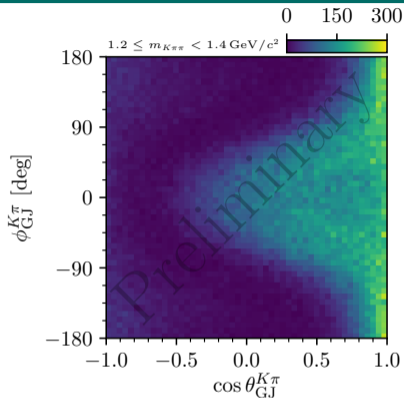


- ▶ Also structure in  $\pi^-\pi^+$  and  $K^-\pi^+$  subsystems
  - ↳ Successive 2-body decay via  $\pi^-\pi^+$  /  $K^-\pi^+$  resonance called **isobar**
- ▶ Also structure in angular distributions

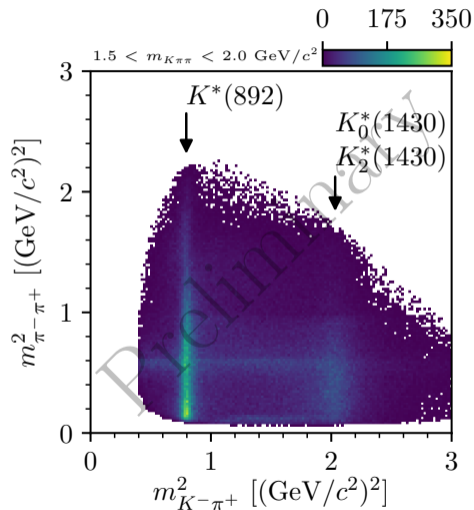
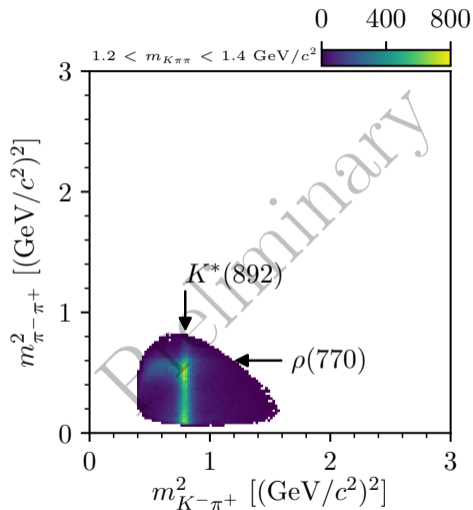




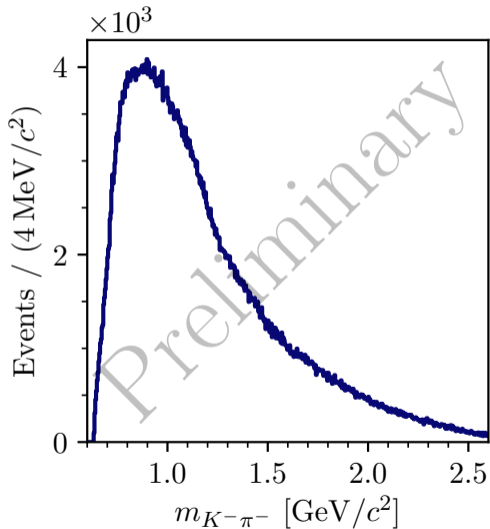
- ▶ Also structure in  $\pi^-\pi^+$  and  $K^-\pi^+$  subsystems
  - ↳ Successive 2-body decay via  $\pi^-\pi^+$  /  $K^-\pi^+$  resonance called **isobar**
- ▶ Also structure in angular distributions



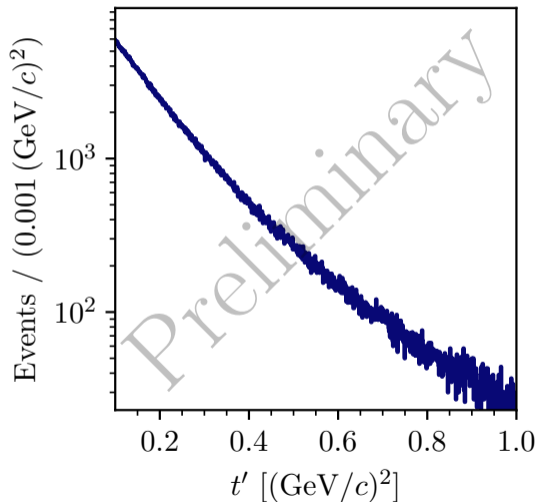
- ▶ Also structure in  $\pi^-\pi^+$  and  $K^-\pi^+$  subsystems
  - ↳ Successive 2-body decay via  $\pi^-\pi^+$  /  $K^-\pi^+$  resonance called **isobar**
- ▶ Also structure in angular distributions



- ▶ No dominant resonant structures

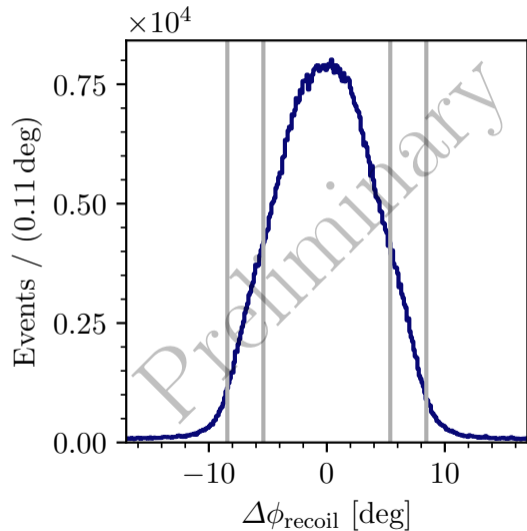
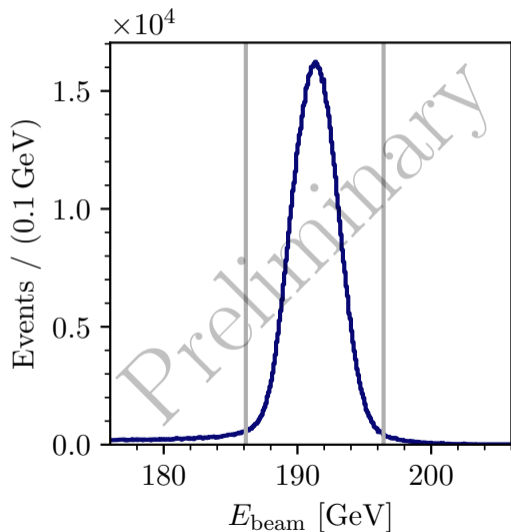


- ▶ Exponential shape
- ▶ Shallower for larger  $t'$



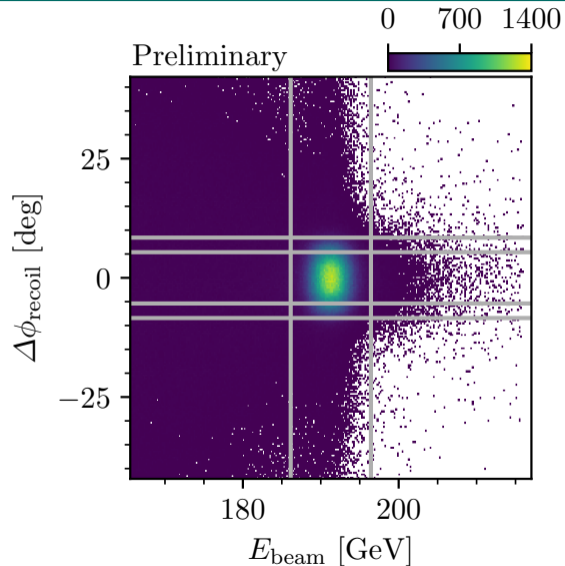
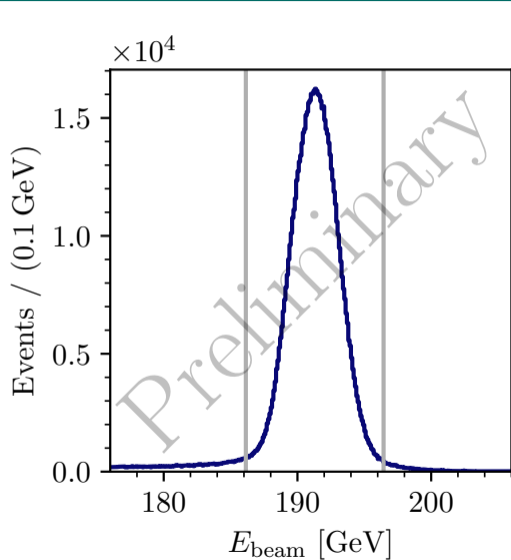
# Kinematic Distribution of $K^-\pi^-\pi^+$ Events

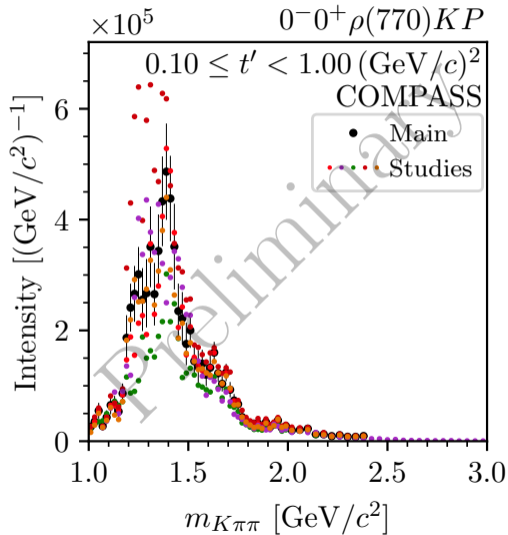
Exclusivity



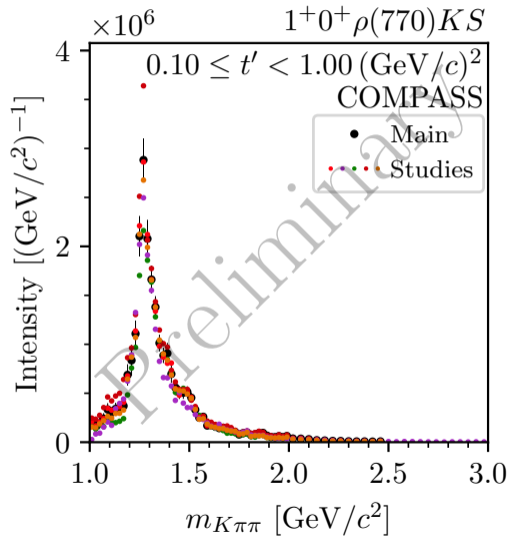
# Kinematic Distribution of $K^-\pi^-\pi^+$ Events

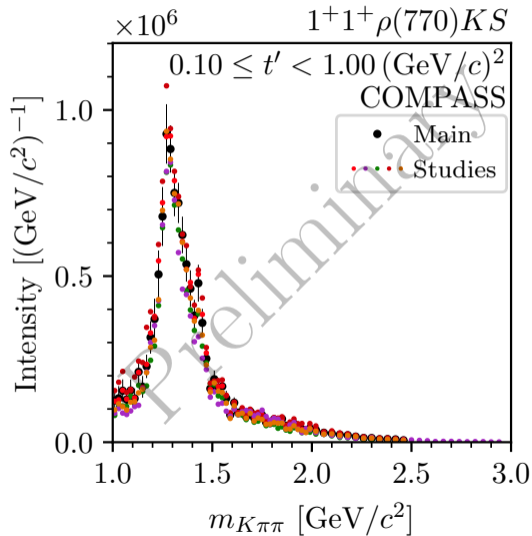
Exclusivity

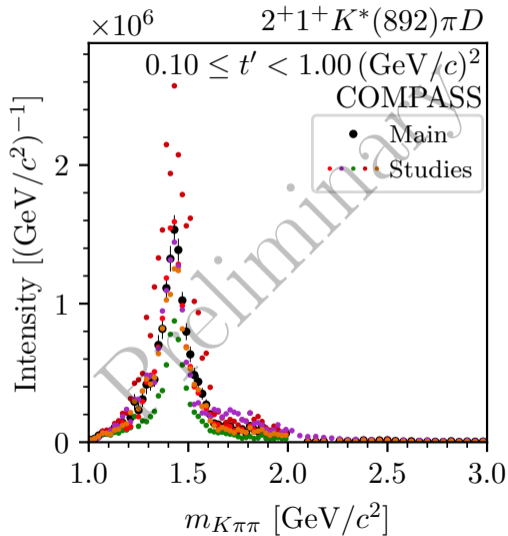


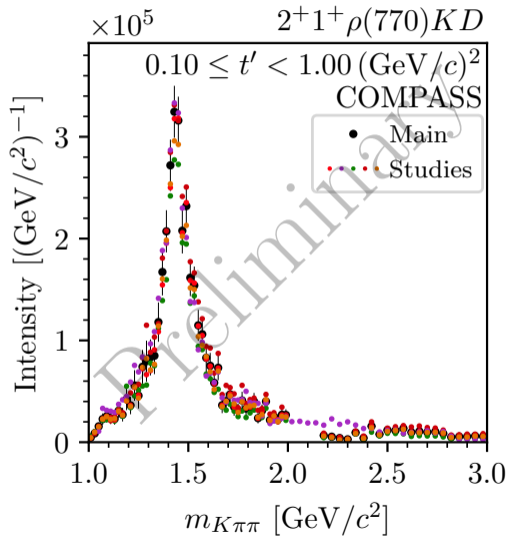


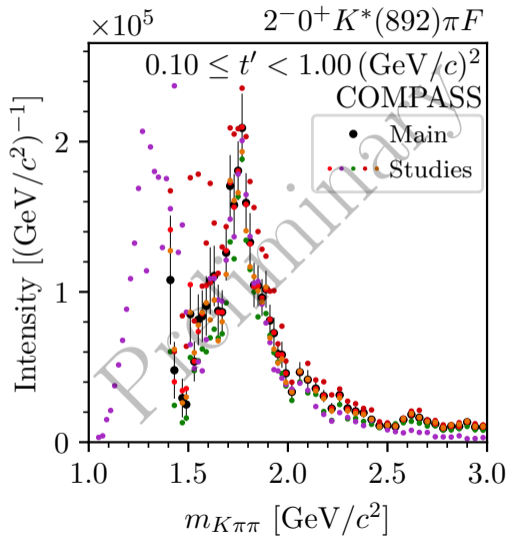


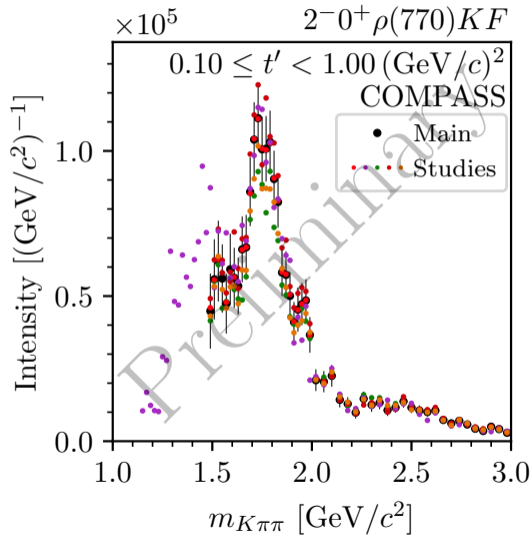


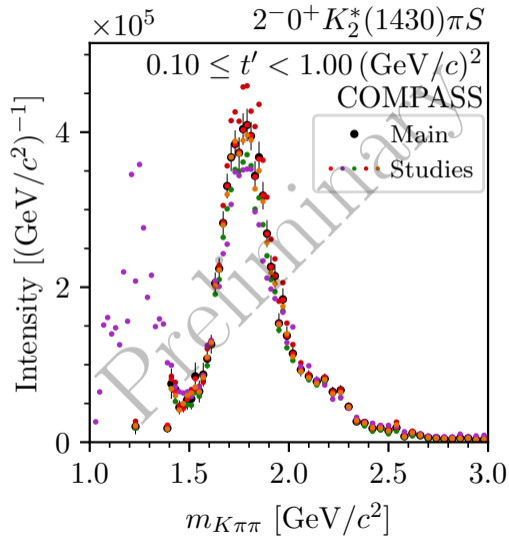


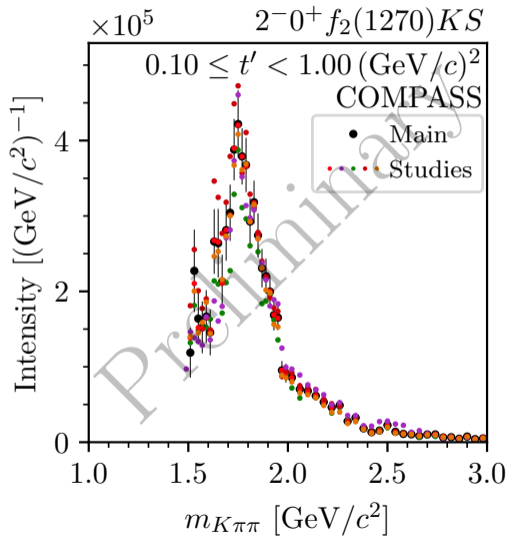




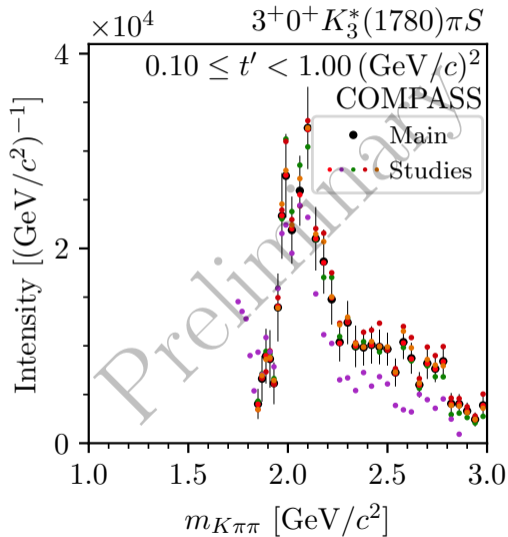


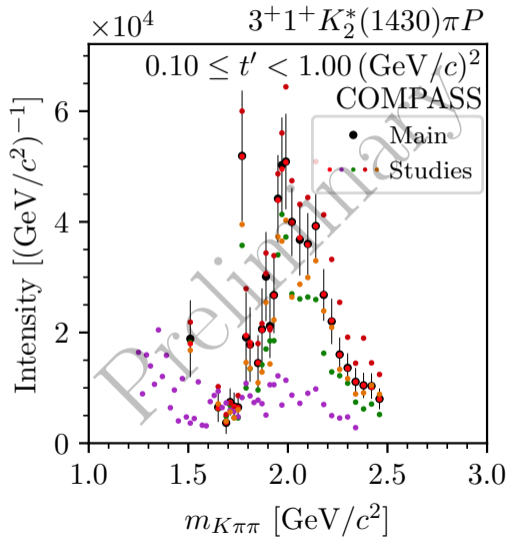


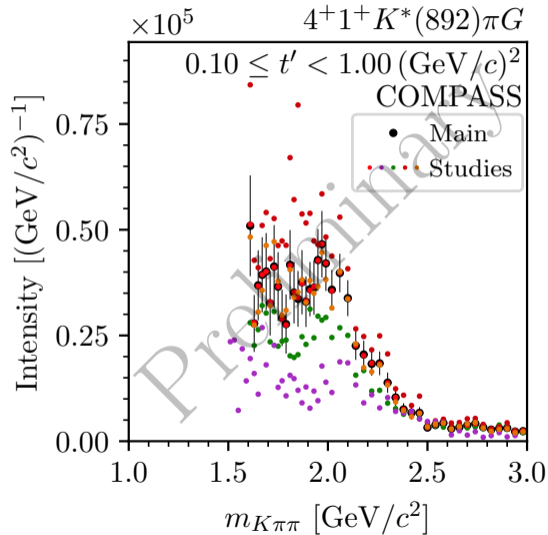


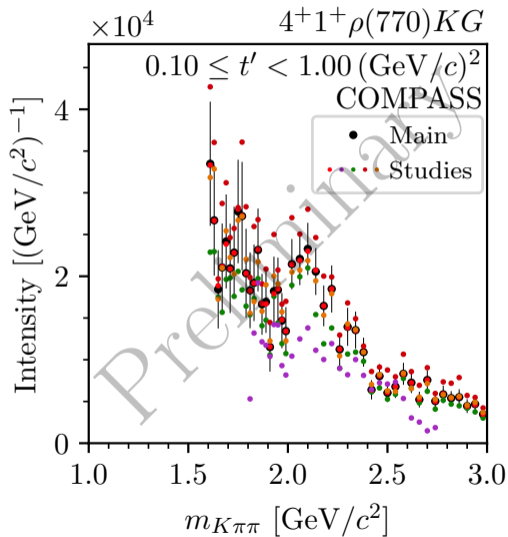


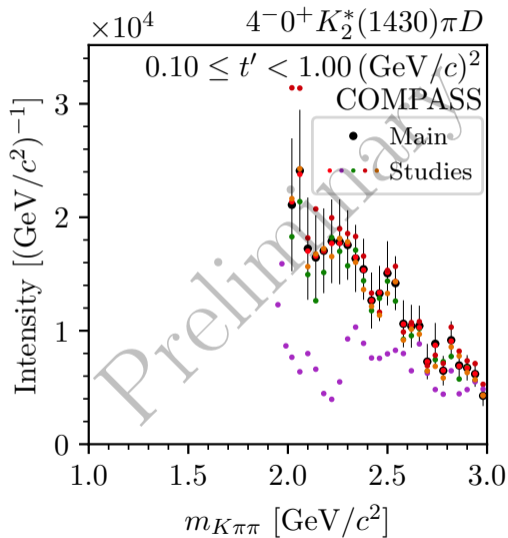


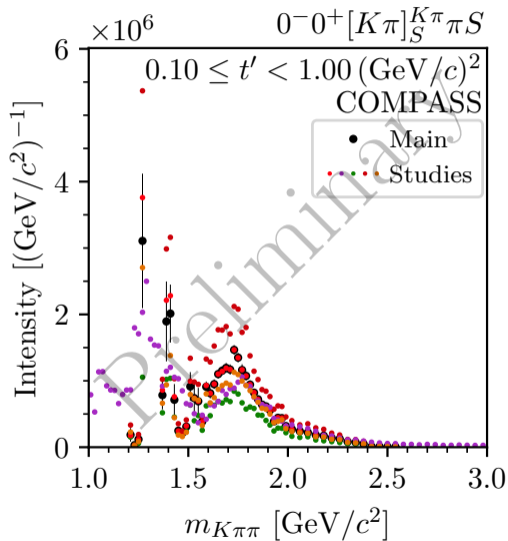


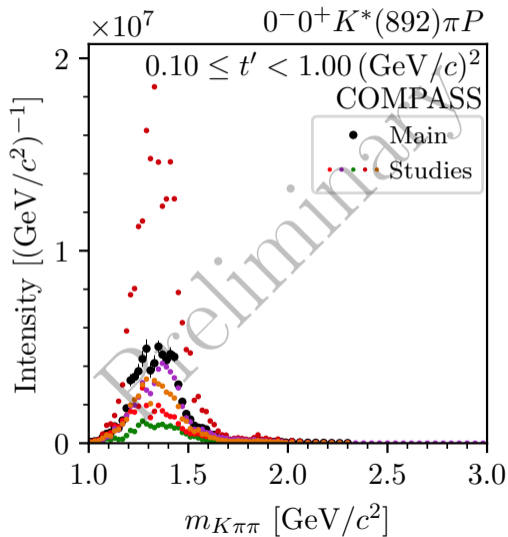


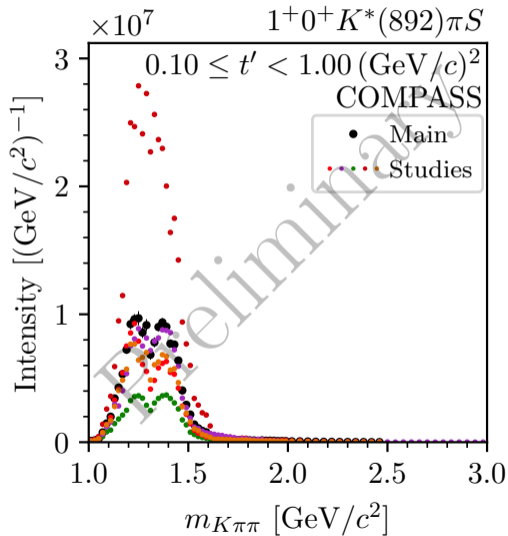




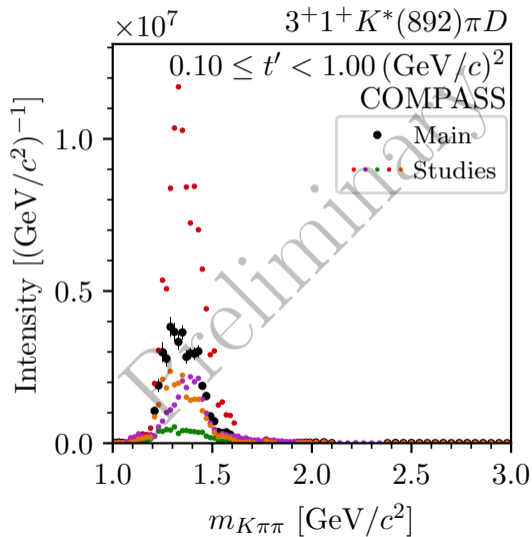




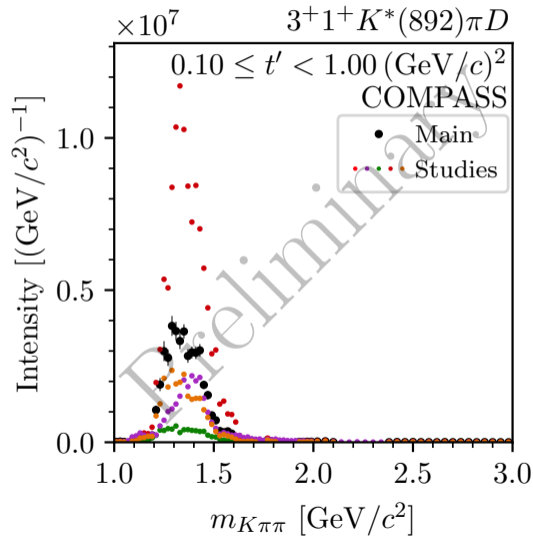




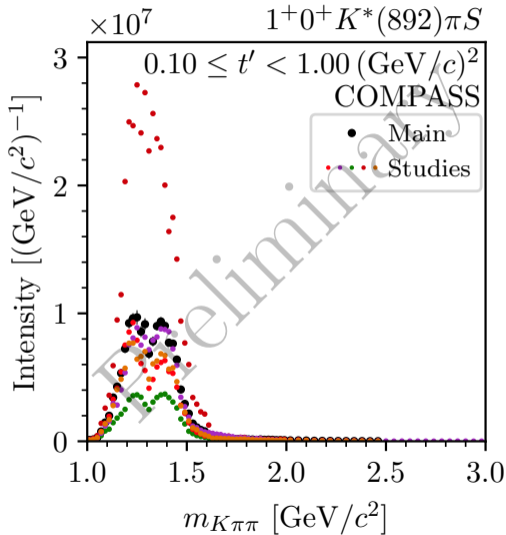




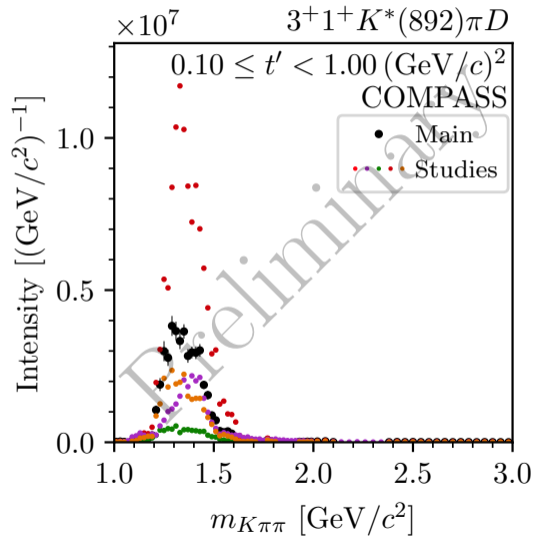
- ▶ Unexpected low-mass enhancement in  $3^+ 1^+$   $K^*(892)\pi D$  wave
- ▶ Similar to dominant  $1^+$  wave
- ▶ Sensitive to systematic effects
- ▶ Decay amplitudes of different  $J^P$  are orthogonal
- ▶ Event selection requires to identify one of the two negative particles
  - ▶ Limited acceptance due to limited kinematic range of final-state PID
- ▶ Loss of orthogonality taking acceptance into account
  - ▶ Reduced differentiability of certain partial waves
- ▶ Only a sub-set of partial waves affected



- ▶ Unexpected low-mass enhancement in  $3^+ 1^+$   $K^*(892)\pi D$  wave
- ▶ Similar to dominant  $1^+$  wave
- ▶ Sensitive to systematic effects
- ▶ Decay amplitudes of different  $J^P$  are orthogonal
- ▶ Event selection requires to identify one of the two negative particles
  - ▶ Limited acceptance due to limited kinematic range of final-state PID
- ▶ Loss of orthogonality taking acceptance into account
  - ▶ Reduced differentiability of certain partial waves
- ▶ Only a sub-set of partial waves affected

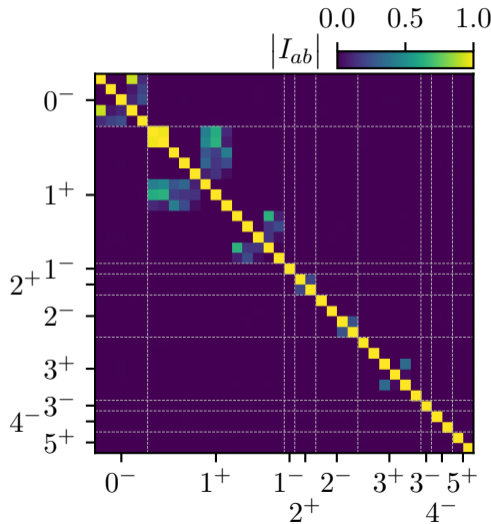


- ▶ Unexpected low-mass enhancement in  $3^+ 1^+$   $K^*(892)\pi D$  wave
- ▶ Similar to dominant  $1^+$  wave
- ▶ Sensitive to systematic effects
- ▶ Decay amplitudes of different  $J^P$  are orthogonal
- ▶ Event selection requires to identify one of the two negative particles
  - ▶ Limited acceptance due to limited kinematic range of final-state PID
- ▶ Loss of orthogonality taking acceptance into account
  - ▶ Reduced differentiability of certain partial waves
- ▶ Only a sub-set of partial waves affected

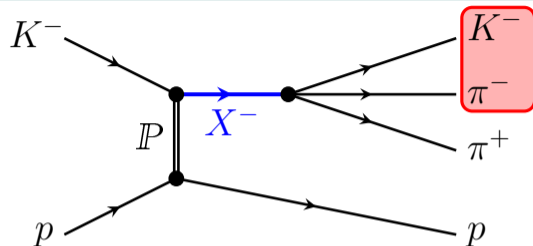


- ▶ Unexpected low-mass enhancement in  $3^+ 1^+$   $K^*(892) \pi D$  wave
- ▶ Similar to dominant  $1^+$  wave
- ▶ Sensitive to systematic effects
- ▶ Decay amplitudes of different  $J^P$  are orthogonal
- ▶ Event selection requires to identify one of the two negative particles
  - ▶ Limited acceptance due to limited kinematic range of final-state PID
- ▶ Loss of orthogonality taking acceptance into account
  - ▶ Reduced differentiability of certain partial waves
- ▶ Only a sub-set of partial waves affected

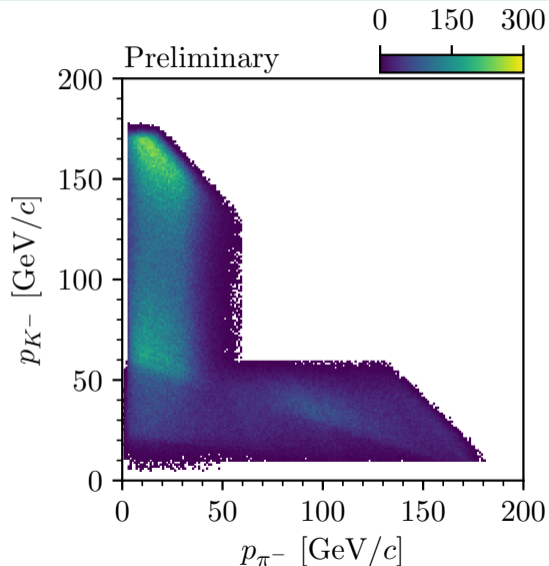
$$I_{a,b} = \int d\varphi_3(\tau) \Psi_a(\tau) \Psi_b^*(\tau)$$



- ▶ Unexpected low-mass enhancement in  $3^+ 1^+$   $K^*(892) \pi D$  wave
- ▶ Similar to dominant  $1^+$  wave
- ▶ Sensitive to systematic effects
- ▶ Decay amplitudes of different  $J^P$  are orthogonal
- ▶ Event selection requires to identify one of the two negative particles
  - ▶ Limited acceptance due to limited kinematic range of final-state PID
- ▶ Loss of orthogonality taking acceptance into account
  - ↳ Reduced differentiability of certain partial waves
- ▶ Only a sub-set of partial waves affected

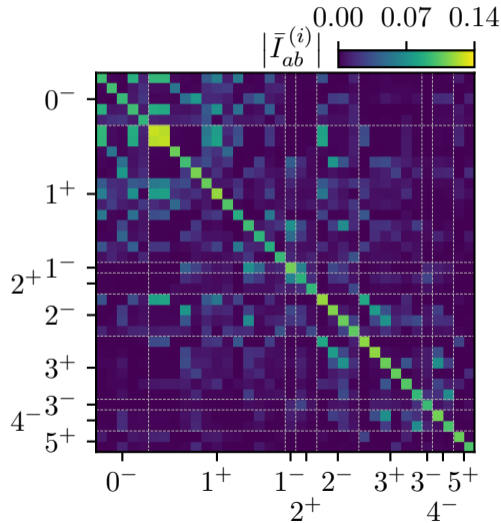


- ▶ Unexpected low-mass enhancement in  $3^+ 1^+$   $K^*(892) \pi D$  wave
- ▶ Similar to dominant  $1^+$  wave
- ▶ Sensitive to systematic effects
- ▶ Decay amplitudes of different  $J^P$  are orthogonal
- ▶ Event selection requires to identify one of the two negative particles
  - ▶ Limited acceptance due to limited kinematic range of final-state PID
- ▶ Loss of orthogonality taking acceptance into account
  - ▶ Reduced differentiability of certain partial waves
- ▶ Only a sub-set of partial waves affected



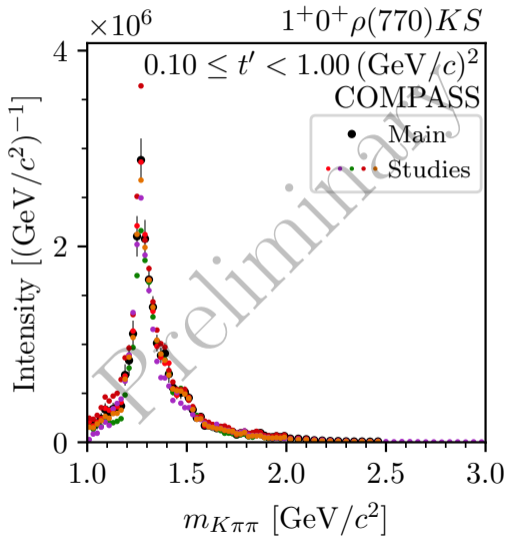
- ▶ Unexpected low-mass enhancement in  $3^+ 1^+$   $K^*(892) \pi D$  wave
- ▶ Similar to dominant  $1^+$  wave
- ▶ Sensitive to systematic effects
- ▶ Decay amplitudes of different  $J^P$  are orthogonal
- ▶ Event selection requires to identify one of the two negative particles
  - ▶ Limited acceptance due to limited kinematic range of final-state PID
- ▶ Loss of orthogonality taking acceptance into account
  - ➡ Reduced differentiability of certain partial waves
- ▶ Only a sub-set of partial waves affected

$$\bar{I}_{a,b} = \int d\varphi_3(\tau) \eta(\tau) \Psi_a(\tau) \Psi_b^*(\tau)$$



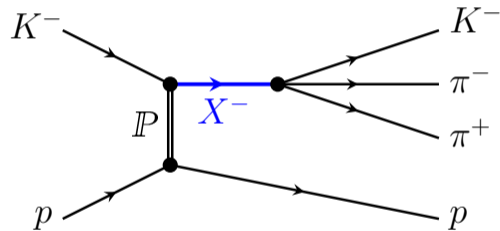


- ▶ Unexpected low-mass enhancement in  $3^+ 1^+$   $K^*(892)\pi D$  wave
- ▶ Similar to dominant  $1^+$  wave
- ▶ Sensitive to systematic effects
- ▶ Decay amplitudes of different  $J^P$  are orthogonal
- ▶ Event selection requires to identify one of the two negative particles
  - ▶ Limited acceptance due to limited kinematic range of final-state PID
- ▶ Loss of orthogonality taking acceptance into account
  - ➡ Reduced differentiability of certain partial waves
- ▶ Only a sub-set of partial waves affected

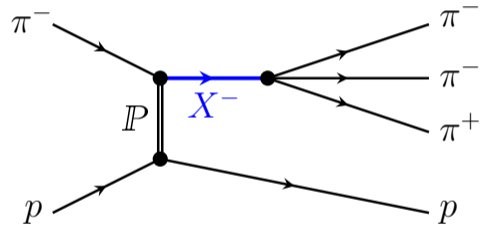


- ▶ Unexpected low-mass enhancement in  $3^+ 1^+$   $K^*(892) \pi D$  wave
- ▶ Similar to dominant  $1^+$  wave
- ▶ Sensitive to systematic effects
- ▶ Decay amplitudes of different  $J^P$  are orthogonal
- ▶ Event selection requires to identify one of the two negative particles
  - ▶ Limited acceptance due to limited kinematic range of final-state PID
- ▶ Loss of orthogonality taking acceptance into account
  - ➡ Reduced differentiability of certain partial waves
- ▶ Only a sub-set of partial waves affected

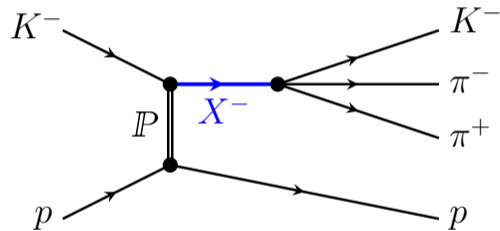
- ▶  $K^- \pi^- \pi^+$  and  $\pi^- \pi^- \pi^+$  similar experimental footprint
- ▶ Distinguishable only by
  - ▶ Beam particle identification
  - ▶ Final-state particle identification
- ▶ Excellent beam PID:
  - ▶ Expect small contamination from beam  $\pi^-$
- ▶ Final-state PID does not suppress  $\pi^- \pi^- \pi^+$  background
  - ➔ Non-negligible  $\pi^- \pi^- \pi^+$  background in  $K^- \pi^- \pi^+$  sample of about 7%
  - ➔ Dominant background in  $K^- \pi^- \pi^+$  sample



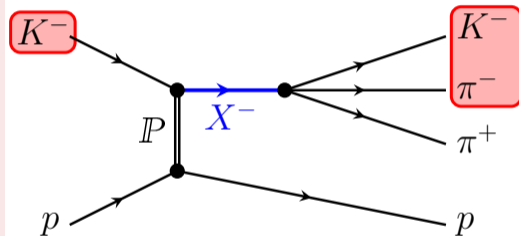
- ▶  $K^- \pi^- \pi^+$  and  $\pi^- \pi^- \pi^+$  similar experimental footprint
- ▶ Distinguishable only by
  - ▶ Beam particle identification
  - ▶ Final-state particle identification
- ▶ Excellent beam PID:
  - ▶ Expect small contamination from beam  $\pi^-$
- ▶ Final-state PID does not suppress  $\pi^- \pi^- \pi^+$  background
  - ➔ Non-negligible  $\pi^- \pi^- \pi^+$  background in  $K^- \pi^- \pi^+$  sample of about 7%
  - ➔ Dominant background in  $K^- \pi^- \pi^+$  sample



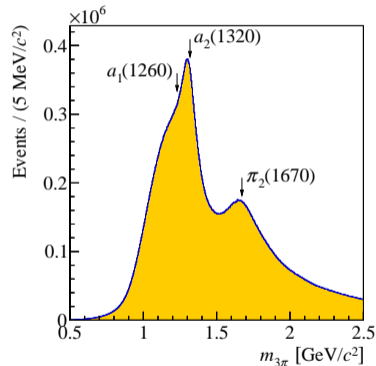
- ▶  $K^- \pi^- \pi^+$  and  $\pi^- \pi^- \pi^+$  similar experimental footprint
- ▶ Distinguishable only by
  - ▶ Beam particle identification
  - ▶ Final-state particle identification
- ▶ Excellent beam PID:
  - ▶ Expect small contamination from beam  $\pi^-$
- ▶ Final-state PID does not suppress  $\pi^- \pi^- \pi^+$  background
  - ➔ Non-negligible  $\pi^- \pi^- \pi^+$  background in  $K^- \pi^- \pi^+$  sample of about 7%
  - ➔ Dominant background in  $K^- \pi^- \pi^+$  sample



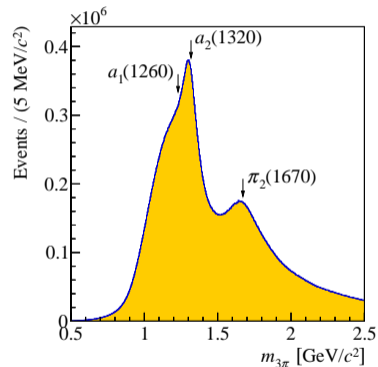
- ▶  $K^- \pi^- \pi^+$  and  $\pi^- \pi^- \pi^+$  similar experimental footprint
- ▶ Distinguishable only by
  - ▶ Beam particle identification
  - ▶ Final-state particle identification
- ▶ Excellent beam PID:
  - ▶ Expect small contamination from beam  $\pi^-$
- ▶ Final-state PID does not suppress  $\pi^- \pi^- \pi^+$  background
  - ▶ Non-negligible  $\pi^- \pi^- \pi^+$  background in  $K^- \pi^- \pi^+$  sample of about 7%
  - ▶ Dominant background in  $K^- \pi^- \pi^+$  sample



- ▶ Well established model for  $\pi^- + p \rightarrow \pi^- \pi^- \pi^+ + p$ 
  - ▶ From very same data set
  - ▶ Measured with high precision
  - ▶ Acceptance corrected
- ▶ Generate  $\pi^- \pi^- \pi^+$  Monte Carlo sample
- ▶ Mis-interpret  $\pi^- \pi^- \pi^+$  Monte Carlo events as  $K^- \pi^- \pi^+$ 
  - ▶ Apply wrong mass assumption
  - ▶ Same event reconstruction and selection as for  $K^- \pi^- \pi^+$
- ▶ Perform partial-wave decomposition of mis-interpreted  $\pi^- \pi^- \pi^+$  Monte Carlo sample
  - ▶ Using the same PWA model as for measured  $K^- \pi^- \pi^+$  sample

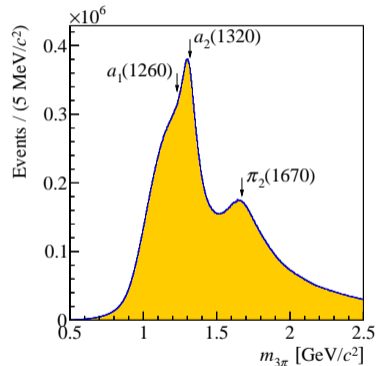


- ▶ Well established model for  $\pi^- + p \rightarrow \pi^- \pi^- \pi^+ + p$ 
  - ▶ From very same data set
  - ▶ Measured with high precision
  - ▶ Acceptance corrected
- ▶ Generate  $\pi^- \pi^- \pi^+$  Monte Carlo sample
- ▶ Mis-interpret  $\pi^- \pi^- \pi^+$  Monte Carlo events as  $K^- \pi^- \pi^+$ 
  - ▶ Apply wrong mass assumption
  - ▶ Same event reconstruction and selection as for  $K^- \pi^- \pi^+$
- ▶ Perform partial-wave decomposition of mis-interpreted  $\pi^- \pi^- \pi^+$  Monte Carlo sample
  - ▶ Using the same PWA model as for measured  $K^- \pi^- \pi^+$  sample

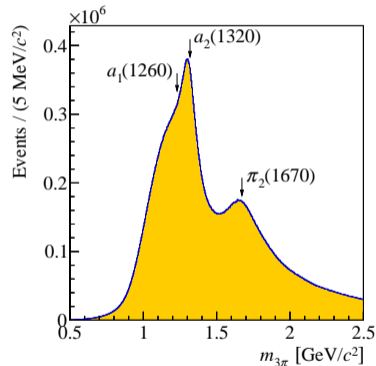




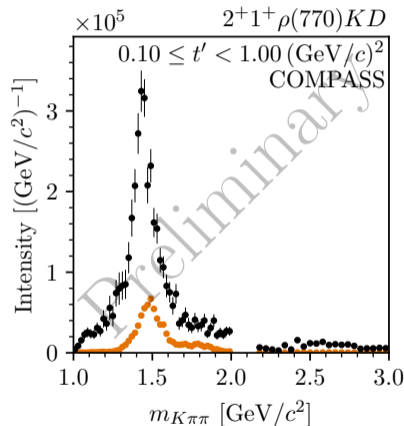
- ▶ Well established model for  $\pi^- + p \rightarrow \pi^- \pi^- \pi^+ + p$ 
  - ▶ From very same data set
  - ▶ Measured with high precision
  - ▶ Acceptance corrected
- ▶ Generate  $\pi^- \pi^- \pi^+$  Monte Carlo sample
- ▶ Mis-interpret  $\pi^- \pi^- \pi^+$  Monte Carlo events as  $K^- \pi^- \pi^+$ 
  - ▶ Apply wrong mass assumption
  - ▶ Same event reconstruction and selection as for  $K^- \pi^- \pi^+$
- ▶ Perform partial-wave decomposition of mis-interpreted  $\pi^- \pi^- \pi^+$  Monte Carlo sample
  - ▶ Using the same PWA model as for measured  $K^- \pi^- \pi^+$  sample



- ▶ Well established model for  $\pi^- + p \rightarrow \pi^- \pi^- \pi^+ + p$ 
  - ▶ From very same data set
  - ▶ Measured with high precision
  - ▶ Acceptance corrected
- ▶ Generate  $\pi^- \pi^- \pi^+$  Monte Carlo sample
- ▶ Mis-interpret  $\pi^- \pi^- \pi^+$  Monte Carlo events as  $K^- \pi^- \pi^+$ 
  - ▶ Apply wrong mass assumption
  - ▶ Same event reconstruction and selection as for  $K^- \pi^- \pi^+$
- ▶ Perform partial-wave decomposition of mis-interpreted  $\pi^- \pi^- \pi^+$  Monte Carlo sample
  - ▶ Using the same PWA model as for measured  $K^- \pi^- \pi^+$  sample
- ➔ Study  $\pi^- \pi^- \pi^+$  background in individual  $K^- \pi^- \pi^+$  partial waves

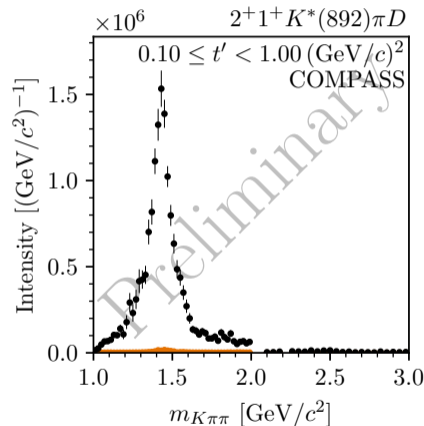


- ▶ Significant contribution to waves with  $\rho(770)$  isobar
- ▶  $\pi^- \pi^- \pi^+$  produces peaking structures
- ▶ Largest relative contribution to  $2^+ 1^+ \rho(770) K D$  wave
- ▶ Small contribution to waves with  $K^*(892)$  isobar
- ▶ Also significant contribution to waves with  $f_2(1270)$  and  $K_2^*(1430)$  isobars
- ▶ No contribution to flat wave



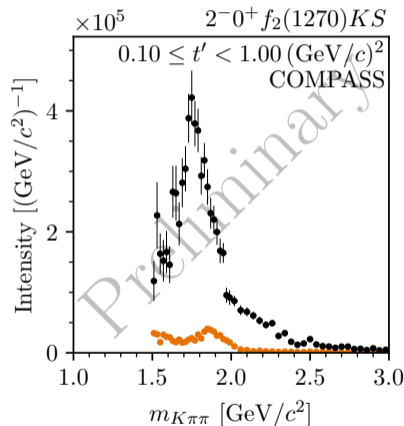
$K^- \pi^- \pi^+$  data,  $\pi^- \pi^- \pi^+$  pseudo data

- ▶ Significant contribution to waves with  $\rho(770)$  isobar
- ▶  $\pi^- \pi^- \pi^+$  produces peaking structures
- ▶ Largest relative contribution to  $2^+ 1^+ \rho(770) K D$  wave
- ▶ Small contribution to waves with  $K^*(892)$  isobar
- ▶ Also significant contribution to waves with  $f_2(1270)$  and  $K_2^*(1430)$  isobars
- ▶ No contribution to flat wave



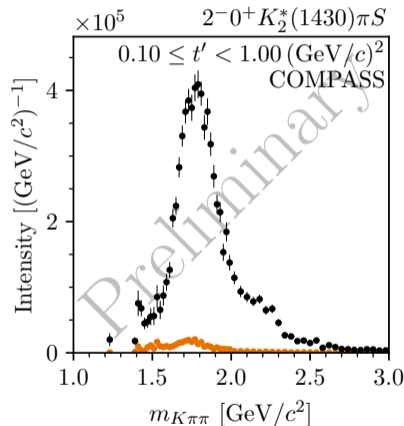
$K^- \pi^- \pi^+$  data,  $\pi^- \pi^- \pi^+$  pseudo data

- ▶ Significant contribution to waves with  $\rho(770)$  isobar
- ▶  $\pi^- \pi^- \pi^+$  produces peaking structures
- ▶ Largest relative contribution to  $2^+ 1^+ \rho(770) K D$  wave
- ▶ Small contribution to waves with  $K^*(892)$  isobar
- ▶ Also significant contribution to waves with  $f_2(1270)$  and  $K_2^*(1430)$  isobars
- ▶ No contribution to flat wave



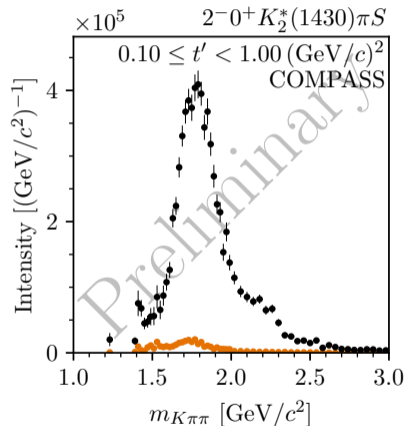
$K^- \pi^- \pi^+$  data,  $\pi^- \pi^- \pi^+$  pseudo data

- ▶ Significant contribution to waves with  $\rho(770)$  isobar
- ▶  $\pi^- \pi^- \pi^+$  produces peaking structures
- ▶ Largest relative contribution to  $2^+ 1^+ \rho(770) K D$  wave
- ▶ Small contribution to waves with  $K^*(892)$  isobar
- ▶ Also significant contribution to waves with  $f_2(1270)$  and  $K_2^*(1430)$  isobars
- ▶ No contribution to flat wave



$K^- \pi^- \pi^+$  data,  $\pi^- \pi^- \pi^+$  pseudo data

- ▶ Significant contribution to waves with  $\rho(770)$  isobar
- ▶  $\pi^- \pi^- \pi^+$  produces peaking structures
- ▶ Largest relative contribution to  $2^+ 1^+ \rho(770) K D$  wave
- ▶ Small contribution to waves with  $K^*(892)$  isobar
- ▶ Also significant contribution to waves with  $f_2(1270)$  and  $K_2^*(1430)$  isobars
- ▶ No contribution to flat wave



$K^- \pi^- \pi^+$  data,  $\pi^- \pi^- \pi^+$  pseudo data

- ▶ 238-wave set can describe main features of  $\pi^- \pi^- \pi^+$  pseudodata sufficiently well
- ▶ Largest deviation for  $K^- \pi^+$  isobar system at thigh  $m_{K\pi\pi}$

$\pi^- \pi^- \pi^+$  pseudo data,  
prediction (weighted-MC) of  $K^- \pi^- \pi^+$  PWD  
to  $\pi^- \pi^- \pi^+$  pseudo data

